

LECTURE NOTE
ADVANCED SOIL MECHANICS
FIRST SEMESTER
M.TECH (GTE)



Dr. Debabrata Giri, Associate Professor
Department of Civil Engineering
Veer Surendra Sai University of Technology, Burla
Email: dgiri_ce@vssut.ac.in

DISCLAIMER

These lecture notes are being prepared and printed for the use in training the students. No commercial use of these notes is permitted and copies of these will not be offered for sale in any manner. The readers are encouraged to provide written feedbacks for improvement of course materials.

Dr. Debabrata Giri

COURSE CONTENTS

Module-I
Compressibility of soils: consolidation theory (one, two, and three dimensional consolidation theories), consolidation in layered soil and consolidation for time dependent loading, determination of coefficient of consolidation (Casagrande method and Taylors method)
Module-II
Strength behavior of soils; Mohr Circle of Stress; UU, CU, CD tests, drained and undrained behavior of sand and clay, significance of pore pressure parameters; determination of shear strength of soil; Interpretation of triaxial test results.
Module-III
Stress path; Drained and undrained stress path; Stress path with respect to different initial state of the soil; Stress path for different practical situations.
Module-IV
Elastic and plastic deformations: elastic wall; introduction to yielding and hardening; yield curve and yield surface, associated and non-associated flow rule, Failure theories and constitutive modelling.
Module-V
Critical state soil mechanics; Critical state parameters; Critical state for normally consolidated and over consolidated soil; Significance of Roscoe and Hvorslev state boundary surface; drained and un drained plane. Critical void ratio; effect of dilation in sands; different dilation-models.
Reference Books:
Atkinson, J.H. and Bransby, P.L, The Mechanics of Soils: An introduction to Critical soil mechanics, McGraw Hill, 1978. Atkinson J.H, An introduction to the Mechanics of soils and Foundation, McGraw- Hill Co., 1993. Das, B.M., Advanced Soil Mechanics, Taylor and Francis, 2nd Edition, 1997. Wood, D.M., Soil Behavior and Critical State Soil Mechanics, Cambridge University Press, 1990. Craig, R.F., Soil Mechanics, Van Nostrand Reinhold Co. Ltd., 1987. Terzaghi, K., and Peck, R.B., Soil Mechanics in Engineering Practice, John Wiley & Sons, 1967. Lambe, T.W. and Whitman, R.V., Soil Mechanics, John Wiley & Sons, 1979
COURSE OUTCOME
1. The students obtain knowledge on compressibility parameters of soil mass.
2. The students are able to select the shear strength to design different structures for different conditions of loading, drainage and failure criteria.
3. The students can estimate the stress path in soil under drainage condition.
4. The students can describe the mathematical models for solving different problems in soil mechanics.
5. The students can illustrate the deformation behavior of soil mass.

1.0 Consolidation and Compression of Soils

When a soil layer is subjected to vertical stress, volume change can take place through rearrangement of soil grains, and some amount of grain fracture may also take place. The volume of soil grains remains constant, so change in total volume is due to change in volume of water. In saturated soils, this can happen only if water is pushed out of the voids. The movement of water takes time and is controlled by the **permeability** of the soil and the locations of free draining boundary surfaces.

It is necessary to determine both the magnitude of volume change (or the settlement) and the time required for the volume change to occur. The magnitude of settlement is dependent on the magnitude of applied stress, thickness of the soil layer, and the **compressibility** of the soil.

When soil is loaded undrained, the pore pressure increases. As the excess pore pressure dissipates and water leaves the soil, settlement takes place. This process takes time, and the rate of settlement decreases over time. In coarse soils (sands and gravels), volume change occurs immediately as pore pressures are dissipated rapidly due to high permeability. In fine soils (silts and clays), slow seepage occurs due to low permeability.

Elastic settlement is on account of change in shape at constant volume, i.e. due to vertical compression and lateral expansion. **Primary consolidation** (or simply **consolidation**) is on account of flow of water from the voids, and is a function of the permeability and compressibility of soil. **Secondary compression** is on account of creep-like behaviour.

Primary consolidation is the major component and it can be reasonably estimated. A general theory for consolidation, incorporating three-dimensional flow is complicated and only applicable to a very limited range of problems in geotechnical engineering. For the vast majority of practical settlement problems, it is sufficient to consider that both seepage and strain take place in one direction only, as **one-dimensional consolidation** in the vertical direction.

1.1 Compressibility Characteristics

Soils are often subjected to uniform loading over large areas, such as from wide foundations, fills or embankments. Under such conditions, the soil which is remote from the edges of the loaded area undergoes vertical strain, but no horizontal strain. Thus, the settlement occurs only in one-dimension.

The compressibility of soils under one-dimensional compression can be described from the decrease in the volume of voids with the increase of effective stress. This relation of void ratio and effective stress can be depicted either as an **arithmetic plot** or a **semi-log plot**.

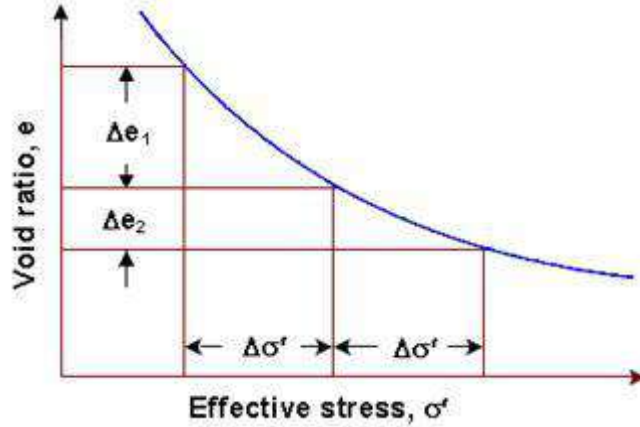


Fig.1.1 Effective stress versus void ratio

In the arithmetic plot as shown, as the soil compresses, for the same increase of effective stress σ' , the void ratio reduces by a smaller magnitude, from Δe_1 to Δe_2 . This is on account of an increasingly denser packing of the soil particles as the pore water is forced out. In fine soils, a much longer time is required for the pore water to escape, as compared to coarse soils.

It can be said that the compressibility of a soil decreases as the effective stress increases. This can be represented by the slope of the void ratio – effective stress relation, which is called the **coefficient of compressibility**, a_v .

$$a_v = - \frac{de}{d\sigma'} \text{-----} \quad \text{Eq.1.1}$$

Or

$$a_v = - \frac{\Delta e}{\Delta \sigma'} \text{-----} \quad \text{Eq.1.2}$$

For a small range of effective stress, $a_v = - \frac{\Delta e}{\Delta \sigma'}$

The -ve sign is introduced to make a_v a positive parameter.

If e_0 is the initial void ratio of the consolidating layer, another useful parameter is the **coefficient of volume compressibility**, m_v , which is expressed as

$$m_v = \frac{a_v}{1+e_0} \text{-----} \quad \text{Eq.1.3}$$

It represents the compression of the soil, per unit original thickness, due to a unit increase of pressure.

1.2 Normally Consolidated and Over Consolidated

If the current effective stress, σ' , is equal (note that it cannot be greater than) to the pre-consolidation stress, then the deposit is said to be **normally consolidated (NC)**. If the current effective stress is less than the pre-consolidation stress, then the soil is said to be **over-consolidated (OC)**.

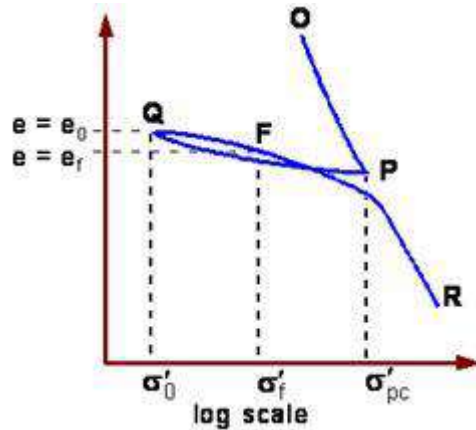


Fig.1.2: Relation between void ratio and logarithmic effective stress

The figure shows the relation of void ratio and effective stress of a clay soil as a **semi-log plot**.

OP corresponds to initial loading of the soil. **PQ** corresponds to unloading of the soil. **QFR** corresponds to a reloading of the soil. Upon reloading beyond **P**, the soil continues along the path that it would have followed if loaded from **O to R** continuously.

The **pre-consolidation stress**, s'_{pc} , is defined to be the maximum effective stress experienced by the soil. This stress is identified in comparison with the effective stress in its present state. For soil at state **Q or F**, this would correspond to the effective stress at point **P**.

It may be seen that for the same increase in effective stress, the change in void ratio is much less for an over-consolidated soil (**from e_0 to e_1**), than it would have been for a normally consolidated soil as in path **OP**. In unloading, the soil swells but the increase in volume is much less than the initial decrease in volume for the same stress difference.

The distance from the normal consolidation line has an important influence on soil behaviour. This is described numerically by the **over-consolidation ratio (OCR)**, which is defined as the ratio of the pre-consolidation stress to the current effective stress.

$$OCR = \frac{\sigma'_{pc}}{\sigma'} \text{-----} \quad \text{Eq.1.4}$$

Note that when the soil is normally consolidated, **OCR = 1**

Settlements will generally be much smaller for structures built on over consolidated soils. Most soils are over-consolidated to some degree. This can be due to shrinking and swelling of the soil on drying and rewetting, changes in ground water levels, and unloading due to erosion of overlying strata.

For **NC clays**, the plot of void ratio versus log of effective stress can be approximated to a straight line, and the slope of this line is indicated by a parameter termed as **compression index, C_c** .

$$C_c = \frac{\Delta e}{\log_{10}\left(\frac{\sigma_2}{\sigma_1}\right)}$$

Eq.1.5

1.3 Estimation of Pre-Consolidation Stress

It is possible to determine the pre-consolidation stress that the soil had experienced. The soil sample is to be loaded in the laboratory so as to obtain the void ratio - effective stress relationship. Empirical procedures are used to estimate the pre-consolidation stress, the most widely used being **Casagrande's construction** which is illustrated.

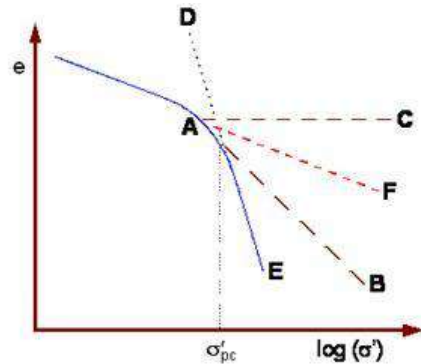


Fig.1.3: Casagrande's construction method to find pre-consolidation pressure

The steps in the construction are:

1. Draw the graph using an appropriate scale.
2. Determine the point of maximum curvature **A**.
3. At **A**, draw a tangent **AB** to the curve.
4. At **A**, draw a horizontal line **AC**.
5. Draw the extension **ED** of the straight line portion of the curve.

Where the line **ED** cuts the bisector **AF** of angle **CAB** that point corresponds to the pre-consolidation stress.

The total stress increases when additional vertical load is first applied. Instantaneously, the pore water pressure increases by exactly the same amount. Subsequently there will be flow from regions of higher excess pore pressure to regions of lower excess pore pressure causing dissipation. The effective stress will change and the soil will consolidate with time. This is shown schematically.

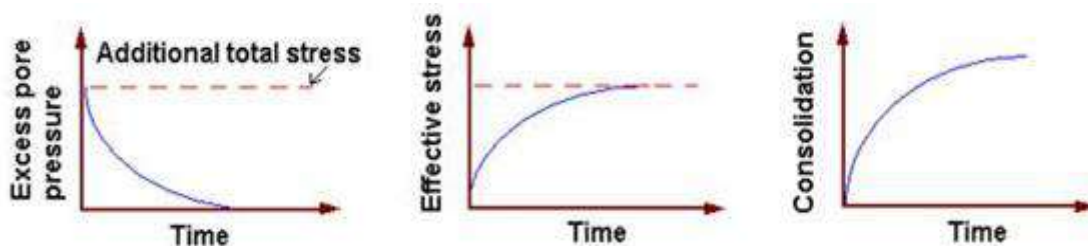


Fig.1.4: Change of effective stress, consolidation with time

1.4 SPRING ANALOGY TO EXPLAIN CONSOLIDATION THEORY

A mechanistic model for the phenomenon of consolidation was given by Taylor (1948), by which the process can be better understood. This model, with slight modifications, is presented in Fig. 1 and is explained below:

A spring of initial height H_i is surrounded by water in a cylinder. The spring is analogous to the soil skeleton and the water to the pore water. The cylinder is fitted with a piston of area A through which a certain load may be transmitted to the system representing a saturated soil. The piston, in turn, is fitted with a vent, and a valve by which the vent may be opened or closed.

Referring to Fig.1.5 (a), let a load P be applied on the piston. Let us assume that the valve of the vent is open and no flow is occurring. This indicates that the system is in equilibrium under the total stress P/A which is fully borne by the spring, the pressure in the water being zero.

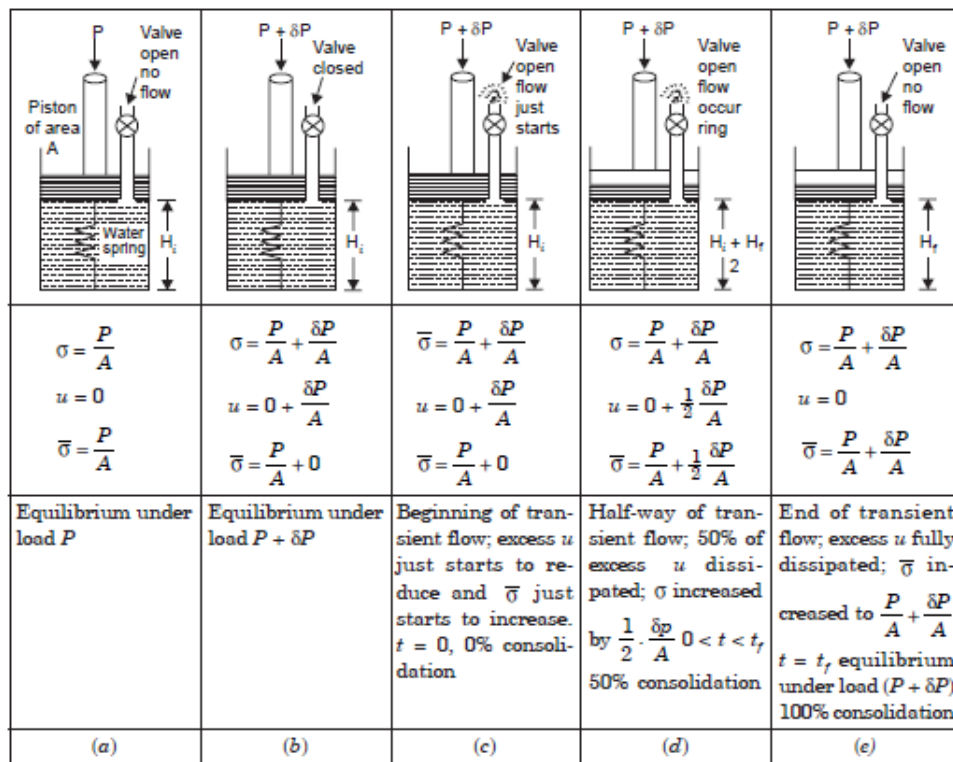


Fig.1.5: Spring Model for Consolidation of Soil mass

Referring to Fig.1.5 (b), let us apply an increment of load δP to the piston, the valve being kept closed. Since no water is allowed to flow out, the piston cannot move downwards and compress the spring; therefore, the spring carries the earlier stress of P/A , while the water is forced to carry the additional stress of $\delta P/A$ imposed on the system, the sum counteracting the total stress imposed. This additional stress $\delta P/A$ in the water is known as the hydrostatic excess pressure.

Referring to Fig.1.5(c), let us open the valve and start reckoning time from that instant. Water just starts to flow under the pressure gradient between it and the atmosphere seeking to return to its equilibrium or atmospheric pressure. The excess pore pressure begins to diminish, the spring starts getting compressed as the piston descends consequent to expulsion of pore water. It is just

the beginning of transient flow, simulating the phenomenon of consolidation. The openness of the valve is analogous to the permeability of soil.

Referring to Fig.1.5 (d), flow has occurred to the extent of dissipating 50% of the excess pore pressure. The pore water pressure at this instant is half the initial value, *i.e.*, $1/2(\delta P/A)$. This causes a corresponding increase in the stress in the spring of $1/2 (\delta P/A)$, the total stress remaining constant at $[(P/A) + (\delta P/A)]$. This stage refers to that of “50% consolidation”.

Referring to Fig.5 (e), the final equilibrium condition is reached when the transient flow situation ceases to exist, consequent to the complete dissipation of the pore water pressure. The spring compresses to a final height $H_f < H_i$, carrying the total stress of $(P + \delta P)/A$, all by itself, since the excess pore water pressure has been reduced to zero, the pressure in it having equalled the atmospheric. The system has reached the equilibrium condition under the load $(P + \delta P)$. This represents “100% consolidation” under the applied load or stress increment. We may say that the “soil” has been consolidated to an effective stress of $(P + \delta P)/A$.

In this mechanistic model, the compressible soil skeleton is characterised by the spring and the pore water by the water in the cylinder. The more compressible the soil, the longer the time required for consolidation; the more permeable the soil, the shorter the time required. There is one important aspect in which this analogy fails to simulate consolidation of a soil. It is that the pressure conditions are the same throughout the height of the cylinder, whereas the consolidation of a soil begins near the drainage surfaces and gradually progresses inward. It may be noted that soil consolidates only when effective stress increases; that is to say, the volume change behaviour of a soil is a function of the effective stress and not the total stress.

Similar arguments may be applied to the expansion characteristics under the decrease of load.

An alternative mechanical analogy to the consolidation process is shown in Fig. 6. A cylinder is fitted with a number of pistons connected by springs to one another. Each of the compartments thus formed is connected to the atmosphere with the aid of standpipes. The cylinder is full of water and is considered to be airtight. The pistons are provided with perforations through which water can move from one compartment to another. The topmost piston is fitted with valves which may open or close to the atmosphere. It is assumed that any pressure applied to the top piston gets transmitted undiminished to the water and springs.

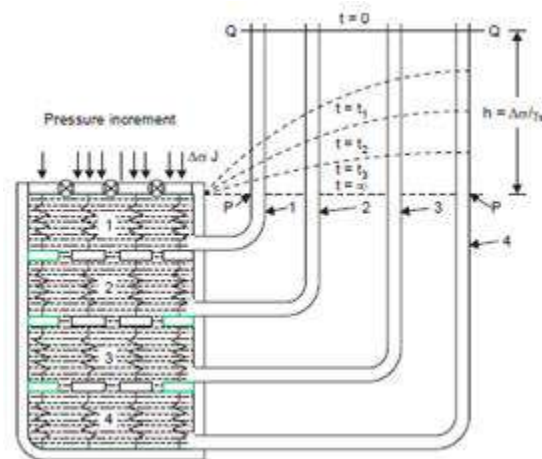


Fig.1.6: Mechanical Analogy to Consolidation process

Initially, the cylinder is full of water and weights of the pistons are balanced by the springs; the water is at atmospheric pressure and the valves may be open. The water level stands at the elevation **PP** in the standpipes as shown. The valves are now closed, the water level continuing to remain at **PP**. An increment of pressure $\Delta\sigma$ is applied on the top piston. It will be observed that the water level rises instantaneously in all the stand pipes to an elevation

QQ, above **PP** by a height $h = \Delta\sigma/\gamma_w$. Let all the valves be opened simultaneously with the application of the pressure increment, the time being reckoned from that instant. The height of the springs remains unchanged at that instant and the applied increment of pressure is fully taken up by water as the hydrostatic excess pressure over and above the atmospheric. An equal rise of water in all the standpipes indicates that the hydrostatic excess pressure is the same in all compartments immediately after application of pressure. As time elapses, the water level in the pipes starts falling, the pistons move downwards gradually and water comes out through the open valves. At any time $t = t_1$, the water pressure in the first compartment is least and that in the last or the bottommost is highest, as indicated by the water levels in the standpipes. The variation of hydrostatic excess pressure at various points in the depth of the cylinder, as shown by the dotted lines, varies with time. Ultimately, the hydrostatic excess pressure reduces to zero in all compartments, the water levels in the standpipes reaching elevation **PP**; this theoretically speaking, is supposed to happen after the lapse of infinite time. As the hydrostatic excess pressure decreases in each compartment, the springs in each compartment experience a corresponding pressure and get compressed. For example, at time $t = t_1$, the hydrostatic excess pressure in the first compartment is given by the head **PJ**; the pressure taken by the springs is indicated by the head **JQ**, the sum of the two at all times being equivalent to the applied pressure increment; that is to say, it is analogous to the effective stress principle: $\sigma = \sigma' + u$, the pressure transferred to the springs being analogous to inter-granular or effective stress in a saturated soil, and the hydrostatic excess pressure to the neutral pressure or excess pore water pressure.

Since water is permitted to escape only at one end, it is similar to the case of a single drainage face for a consolidating clay sample. The distribution of hydrostatic excess pressure will be symmetrical about mid-depth for the situation of a double drainage face, the maximum occurring at mid-depth and the minimum or zero values occurring at the drainage faces.

1.5 TERZAGHI'S THEORY OF ONE-DIMENSIONAL CONSOLIDATION

Terzaghi (1925) advanced his theory of one-dimensional consolidation based upon the following assumptions, the mathematical implications being given in parentheses:

1. The soil is homogeneous (k_z is independent of z).
2. The soil is completely saturated ($S = 100\%$).
3. The soil grains and water are virtually incompressible (γ_w is constant and volume change of soil is only due to change in void ratio).
4. The behaviour of infinitesimal masses in regard to expulsion of pore water and consequent consolidation is no different from that of larger representative masses (Principles of calculus may be applied).

5. The compression is one-dimensional (u varies with z only).
6. The flow of water in the soil voids is one-dimensional, Darcy's law being valid.

$$\frac{\partial v_x}{\partial x} = \frac{\partial v_y}{\partial y} = 0 \text{ and } v_z = k_z \frac{\partial h}{\partial z} \text{-----} \quad \text{Eq.1.6}$$

Also, flow occurs on account of hydrostatic excess pressure ($h = u/\gamma_w$).

7. Certain soil properties such as permeability and modulus of volume change are constant; these actually vary somewhat with pressure. (k and m_v are independent of pressure).
8. The pressure versus void ratio relationship is taken to be the idealised one, a_v is constant).
9. Hydrodynamic lag alone is considered and plastic lag is ignored, although it is known to exist. (The effect of k alone is considered on the rate of expulsion of pore water).

The first three assumptions represent conditions that do not vary significantly from actual conditions.

The fourth assumption is purely of academic interest and is stated because the differential equations used in the derivation treat only infinitesimal distances. It has no significance for the laboratory soil sample or for the field soil deposit.

The fifth assumption is certainly valid for deeper strata in the field owing to lateral confinement and is also reasonably valid for an oedometer sample.

The sixth assumption regarding flow of pore water being one-dimensional may be taken to be valid for the laboratory sample, while its applicability to a field situation should be checked. However, the validity of Darcy's law for flow of pore water is unquestionable.

The seventh assumption may introduce certain errors in view of the fact that certain soil properties which enter into the theory vary somewhat with pressure but the errors are considered to be of minor importance.

The eighth and ninth assumptions lead to the limited validity of the theory. The only justification for the use of the eighth assumption is that, otherwise, the analysis becomes unduly complex.

The ninth assumption is necessitated because it is not possible to take the plastic lag into account in this theory. These two assumptions also may be considered to introduce some errors.

Now let us see the derivation of Terzaghi's theory with respect to the laboratory oedometer sample with double drainage as shown in Fig. 1.7.

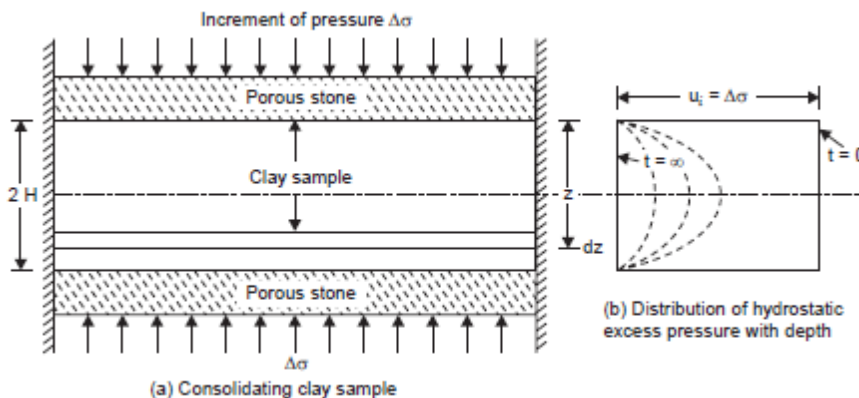


Fig.1.7: Consolidation of clay soil sample with double drainage

Let us consider a layer of unit area of cross-section and of elementary thickness dz at depth z from the pervious boundary. Let the increment of pressure applied be $\Delta\sigma$. immediately on application of the pressure increment, pore water starts to flow towards the drainage faces. Let ∂h be the head lost between the two faces of this elementary layer, corresponding to a decrease of hydrostatic excess pressure ∂u .

Equation 2, for flow of water through soil, holds here also,

$$k_x \frac{\partial^2 h}{\partial x^2} + k_z \frac{\partial^2 h}{\partial z^2} = \frac{1}{1+e} \left[e \frac{\partial s}{\partial t} + S \frac{\partial e}{\partial t} \right] \text{-----} \quad \text{Eq.1.7}$$

For one-dimensional flow situation, this reduces to:

$$k_z \frac{\partial^2 h}{\partial z^2} = \frac{1}{1+e} \left[e \frac{\partial s}{\partial t} + S \frac{\partial e}{\partial t} \right] \text{-----} \quad \text{Eq.1.8}$$

During the process of consolidation, the degree of saturation is taken to remain constant at 100%, while void ratio changes causing reduction in volume and dissipation of excess hydrostatic pressure through expulsion of pore water; that is,

$$S=0 \text{ or unity and } \frac{\partial s}{\partial t} = 0$$

$$\text{Hence } k_z \frac{\partial^2 h}{\partial z^2} = \frac{1}{1+e} \left[\frac{\partial e}{\partial t} \right] = \frac{\partial}{\partial t} \left[\frac{e}{1+e} \right] \text{-----} \quad \text{Eq.1.9}$$

Negative sign denoting decrease of e for increase of h .

Since volume decrease can be due to a decrease in the void ratio only as the pore water and soil grains are virtually incompressible, $\frac{\partial}{\partial t} \left[\frac{e}{1+e} \right]$ represents time-rate of volume change per unit volume

The flow is only due to the hydrostatic excess pressure, $h = \frac{u}{\gamma_w}$

$$\text{So } \frac{k}{\gamma_w} \frac{\partial^2 u}{\partial z^2} = - \frac{\partial V}{\partial t} \text{-----} \quad \text{Eq.1.10}$$

Here k is the permeability of soil in the direction of flow, and ∂V represents the change in volume per unit volume. The change in hydrostatic excess pressure, ∂u , changes the intergranular or effective stress by the same magnitude, the total stress remaining constant.

The change in volume per unit volume, ∂V , may be written, as per the definition of the modulus of volume change, m_v

$$\partial V = m_v \partial \sigma = -m_v \partial u \text{-----} \quad \text{Eq.1.11}$$

Negative sign is used, since increase in stress reduces pore water pressure.

Differentiating both sides with respect to time,

$$\frac{\partial V}{\partial t} = -m_v \frac{\partial u}{\partial t} \text{-----} \quad \text{Eq.1.12}$$

From Eq. 1.11 and 1.12, we get

$$\frac{\partial u}{\partial t} = \frac{k}{\gamma_w m_v} \frac{\partial^2 u}{\partial z^2} \text{-----} \quad \text{Eq.1.13}$$

This is written as:

$$\frac{\partial u}{\partial t} = c_v \frac{\partial^2 u}{\partial z^2} \text{-----} \quad \text{Eq.1.14}$$

Where $c_v = \frac{k}{\gamma_w m_v}$

c_v is known as the “Coefficient of consolidation”. u represents the hydrostatic excess pressure at a depth z from the drainage face at time t from the start of the process of consolidation.

The coefficient of consolidation may also be written in terms of the coefficient of compressibility

$$c_v = \frac{k}{\gamma_w m_v} = \frac{k(1+e_0)}{a_v \gamma_w} \text{-----} \quad \text{Eq.1.15}$$

Equation 1.13 is the basic differential equation of consolidation according to Terzaghi’s theory of one-dimensional consolidation. The coefficient of consolidation combines the effect of permeability and compressibility characteristics on volume change during consolidation. Its units can be shown to be mm^2/s or $\text{L}^2 \text{T}^{-1}$.

The initial hydrostatic excess pressure, u_i , is equal to the increment of pressure $\Delta\sigma$, and is the same throughout the depth of the sample, immediately on application of the pressure, and is shown by the heavy line in Fig. 1.7 (b). The horizontal portion of the heavy line indicates the fact that, at the drainage face, the hydrostatic excess pressure instantly reduces to zero, theoretically speaking. Further, the hydrostatic excess pressure would get fully dissipated throughout the depth of the sample only after the lapse of infinite time*, as indicated by the heavy vertical line on the left of the figure. At any other instant of time, the hydrostatic excess pressure will be maximum at the farthest point in the depth from the drainage faces, that is, at the middle and it is zero at the top and bottom. The distribution of the hydrostatic excess pressure with depth is sinusoidal at other instants of time, as shown by dotted lines. These curves are called “Isochrones”.

1.6 Alternative Method:

With reference to Fig.1, the hydraulic gradient i_1 at depth z

$$\frac{\partial h}{\partial z} = \frac{1}{\gamma_w} \frac{\partial u}{\partial z} \text{-----} \quad \text{Eq.1.16}$$

$$\text{The hydraulic gradient } i_2 \text{ at depth } z+\partial z = \frac{1}{\gamma_w} \left(\frac{\partial u}{\partial z} + \frac{\partial^2 u}{\partial z^2} dz \right) \text{-----} \quad \text{Eq.1.17}$$

Rate of inflow per unit area = Velocity at depth $z = k.i_1$, by Darcy’s law.

Rate of outflow per unit area = Velocity at $(z + dz) = k.i_2$

$$\text{Water lost per unit time} = k(i_2 - i_1) = \frac{k}{\gamma_w} \left(\frac{\partial^2 u}{\partial z^2} dz \right) \text{-----} \quad \text{Eq.1.18}$$

This should be the same as the time-rate of volume decrease.

$$\text{Volumetric strain} = m_v \cdot \Delta\sigma = -m_v \partial(\sigma - u) \text{-----} \quad \text{Eq.1.19}$$

As per the definition of the modulus of volume change, m_v

(The negative sign denotes decrease in volume with increase in pressure).

$$\therefore \text{Change of volume} = -m_v \partial(\sigma - u) \cdot dz \text{-----} \quad \text{Eq.1.20}$$

Since the elementary layer of thickness dz and unit cross-sectional area is considered.

$$\text{Time-rate of change of volume} = -m_v \frac{\partial}{\partial t} (\sigma - u) dz \text{-----} \quad \text{Eq.1.21}$$

But $\frac{\partial \sigma}{\partial t} = 0$, since σ is constant.

$$\therefore \text{Time-rate of change of volume} = +m_v \frac{\partial u}{\partial t} dz \text{-----} \quad \text{Eq.1.22}$$

Equating this to water lost per unit time

$$\frac{k}{\gamma_w m_v} \frac{\partial^2 u}{\partial z^2} dz = -m_v \frac{\partial u}{\partial t} dz \text{-----} \quad \text{Eq.1.23}$$

$$\frac{\partial u}{\partial t} = c_v \frac{\partial^2 u}{\partial z^2} \text{-----} \quad \text{Eq.1.24}$$

$$\text{Where } c_v = \frac{k}{\gamma_w m_v} \text{-----} \quad \text{Eq.1.25}$$

1.7 SOLUTION OF TERZAGHI'S EQUATION FOR ONE-DIMENSIONAL CONSOLIDATION

Terzaghi solved the differential equation for a set of boundary conditions which have utility in solving numerous engineering problems and presented the results in graphical form using dimensional parameters.

The following are the boundary conditions:

1. There is drainage at the top of the sample: At $z = 0$, $u = 0$, for all t .
2. There is drainage at the bottom of the sample: At $z = 2H$, $u = 0$, for all t .
3. The initial hydrostatic excess pressure u_i is equal to the pressure increment, $\Delta\sigma$ $u = u_i = \Delta\sigma$, at $t = 0$.

Terzaghi chose to consider this situation where $u = u_i$ initially *throughout the depth*, although solutions are possible when u_i varies with depth in any specified manner. The thickness of the sample is designated by $2H$, the distance H thus being the length of the longest drainage path, *i.e.*, maximum distance water has to travel to reach a drainage face because of the existence of two drainage faces. (In the case of only one drainage face, this will be equal to the total thickness of the clay layer).

The general solution for the above set of boundary conditions has been obtained on the basis of separation of variables and Fourier Series expansion and is as follows:

$$u = f(z, t) = \sum_{n=1}^{\infty} \left\{ \frac{1}{H} \int_0^{2H} u_i \sin \frac{n\pi z}{2H} dz \right\} \left(\sin \frac{n\pi z}{2H} \right) e^{-n^2 \pi^2 c_v / 4H^2 t} \text{-----} \quad \text{Eq.1.26}$$

This solution enables the hydrostatic excess u to be computed for a soil mass under any initial system of stress u_i , at any depth z , and at any time t .

In particular, if u_i is considered constant with respect to depth, this equation reduces to

$$u = \sum_{n=1}^{\infty} \left\{ \frac{2u_i}{n\pi} (1 - \cos n\pi) \right\} \left(\sin \frac{n\pi z}{2H} \right) e^{-n^2 \pi^2 c_v / 4H^2 t} \text{-----} \quad \text{Eq.1.27}$$

When n is even, $(1 - \cos n\pi)$ vanishes; when n is odd, this factor becomes 2. Therefore it is convenient to replace n by $(2m + 1)$, m being an integer. Thus, we have

$$u = \sum_{n=1}^{\infty} \frac{4u_i}{(2m+1)\pi} \left[\sin \frac{(2m+1)z}{2H} \right] e^{-(2m+1)^2 \pi^2 c_v / 4H^2 t} \text{-----} \quad \text{Eq.1.28}$$

Three-dimensionless parameters are introduced for convenience in presenting the results in a form usable in practice. The first is z/H , relating to the location of the point at which consolidation is considered, H being the maximum length of the drainage path. The second is the consolidation ratio, U_z , to indicate the extent of dissipation of the hydrostatic excess pressure in relation to the initial value:

$$U_z = \frac{u_i - u}{u_i} = \left[1 - \frac{u}{u_i} \right] \text{-----} \quad \text{Eq.1.29}$$

The subscript z is significant, since the extent of dissipation of excess pore water pressure is different for different locations, except at the beginning and the end of the consolidation process.

The third dimensionless parameter, relating to time, and called ‘Time-factor’, T , is defined as follows:

$$T = \frac{c_v t}{H^2} \text{-----} \quad \text{Eq.1.30}$$

where c_v is the coefficient of consolidation,

H is the length drainage path, and t is the elapsed time from the start of consolidation process.

In the context of consolidation process at a particular site, c_v and H are constants, and the time factor is directly proportional to time. Introducing the time factor we have

$$u = \sum_{m=0}^{\infty} \frac{2u_i}{M} \left[\sin \frac{M_z}{H} \right] e^{-M^2 T} \text{-----} \quad \text{Eq.1.31}$$

Introducing the consolidation ratio, U_z , we have:

$$U_z = 1 - \frac{u}{u_i} = 1 - \sum_{m=0}^{\infty} \frac{2}{M} \left[\sin \frac{M_z}{H} \right] e^{-M^2 T} \text{-----} \quad \text{Eq.1.32}$$

The following approximate expressions have been found to yield values for T with good degree of precision:

$$\text{When } U < 60\%, T = (\pi/4)U^2 \text{-----} \quad \text{Eq.1.33}$$

$$\text{When } U > 60\%, T = -0.9332 \log_{10} (1 - U) - 0.0851 \quad \text{Eq.1.34}$$

1.8 THREE-DIMENSIONAL CONSOLIDATION OF SOIL

Terzaghi’s theory of consolidation assumes that the expulsion of pore water during consolidation takes place in vertical direction alone. This is generally true for most of the cases, where the pervious layers, which form the drainage faces, are horizontal, located above and /or below the compressible soil layer. In some special cases, where vertical sand drains or sand wicks are installed to accelerate the consolidation of a natural or man-made fill, the compressible soil layer is surrounded by vertical drainage face, facilitating the pore water flow in horizontal direction from the stressed zone of compressible soil.

In such cases, where horizontal flow of pore water takes place, Terzaghi’s 1D theory of consolidation grossly underestimates the rate of consolidation. This is because the time required for dissipation of pore water pressure reduces because of additional flow in horizontal (lateral) direction and it is also because the permeability of soils in horizontal direction is several times (up to 25 times or more) more than that in vertical direction. For such cases, it is necessary to consider the flow in all directions to estimate the rate of consolidation

1.9 THREE-DIMENSIONAL CONSOLIDATION EQUATION IN CARTESIAN COORDINATES

Consider the flow that is taking place through a small soil element of dimensions dx , dy , and dz in x , y , and z coordinate directions, respectively, as shown in Fig. 1.8. Let v_x be the velocity of pore water entering the soil element in X-direction, v_y be the velocity of pore water entering the soil element in Y-direction, and v_z be the velocity of pore water entering the soil element in Z-direction.

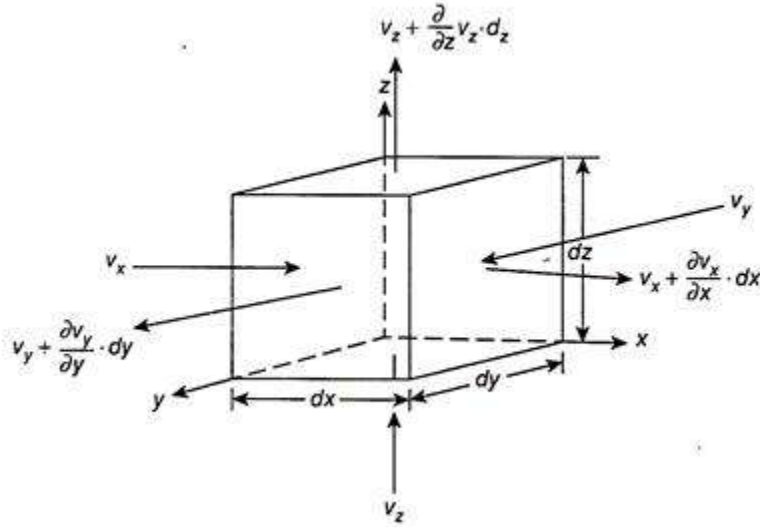


Fig.1.8: Flow through soil mass during 3D consolidation

Then the velocity of pore water leaving the soil element can be expressed as

in X-direction = $v_x + (\partial v_x / \partial x) \times dx$

in Y-direction = $v_y + (\partial v_y / \partial y) \times dy$

in Z-direction = $v_z + (\partial v_z / \partial z) \times dz$

We know that the rate of flow (i.e., volume per unit time) of pore water is given by $q = v \times A$, where v is the velocity of flow and A is the area of flow. Hence, the total volume of water entering the soil element per unit time is

$$q_i = v_x \times dy \times dz + v_y \times dz \times dx + v_z \times dx \times dy \text{-----} \quad \text{Eq.1.35}$$

Volume of the water leaving the soil element per unit time is given as

$$q_o = \left[v_x + \left(\frac{\partial v_x}{\partial x} \times dx \right) \right] \times dy \times dz + \left[v_y + \left(\frac{\partial v_y}{\partial y} \times dy \right) \right] \times dz \times dx + \left[v_z + \left(\frac{\partial v_z}{\partial z} \times dz \right) \right] \times dx \times dy \text{-----} \quad \text{Eq.1.36}$$

Volume of pore water squeezed (expelled) out of the element per unit time is expressed as

$$\Delta q = q_o - q_i = \left[\left\{ v_x + \left(\frac{\partial v_x}{\partial x} \times dx \right) \right\} \times dy \times dz + \left\{ v_y + \left(\frac{\partial v_y}{\partial y} \times dy \right) \right\} \times dz \times dx + \left\{ v_z + \left(\frac{\partial v_z}{\partial z} \times dz \right) \right\} \times dx \times dy \right] \text{--} \quad \text{Eq.1.37}$$

$$\Delta q = \frac{\partial v_x}{\partial x} \times dx \times dy \times dz + \frac{\partial v_y}{\partial y} \times dx \times dy \times dz + \frac{\partial v_z}{\partial z} \times dx \times dy \times dz \text{-----} \quad \text{Eq.1.38}$$

$$\text{Or } \Delta q = \left[\frac{\partial v_x}{\partial x} + \frac{\partial v_y}{\partial y} + \frac{\partial v_z}{\partial z} \right] \times V_1 \text{-----} \quad \text{Eq.1.39}$$

where V_1 the initial volume = $dx \times dy \times dz$. From Eq. (11.22), we have

$$\frac{\partial v_z}{\partial z} = \frac{\partial}{\partial z} \left[k \times \frac{1}{\gamma_w} \left(\frac{\partial u}{\partial z} \right) \right] \text{-----} \quad \text{Eq.1.40}$$

Since the permeability of soil is not identical in x-, y-, and z-directions, we can write

$$\frac{\partial v_z}{\partial z} = \frac{\partial}{\partial z} \left[k_z \times \frac{1}{\gamma_w} \left(\frac{\partial u}{\partial z} \right) \right] \text{-----} \quad \text{Eq.1.41}$$

where k_z is the permeability of soil in z-direction. Similarly we can obtain

$$\frac{\partial v_x}{\partial x} = \frac{\partial}{\partial x} \left[k_x \times \frac{1}{\gamma_w} \left(\frac{\partial u}{\partial x} \right) \right] \text{-----} \quad \text{Eq.1.42}$$

$$\frac{\partial v_y}{\partial y} = \frac{\partial}{\partial y} \left[k_y \times \frac{1}{\gamma_w} \left(\frac{\partial u}{\partial y} \right) \right] \text{-----} \quad \text{Eq.1.43}$$

where k_x and k_y are the permeability of soil in x-direction and y-direction respectively.

Substituting the value of $\frac{\partial v_x}{\partial x}$, $\frac{\partial v_y}{\partial y}$, and $\frac{\partial v_z}{\partial z}$ in Eq. (1.39), we have

$$\Delta q = \left[\frac{\partial}{\partial x} \left\{ k_x \times \frac{1}{\gamma_w} \left(\frac{\partial u}{\partial x} \right) \right\} + \frac{\partial}{\partial y} \left\{ k_y \times \frac{1}{\gamma_w} \left(\frac{\partial u}{\partial y} \right) \right\} + \frac{\partial}{\partial z} \left\{ k_z \times \frac{1}{\gamma_w} \left(\frac{\partial u}{\partial z} \right) \right\} \right] \times V_1 \text{-----} \quad \text{Eq.1.44}$$

Assuming the soil to be homogeneous, density of water (γ_w) is uniform in all directions, while permeability (k) is uniform in the respective coordinate direction, then the above equation can be expressed as

$$\Delta q = \frac{1}{\gamma_w} \left[\left\{ k_x \times \left(\frac{\partial^2 u}{\partial x^2} \right) \right\} + \left\{ k_y \times \left(\frac{\partial^2 u}{\partial y^2} \right) \right\} + \left\{ k_z \times \left(\frac{\partial^2 u}{\partial z^2} \right) \right\} \right] \times V_1 \text{-----} \quad \text{Eq.1.45}$$

From the definition of coefficient of volume compressibility, we have

$$m_v = -\Delta V / V_1 \times \frac{1}{\Delta \sigma'} \text{-----} \quad \text{Eq.1.46}$$

Change in the volume of soil is

$$\Delta V = -m_v \times V_1 \times \Delta \sigma' \text{-----} \quad \text{Eq.1.47}$$

Change in the volume per unit time is given as

$$\partial/\partial t (\Delta V) = \partial/\partial t (-m_v \times V_1 \times \Delta \sigma') \text{-----} \quad \text{Eq.1.48}$$

Assuming that (a) the coefficient of volume compressibility (m_v) remains constant with time and (b) the change in the volume of soil due to consolidation is negligible, we have

$$\frac{\partial}{\partial t} (\Delta V) = -m_v \times V_1 \times \frac{\partial}{\partial t} (\Delta \sigma') \text{-----} \quad \text{Eq.1.49}$$

From Terzaghi's effective stress principle, we have $\Delta \sigma = \Delta \sigma' + u$. Differentiating both sides with respect to time, we have

$$\frac{\partial}{\partial t} \Delta \sigma = \frac{\partial}{\partial t} \Delta \sigma' + \frac{\partial u}{\partial t} \text{-----} \quad \text{Eq.1.50}$$

As the total stress, $\Delta \sigma$, is constant with time during the consolidation, so

$$(\partial/\partial t) \Delta \sigma = 0 \text{-----} \quad \text{Eq.1.51}$$

we have, $\frac{\partial}{\partial t} \Delta \sigma = 0$ or $\frac{\partial}{\partial t} \Delta \sigma' + \frac{\partial u}{\partial t} = 0$

$$\text{Hence } \frac{\partial}{\partial t} (\Delta \sigma') = -\frac{\partial u}{\partial t}$$

Substituting this value in Eq. (1.49), we have

$$\frac{\partial}{\partial t} (\Delta V) = -m_v \times V_1 \times \left(-\frac{\partial u}{\partial t} \right) = m_v \times V_1 \times \frac{\partial u}{\partial t} \text{-----} \quad \text{Eq.1.52}$$

As the change in the volume of soil is only due to expulsion of pore water, we get

$$(\partial/\partial t) (\Delta V) = \Delta q$$

Hence, equating Eqs. (1.52) and (1.45), we have

$$m_v \times V_1 \times \frac{\partial u}{\partial t} = \frac{1}{\gamma_w} \left[\left\{ k_x \times \left(\frac{\partial^2 u}{\partial x^2} \right) \right\} + \left\{ k_y \times \left(\frac{\partial^2 u}{\partial y^2} \right) \right\} + \left\{ k_z \times \left(\frac{\partial^2 u}{\partial z^2} \right) \right\} \right] \times V_1 \text{-----} \quad \text{Eq.1.53}$$

$$\text{Or } \frac{\partial u}{\partial t} = \frac{1}{\gamma_w \times m_v} \left[\left\{ k_x \times \left(\frac{\partial^2 u}{\partial x^2} \right) \right\} + \left\{ k_y \times \left(\frac{\partial^2 u}{\partial y^2} \right) \right\} + \left\{ k_z \times \left(\frac{\partial^2 u}{\partial z^2} \right) \right\} \right] \times V_1 \text{-----} \quad \text{Eq.1.54}$$

$$\frac{\partial u}{\partial t} = \left[\left\{ C_{vx} \times \left(\frac{\partial^2 u}{\partial x^2} \right) \right\} + \left\{ C_{vy} \times \left(\frac{\partial^2 u}{\partial y^2} \right) \right\} + \left\{ C_{vz} \times \left(\frac{\partial^2 u}{\partial z^2} \right) \right\} \right] \text{-----} \quad \text{Eq.1.55}$$

Here C_{vx} , C_{vy} , and C_{vz} are coefficient of consolidation in x-, y-, and z-directions, respectively.

1.10 SUMMARIZING THE ASSUMPTIONS MADE IN THE DERIVATION OF TERZAGHI'S CONSOLIDATION EQUATION, WE HAVE THE FOLLOWING

- i. The soil is homogeneous and fully saturated.
- ii. Soil particles and pore water are incompressible.
- iii. The flow of water during expulsion of pore water occurs only in vertical direction, that is, consolidation is one dimensional
- iv. The change in the volume of soil due to consolidation is negligible compared to the initial volume of soil.
- v. Flow is laminar and Darcy's law is valid.
- vi. Permeability is the same throughout the thickness of the compressible soil layer.
- vii. The coefficient of volume compressibility (m_v) remains constant with time.
- viii. Compression takes place only due to expulsion of pore water, that is, the effect of secondary consolidation is neglected.

1.11 THREE-DIMENSIONAL CONSOLIDATION EQUATION IN POLAR COORDINATES

For most practical cases, the 3D consolidation is identical about the x- and y-axes. Hence, it is more convenient to express the consolidation equation in polar coordinates consisting of only the radial and vertical axes. The 3D consolidation in Cartesian coordinates can be transformed into polar coordinates as follows

$$x = r \cos \theta, y = r \sin \theta, z = z$$

Hence

$$r^2 = x^2 + y^2 \dots \quad \text{Eq.1.56}$$

$$\text{and } y/x = \sin\theta/\cos\theta = \tan\theta \text{ -----} \quad \text{Eq.1.57}$$

Differentiating Eq. 1.56 partially with respect to x we get

$$2r \times \partial r / \partial x = 2x \times \partial x / \partial x \text{-----} \quad \text{Eq.1.57}$$

$$\text{Or } \frac{\partial r}{\partial x} = \frac{x}{r} = \cos\theta \text{-----} \quad \text{Eq.1.58}$$

Similarly,

$$\partial r / \partial y = y/r = \sin\theta \text{-----} \quad \text{Eq.1.59}$$

Differentiating Eq. (1.65) partially with respect to x we get –

$$\partial \theta / \partial x = y/r^2 = \sin\theta/r \text{-----} \quad \text{Eq.1.60}$$

Similarly,

$$\partial \theta / \partial y = x/r^2 = \cos\theta/r \text{-----} \quad \text{Eq.1.61}$$

The excess hydrostatic pressure (u) is a function of r and θ

$$u = f_1(r) \times f_2(\theta) \text{-----} \quad \text{Eq.1.62}$$

$$\frac{\partial u}{\partial x} = \frac{\partial u}{\partial r} \times \frac{\partial r}{\partial x} + \frac{\partial u}{\partial \theta} \times \frac{\partial \theta}{\partial x} \text{-----} \quad \text{Eq.1.63}$$

$$\text{Hence } \frac{\partial u}{\partial x} = \frac{\partial u}{\partial r} \times \cos\theta - \frac{\partial u}{\partial \theta} \times \frac{\sin\theta}{r} \text{-----} \quad \text{Eq.1.64}$$

$$\text{and } \frac{\partial u}{\partial y} = \frac{\partial u}{\partial r} \times \frac{\partial r}{\partial y} + \frac{\partial u}{\partial \theta} \times \frac{\partial \theta}{\partial y} \text{-----} \quad \text{Eq.1.65}$$

Differentiating Eqs. (1.64) and (1.66) again, adding and simplifying, we have

$$\frac{\partial^2 u}{\partial x^2} + \frac{\partial^2 u}{\partial y^2} = \frac{\partial^2 u}{\partial r^2} + \frac{1}{r} \times \frac{\partial u}{\partial r} + \frac{1}{r^2} \times \frac{\partial^2 u}{\partial^2 \theta} \text{-----} \quad \text{Eq.1.66}$$

For the case of radial symmetry, excess pore pressure (u) is independent of θ . Hence

$$\frac{\partial u}{\partial \theta} = 0 \text{-----} \quad \text{Eq.1.67}$$

Therefore, Eq. (1.66) becomes

$$\frac{\partial^2 u}{\partial x^2} + \frac{\partial^2 u}{\partial y^2} = \frac{\partial^2 u}{\partial r^2} + \frac{1}{r} \times \frac{\partial u}{\partial r} \text{-----} \quad \text{Eq.1.68}$$

Rewriting Eq. (1.55), we get

$$\frac{\partial u}{\partial t} = \left[\left\{ C_{vx} \times \left(\frac{\partial^2 u}{\partial x^2} \right) + C_{vy} \times \left(\frac{\partial^2 u}{\partial y^2} \right) + C_{vz} \times \left(\frac{\partial^2 u}{\partial z^2} \right) \right\} \right]$$

For radial symmetry,

$$C_{vx} = C_{vy} = C_{vr} \text{ and } x = y = r$$

Substituting these values in Eq. (1.55), we obtain

$$\frac{\partial u}{\partial t} = C_{vr} \left[\frac{\partial^2 u}{\partial x^2} + \frac{\partial^2 u}{\partial y^2} \right] + C_{vz} \times \left(\frac{\partial^2 u}{\partial z^2} \right) \text{-----} \quad \text{Eq.1.69}$$

Substituting Eq. (1.68) in Eq. (1.69), we get

$$\frac{\partial u}{\partial t} = C_{vr} \left[\frac{\partial^2 u}{\partial r^2} + \frac{1}{r} \frac{\partial u}{\partial r} \right] + C_{vz} \times \left(\frac{\partial^2 u}{\partial z^2} \right) \text{-----} \quad \text{Eq.1.70}$$

1.12 SOLUTION OF 3D CONSOLIDATION EQUATION

Typical solution for 3D consolidation problem can be obtained by considering the expulsion of pore water in vertical and radial directions separately. Thus, Eq. (1.70) consists of two parts as follows –

Vertical flow –

$$\frac{\partial u}{\partial t} = C_{vz} \times \left(\frac{\partial^2 u}{\partial z^2} \right) \text{-----} \quad \text{Eq.1.71}$$

The solution of Eq. (1.71) is given by Terzaghi using Eq. (1.34), which is reproduced below

$$T_z = \frac{C_{vz} \times t}{d^2} \text{-----} \quad \text{Eq.1.72}$$

where T_z is the time factor for vertical flow and C_{vz} the coefficient of consolidation for vertical flow.

Radial flow

$$\frac{\partial u}{\partial t} = C_{vr} \left[\frac{\partial^2 u}{\partial r^2} + \frac{1}{r} \frac{\partial u}{\partial r} \right] \text{-----} \quad \text{Eq.1.73}$$

The solution of Eq. (1.73) was obtained by Rendulic (1935) using an equation similar to that in the vertical flow –

$$U_r = f \times (T_r) \text{-----} \quad \text{Eq.1.74}$$

where U_r is the degree of consolidation in radial direction and T_r the time factor for the radial flow of pore water which is given as

$$T_r = \frac{C_{vr}}{2r} \times t \text{-----} \quad \text{Eq.1.75}$$

Where, C_{vr} is the coefficient of consolidation in radial (horizontal) direction and $2r$ the effective diameter of a soil cylinder from which pore water flows into the sand drain.

1.13 THE SOLUTION OF RADIAL FLOW PROBLEM WAS OBTAINED FOR THE FOLLOWING TWO TYPES OF VERTICAL STRAINS

i. Free Vertical Strain Case:

In this case, it is assumed that the consolidation settlements at the surface do not change the distribution of load to the soil. Solutions for this case were obtained by Glover (1930) and Rendulic (1935), assuming that pore water pressure is uniform at a radial distance equal to $2r$, which is the effective diameter of the soil cylinder as defined in Eq. (1.75).

ii. Equal Vertical Strain Case:

In this case, the redistribution of surface loads due to arching is considered. As the expulsion of pore water occurs faster near the surface of the sand drains, consolidation (settlement) at any time is more near the surface of sand drain than elsewhere. This would redistribute the stress that is known as arching. In extreme limit, the arching action in soil would redistribute the stresses to such an extent that the consolidation settlement at the surface is the same at all points.

Barron (1948) developed solution for equal vertical strain case, given by the following equations

$$U_r = 1 - e^{-\alpha} \text{-----} \quad \text{Eq.1.76}$$

$$\text{Here } \alpha = \frac{-8T_r}{f(n)} \text{-----} \quad \text{Eq.1.77}$$

$$\text{And } f(n) = \frac{n^2}{n^2-1} \log_e n - \frac{3n^2-1}{4n^2}, n = \frac{r}{r_w}$$

where r_w is the radius of sand drains.

It was observed that for values of $n > 10$, free vertical strain, and equal vertical strain case give more or less same results. As the free vertical strain case requires more time for evaluation, equal vertical strain case is commonly used for solving radial consolidation problems.

Equations (1.76) and (1.77) are combined to form Eq. (1.78) to solve the 3D consolidation problems of sand drains

$$(1 - U) = (1 - U_z)(1 - U_r) \text{-----} \quad \text{Eq.1.78}$$

$$(1 - U) = (1 - U_z)(1 - U_r) \dots (1.78)$$

where U is the degree of consolidation for 3D flow, U_z the degree of consolidation for vertical flow, and U_r the degree of consolidation for radial flow.

1.14 LABORATORY CONSOLIDATION TESTS

The one-dimensional consolidation testing procedure was first suggested by Terzaghi. This test is performed in a consolidometer (sometimes referred to as an *oedometer*). The schematic diagram of a consolidometer is shown in Figure 1.9(a). Figure 1.9(b) shows a photograph of a consolidometer. The soil specimen is placed inside a metal ring with two porous stones, one at the top of the specimen and another at the bottom. The specimens are usually 64 mm in diameter and 25 mm thick. The load on the specimen is applied through a lever arm, and compression is measured by a micrometer dial gauge. The specimen is kept under water during the test. Each

load usually is kept for 24 hours. After that, the load usually is doubled, which doubles the pressure on the specimen, and the compression measurement is continued. At the end of the test, the dry weight of the test specimen is determined. Figure 1.9(c) shows a consolidation test in progress. The general shape of the plot of deformation of the specimen against time for a given load increment is shown in Figure 1.10. From the plot, we can observe three distinct stages, which may be described as follows:

Stage I: Initial compression, which is caused mostly by preloading

Stage II: Primary consolidation, during which excess pore water pressure gradually is transferred into effective stress because of the expulsion of pore water

Stage III: Secondary consolidation, which occurs after complete dissipation of the excess pore water pressure, when some deformation of the specimen takes place because of the plastic readjustment of soil fabric

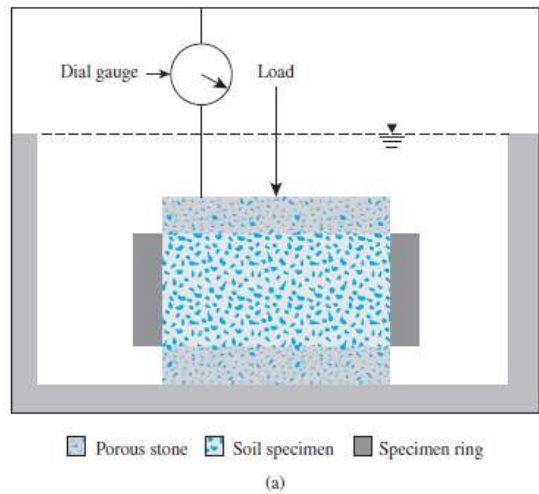


Fig. 1.9 (a): Schematic diagram of a consolidometer

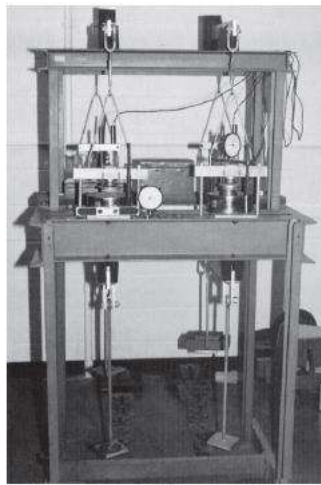
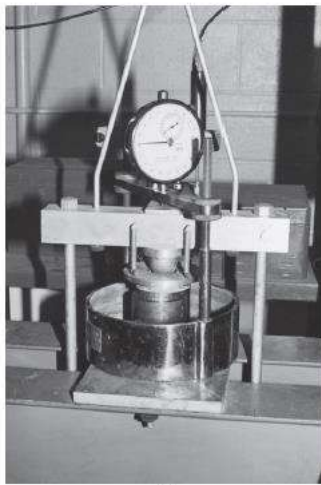


Fig. 1.9 (b): Photograph of a consolidometer

(c): Consolidation test in progress.

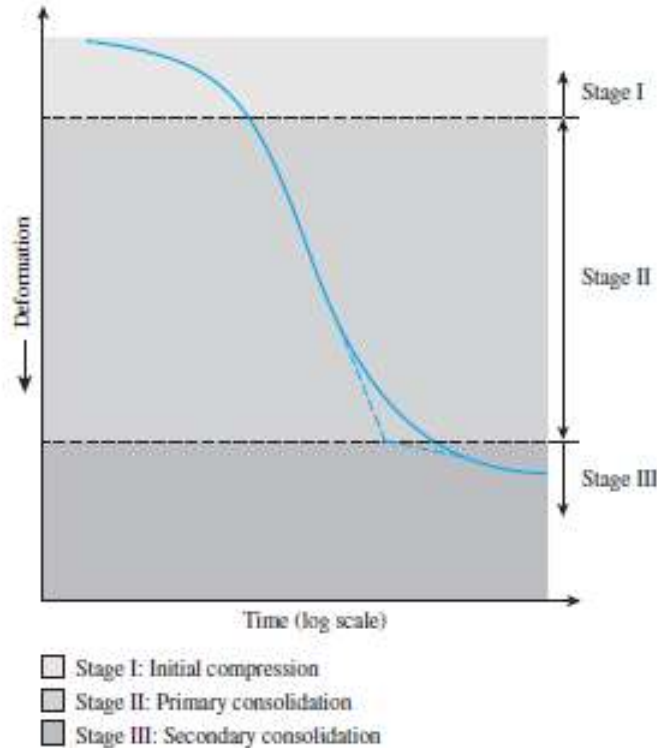


Fig. 1.10: Deformation shape of the specimen

1.15 VOID RATIO–PRESSURE PLOTS

After the time–deformation plots for various loadings are obtained in the laboratory, it is necessary to study the change in the void ratio of the specimen with pressure. Following is a step-by-step procedure for doing so:

Step 1: Calculate the height of solids, H_s , in the soil specimen (Fig.1.11) using the equation

$$H_s = \frac{W_s}{AG_s\gamma_w} = \frac{M_s}{AG_s\rho_w} \text{-----} \quad \text{Eq.1.79}$$

where W_s =dry weight of the specimen

M_s = Dry mass of the specimen

A = Area of the specimen

G_s = Specific gravity of soil solids

γ_w = Unit weight of water

ρ_w =Density of water

Step 2: Calculate the initial height of voids as

$$H_v = H - H_s \text{-----} \quad \text{Eq.1.80}$$

where H_v = initial height of the specimen.

Step 3: Calculate the initial void ratio, of the specimen, using the equation

$$e_0 = \frac{V_v}{V_s} = \frac{H_v A}{H_s A} = \frac{H_v}{H_s} \text{-----} \quad \text{Eq.1.81}$$

Step 4: For the first incremental loading, s_1 (total load/unit area of specimen), which causes a deformation ΔH_1 , calculate the change in the void ratio as

for the stress range under consideration. k may be got from a permeability test conducted on the oedometer sample itself, after complete consolidation under the particular stress increment a_v and e_0 may be obtained from the oedometer test data, by plotting the $e - \sigma$ curve. However, consolidation equation is rarely used for the determination of c_v . Instead, c_v is evaluated from the consolidation test data by the use of characteristics of the theoretical relationship between the time factor T , and the degree of consolidation, U as shown in Fig.1.13. These methods are known as ‘fitting methods’, as one tries to fit in the characteristics of the theoretical curve with the experimental or laboratory curve.

The more generally used fitting methods are the following:

- (a) The square root of time fitting method
- (b) The logarithm of time fitting method

These two methods will be presented in the following sub-sections.

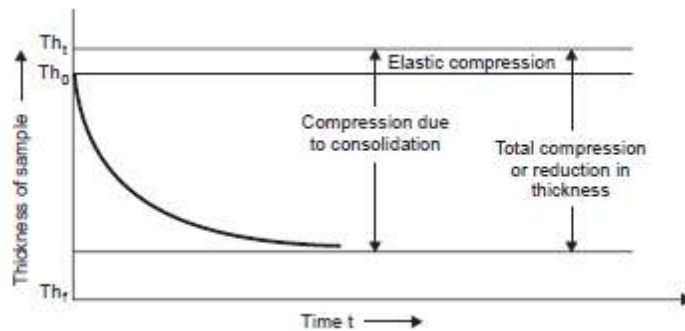


Fig. 1.13: Time versus reduction in sample thickness for a load-increment

1.16.1 The Square Root of Time Fitting Method

This method has been devised by D.W. Taylor (1948). The coefficient of consolidation is the soil property that controls the time-rate or speed of consolidation under a load-increment. The relation between the sample thickness and elapsed time since the application of the loading increment is obtainable from an oedometer test and is somewhat as shown in Fig. 1.13 for a typical load-increment. This figure depicts change in sample thickness with time essentially due to consolidation only the elastic compression which occurs almost instantaneously on application of load increment is shown. The effect of prolonged compression that occurs after 100% dissipation of excess pore pressure is not shown or is ignored; this effect is known as ‘Secondary consolidation which is briefly presented in the following section. The curves of Figs. 1.14 and the theoretical curves bear striking similarity; in fact, one should expect it if Terzaghi’s theory is to be valid for the phenomenon of consolidation. This similarity becomes more apparent if the curves are plotted with square root of time/time factor as the function, as shown in Fig. 1.14 (a) and (b). The theoretical curve on the square root plot is a straight line up to about 60% consolidation with a gentle concave upward curve thereafter. If another straight line, shown dotted, is drawn such that the abscissae of this line are 1.15 times those of the straight line portion of the theoretical curve, it can be shown to cut the theoretical curve at 90% consolidation. This may be established from the values of T at various values of U given in Fig. 7.24 for case I;

that is, the value of T at 90% consolidation is 1.15 times the abscissa of an extension of the straight line portion of the U versus T relation. This property is used for ‘fitting’ the theoretical curve to the laboratory curve.

The laboratory curve shows a sudden initial compression, called ‘elastic compression’ which may be partly due to compression of gas in the pores. The corrected zero point at zero time is obtained by extending the straight line portion of the laboratory plot backward to meet the axis showing the sample thickness/dial gauge reading. The so-called ‘primary compression’ or ‘primary consolidation’ is reckoned from this corrected zero. A dashed line is constructed from the corrected zero such that its abscissa is 1.15 times those of the straight line portion of the laboratory plot. The intersection of the dashed line with the laboratory plot identifies the point representing 90% consolidation in the sample. The time corresponding to this can be read off from the laboratory plot. The point corresponding to 100% primary consolidation may be easily extrapolated on this plot.

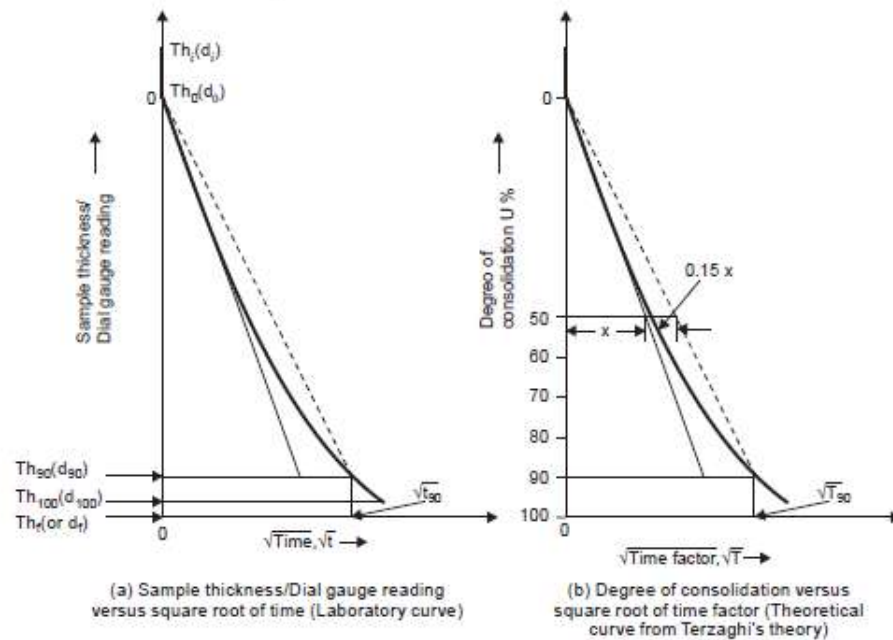


Fig. 1.14: Square root of time fitting method (After Taylor, 1948)

The coefficient of consolidation, c_v , may be obtained from

$$c_v = \frac{T_{90}H^2}{t_{90}} \text{-----} \quad \text{Eq.1.85}$$

Where, t_{90} is read off from Fig. 1.14(a)

T_{90} is 0.848 from Terzaghi's theory

H is the drainage path, which may be taken as half the thickness of the sample for double drainage conditions.

1.16.2 The Logarithm of Time Fitting Method

This method was devised by A. Casagrande and R.E. Fadum (1939). The point corresponding to 100 per cent consolidation curve is plotted on a semi-logarithmic scale, with time factor on a

logarithmic scale and degree of consolidation on arithmetic scale, the intersection of the tangent and asymptote is at the ordinate of 100% consolidation. A comparison of the theoretical and laboratory plots in this regard is shown in Figs. 1.15(a) and (b).

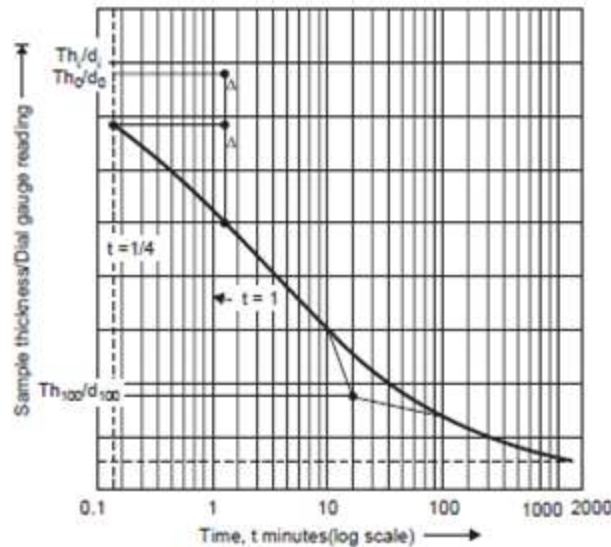


Fig. 1.15(a): Sample thickness/Dial gauge reading versus logarithm of time (Laboratory curve)

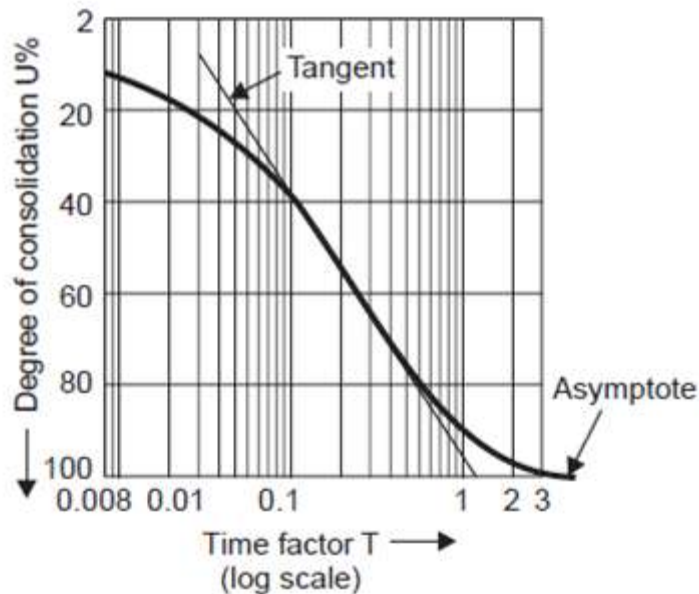


Fig. 1.15 (b): Logarithm of time fitting method (After A. Casagrande, 1939)

Since the early portion of the curve is known to approximate a parabola, the corrected zero point may be located as follows: The difference in ordinates between two points with times in the ratio of 4 to 1 is marked off; then a distance equal to this difference may be stepped off above the upper points to obtain the corrected zero point. This point may be checked by more trials, with

different pairs of points on the curve. After the zero and 100% primary compression points are located, the point corresponding to 50% consolidation and its time may easily be obtained and the coefficient of consolidation computed from:

$$c_v = \frac{T_{50}H^2}{t_{50}} \text{-----} \quad \text{Eq.1.86}$$

where t_{50} is read off from Fig. 1.15(a)

$T_{50} = 0.197$ from Terzaghi's theory, and H is the drainage path as stated in the previous subsection.

1.17 SECONDARY CONSOLIDATION

The time-settlement curve for a cohesive soil has three distinct parts as illustrated in Fig. 1.16. When the hydrostatic excess pressure is fully dissipated, no more consolidation should be expected. However, in practice, the decrease in void ratio continues, though very slowly, for a long time after this stage, called 'Primary Consolidation'. The effect or the phenomenon of continued consolidation after the complete dissipation of excess pore water pressure is termed 'Secondary Consolidation' and the resulting compression is called 'Secondary Compression'. During this stage, plastic readjustment of clay platelets takes place and other effects as well as colloidal-chemical processes and surface phenomena such as induced electro kinetic potentials occur. These are, by their very nature, very slow.

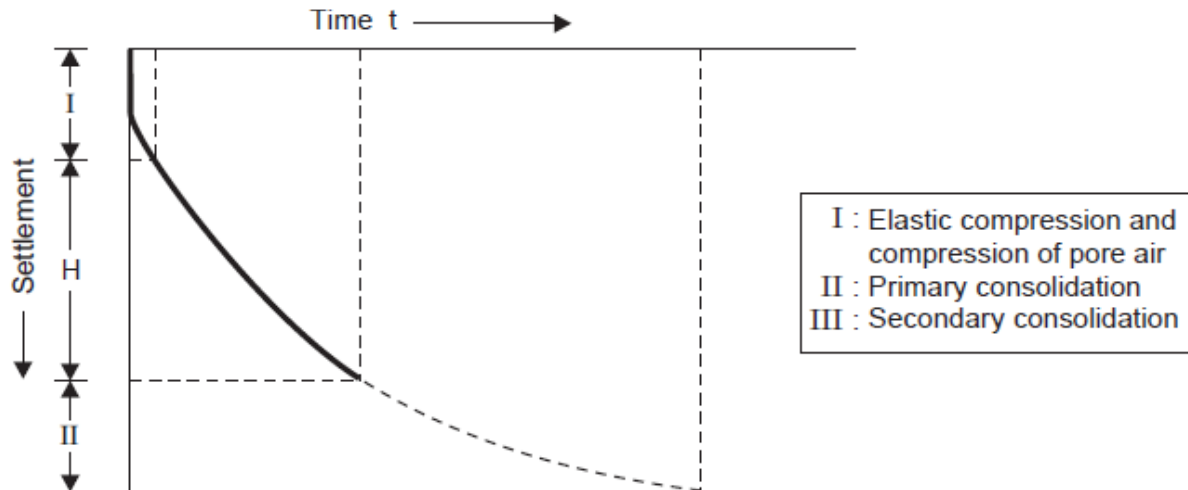


Fig.1.16: Time settlement curve for cohesive soil

Secondary consolidation is believed to come into play even in the range of primary consolidation, although its magnitude is small, because of the existence of a plastic lag right from the beginning of loading. However, it is almost impossible to separate this component from the primary compression. Since dissipation of excess pore pressure is not the criterion here, Terzaghi's theory is inapplicable to secondary consolidation. The fact that experimental time compression curves are in agreement with Terzaghi's theoretical curve only up to about 60%

consolidation is, in itself, an indication of the manifestation of secondary consolidation even during the stage of primary consolidation.

Secondary consolidation of mineral soils is usually negligible but it may be considerable in the case of organic soils due to their colloidal nature. This may constitute a substantial part of total compression in the case of organic soils, micaceous soils, loosely deposited clays, etc. A possible disintegration of clay particles is also mentioned as one of the reasons for this phenomenon. Secondary compression is usually assumed to be proportional to the logarithm of time. Hence, the secondary compression can be identified on a plot of void ratio versus logarithm of time (Fig. 1.17).

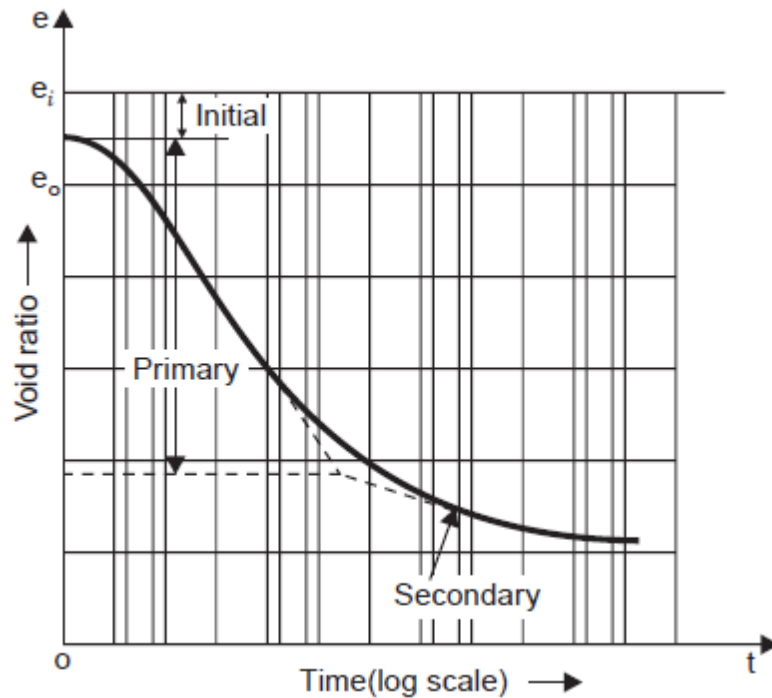


Fig.1.17: Voids ratio versus logarithmic of time

Secondary compression appears as a straight line sloping downward or, in some cases, as a straight line followed by a second straight line with a flatter slope. The void ratio, e_f , at the end of primary consolidation can be found from the intersection of the backward extension of the secondary line with a tangent drawn to the curve of primary compression, as shown in the figure. The rate of secondary compression depends upon the increment of stress and the characteristics of the soil.

The equation for the rate of secondary compression may be approximated as follows:

$$\Delta e = -a \log_{10} \left(\frac{t_2}{t_1} \right) \text{-----} \quad \text{Eq.1.87}$$

Here, t_1 is the time required for the primary compression to be virtually complete, t_2 any later time, and Δe is the corresponding change in void ratio. This means that the secondary

compression which occurs during the hydrodynamic phase is ignored, but the error is not probably serious. α is a coefficient expressing the rate of secondary compression.

Another way of expressing the time–rate of secondary compression is through the ‘coefficient of secondary compression’, C_α , in terms of strain or percentage of settlement as follows:

$$\Delta e = -C_\alpha \log_{10} \left(\frac{t_2}{t_1} \right) \text{-----} \quad \text{Eq.1.88}$$

In other words, C_α may be taken to be the slope of the straight line representing the secondary compression on a plot of strain versus logarithm of time.

The relation between α and C_α is

$$C_\alpha = \frac{\alpha}{1+e} \text{-----} \quad \text{Eq.1.89}$$

Generally α and C_α increase with increasing stress

Some common values of C_α are given below

Table.1: Values of C_α for different soils

Sl. No	Nature of Soil	C_α Value
1	Over consolidated days	0.0005 to 0.0015
2	Normally consolidated days	0.005 to 0.030
3	Organic soils, peats	0.04 to 0.10

1.18 CONSOLIDATION IN A LAYERED SOIL

1.18.1 Numerical solution for one-dimensional consolidation

i) Finite difference solution

In this section, we will consider the finite difference solution for one dimensional consolidation, starting from the basic differential equation of Terzaghi’s consolidation theory:

$$\frac{\partial u}{\partial t} = c_v \frac{\partial^2 u}{\partial z^2} \text{-----} \quad \text{Eq.1.90}$$

Let u_R , t_R , and z_R be any arbitrary reference excess pore water pressure, time, and distance, respectively. From these, we can define the following non-dimensional terms:

$$\text{Non dimensional excess pore water} = \bar{u} = \frac{u}{u_R} \text{-----} \quad \text{Eq.1.91}$$

$$\text{Non dimensional depth, } \bar{z} = \frac{z}{z_R} \text{-----} \quad \text{Eq.1.92}$$

$$\text{Non dimensional time, } \bar{t} = \frac{t}{t_R} \text{-----} \quad \text{Eq.1.93}$$

Now from the above equations, we get

$$\frac{\partial u}{\partial t} = \frac{u_R}{t_R} \frac{\partial \bar{u}}{\partial \bar{t}} \text{-----} \quad \text{Eq.1.94}$$

Again

$$c_v \frac{\partial^2 u}{\partial z^2} = c_v \frac{u_R}{z_R^2} \frac{\partial^2 \bar{u}}{\partial \bar{z}^2} \text{-----} \quad \text{Eq.1.95}$$

$$\text{Hence, } \frac{u_R}{t_R} \frac{\partial \bar{u}}{\partial \bar{t}} = c_v \frac{u_R}{z_R^2} \frac{\partial^2 \bar{u}}{\partial \bar{z}^2} \text{-----} \quad \text{Eq.1.96}$$

Or

$$\frac{1}{t_R} \frac{\partial \bar{u}}{\partial \bar{t}} = \frac{c_v}{z_R^2} \frac{\partial^2 \bar{u}}{\partial \bar{z}^2} \text{-----} \quad \text{Eq.1.97}$$

If we adopt the reference time in such a way that, $t_R = \frac{z_R^2}{c_v}$, then the above differential Eq. will be of the form

$$\frac{\partial \bar{u}}{\partial \bar{t}} = \frac{\partial^2 \bar{u}}{\partial \bar{z}^2} \text{-----} \quad \text{Eq.1.98}$$

The left-hand side of the Eq can be written as

$$\frac{\partial \bar{u}}{\partial \bar{t}} = \frac{1}{\Delta \bar{t}} [\bar{u}_{0,\bar{t}+\Delta \bar{t}} - \bar{u}_{0,\bar{t}}] \text{-----} \quad \text{Eq.1.99}$$

Where, $\bar{u}_{0,\bar{t}}$ and $\bar{u}_{0,\bar{t}+\Delta \bar{t}}$ are the non-dimensional pore water pressures at point 0 (Fig. 1.18 a) at non-dimensional times t and $t + \Delta t$. Again, similarly

$$\frac{\partial^2 \bar{u}}{\partial \bar{z}^2} = \frac{1}{(\Delta \bar{z})^2} [\bar{u}_{1,\bar{t}} + \bar{u}_{3,\bar{t}} - 2\bar{u}_{0,\bar{t}}] \text{-----} \quad \text{Eq.1.100}$$

Equating both left and right hand sides, we get

$$\frac{1}{\Delta \bar{t}} [\bar{u}_{0,\bar{t}+\Delta \bar{t}} - \bar{u}_{0,\bar{t}}] = \frac{1}{(\Delta \bar{z})^2} [\bar{u}_{1,\bar{t}} + \bar{u}_{3,\bar{t}} - 2\bar{u}_{0,\bar{t}}] \text{-----} \quad \text{Eq.1.101}$$

Or

$$[\bar{u}_{0,\bar{t}+\Delta \bar{t}}] = \frac{\Delta \bar{t}}{(\Delta \bar{z})^2} [\bar{u}_{1,\bar{t}} + \bar{u}_{3,\bar{t}} - 2\bar{u}_{0,\bar{t}}] + \bar{u}_{0,\bar{t}} \text{-----} \quad \text{Eq.1.102}$$

To converge the above equation, $\Delta \bar{t}$ and $\Delta \bar{z}$ must be chosen such that $\frac{\Delta \bar{t}}{(\Delta \bar{z})^2}$ be less than 0.5

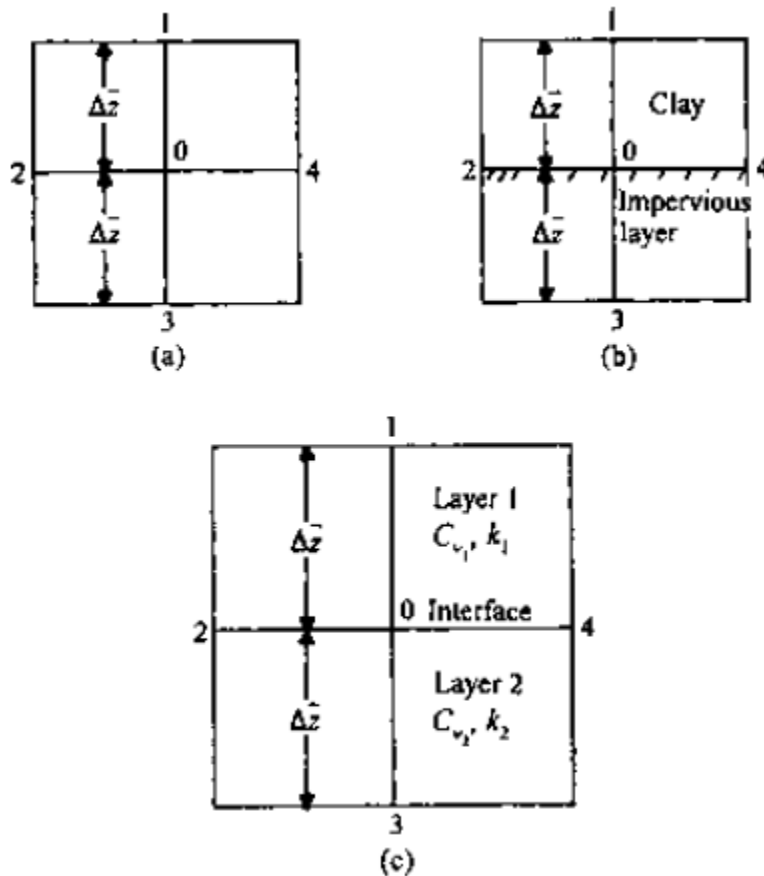


Fig. 1.18: Numerical solution of consolidation

It is not always possible to develop a closed-form solution for consolidation in layered soils. There are several variables involved, such as different coefficients of permeability, the thickness of layers, and different values of coefficient of consolidation. Fig.1.19 shows the nature of the degree of consolidation of a two-layered soil.

In view of the above, numerical solutions provide a better approach. If we are involved with the calculation of excess pore water pressure at the interface of two different types (i.e., different values of C_v) of clayey soils, the general equation will have to be modified to some extent. as follows (Scott, 1963) that

$$\frac{k}{c_v} \frac{\partial u}{\partial t} = k \frac{\partial^2 u}{\partial z^2} \text{-----} \quad \text{Eq.1.103}$$

Now based on permeability of layered soil concept we get

$$k \frac{\partial^2 u}{\partial z^2} = \frac{1}{2} \left[\frac{k_1}{(\Delta z)^2} + \frac{k_2}{(\Delta z)^2} \right] \left(\frac{2k_1}{k_1+k_2} u_{1,t} + \frac{2k_2}{k_1+k_2} u_{3,t} - 2u_{0,t} \right) \text{-----} \quad \text{Eq.1.104}$$

where k_1 and k_2 are the coefficients of permeability in layers 1 and 2, respectively, and $u_{0,t}$, $u_{1,t}$ and $u_{3,t}$ are the excess pore water pressures at time t for points 0, 1, and 3, respectively

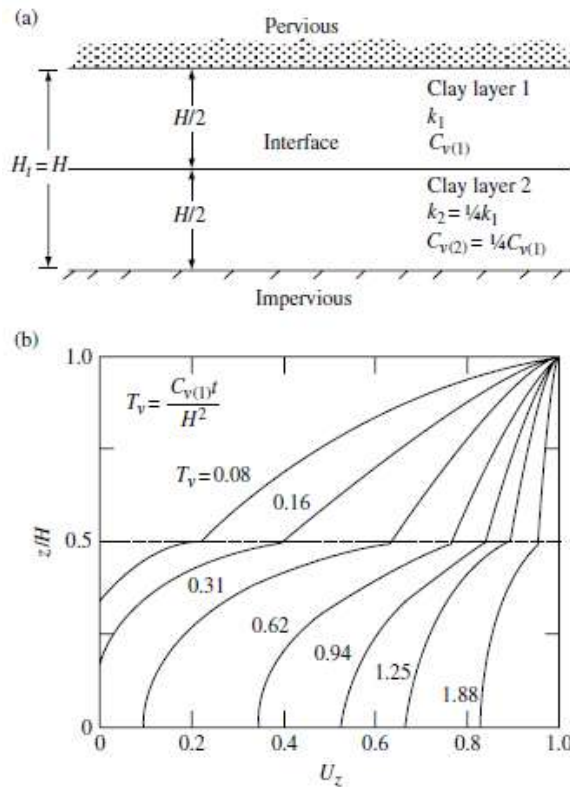


Fig.1.19: Degree of consolidation in two-layered soil [Part (b) after Luscher, 1965]

Also, the average volume change for the element at the boundary is

$$\frac{k}{c_v} \frac{\partial u}{\partial t} = \frac{1}{2} \left(\frac{k_1}{c_{v1}} + \frac{k_2}{c_{v2}} \right) \frac{1}{\Delta t} (u_{0,t+\Delta t} - u_{0,t}) \text{-----} \quad \text{Eq.1.105}$$

where $u_{0,t}$ and $u_{0,t+\Delta t}$ are the excess pore water pressures at point 0 at times t and $t+\Delta t$, respectively. Now equating the right-hand sides of Eqs.1.104 and 1.105, we obtain

$$\left(\frac{k_1}{c_{v1}} + \frac{k_2}{c_{v2}}\right) \frac{1}{\Delta t} (u_{0,t+\Delta t} - u_{0,t}) = \frac{1}{(\Delta z)^2} (k_1 + k_2) \left(\frac{2k_1}{k_1+k_2} u_{1,t} + \frac{2k_2}{k_1+k_2} u_{3,t} - 2u_{0,t}\right) \text{----- Eq.1.106}$$

Or

$$u_{0,t+\Delta t} = \frac{\Delta t}{(\Delta z)^2} \frac{k_1+k_2}{\frac{k_1}{c_{v1}} + \frac{k_2}{c_{v2}}} \times \left(\frac{2k_1}{k_1+k_2} u_{1,t} + \frac{2k_2}{k_1+k_2} u_{3,t} - 2u_{0,t}\right) + 2u_{0,t} \text{----- Eq.1.107}$$

Or

$$u_{0,t+\Delta t} = \frac{\Delta t c_{v1}}{(\Delta z)^2} \frac{1+\frac{k_2}{k_1}}{1+\frac{k_2}{k_1}(c_{v1}/c_{v2})} \times \left(\frac{2k_1}{k_1+k_2} u_{1,t} + \frac{2k_2}{k_1+k_2} u_{3,t} - 2u_{0,t}\right) + 2u_{0,t} \text{----- Eq.1.108}$$

Assuming $\frac{1}{t_R} = \frac{c_{v1}}{z_R^2}$ and introducing

$$\text{Non dimensional excess pore water} = \bar{u} = \frac{u}{u_R} \text{----- Eq.1.109}$$

$$\text{Non dimensional depth, } \bar{z} = \frac{z}{z_R} \text{----- Eq.1.110}$$

From (109)-(110) and combining with Eq. 1.108 we get

$$\bar{u}_{0,t+\Delta t} = \frac{1+\frac{k_2}{k_1}}{1+\frac{k_2}{k_1}(c_{v1}/c_{v2})} \frac{\Delta \bar{t}}{(\Delta \bar{z})^2} \times \left(\frac{2k_1}{k_1+k_2} \bar{u}_{1,t} + \frac{2k_2}{k_1+k_2} \bar{u}_{3,t} - 2\bar{u}_{0,t}\right) + \bar{u}_{0,t} \text{----- Eq.1.111}$$

Example:

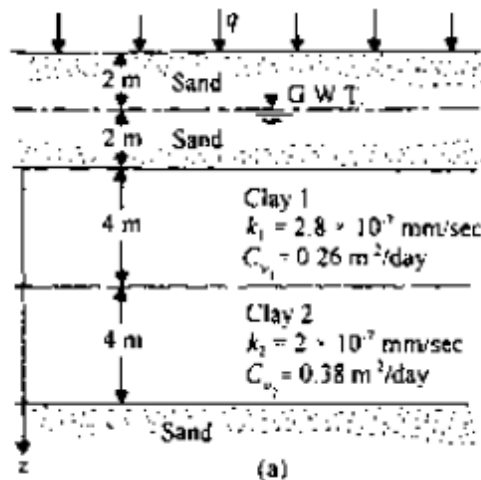
A uniform surcharge of $q = 150\text{kN/m}^2$ is applied at the ground surface of the soil profile shown in Figure 2 a. Using the numerical method, determine the distribution of excess pore water pressure for the clay layers after 10 days of load application

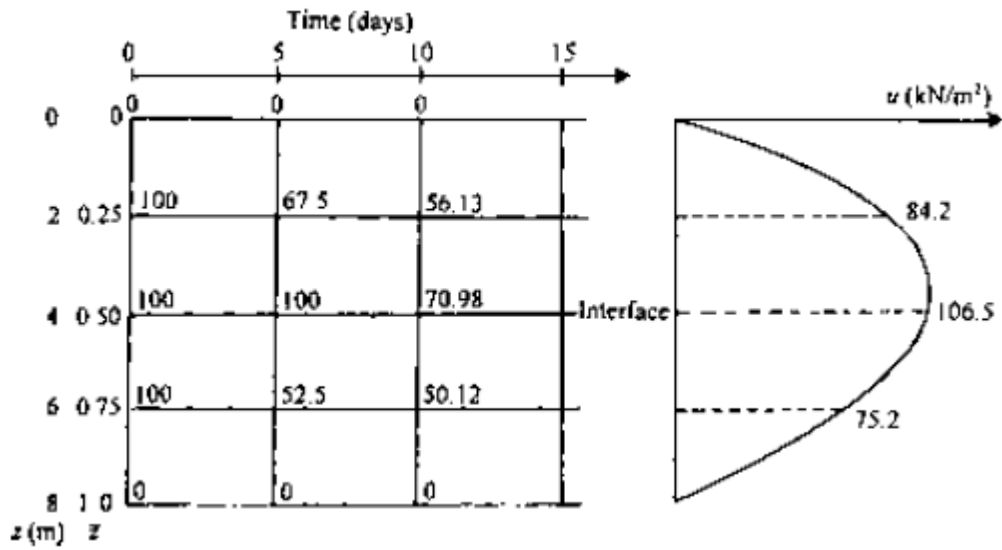
Solution

Since this is a uniform surcharge, the excess pore water pressure immediately after the load application will be 150kN/m^2 throughout the clay layers. However, owing to the drainage conditions, the excess pore water pressures at the top of layer 1 and bottom of layer 2 will immediately become zero. Now, let $z_R = 8\text{m}$ and $u_R = 1.5\text{kN/m}^2$.

So $\bar{z} = \frac{z}{z_R} = 1$ and $\bar{u} = \frac{u}{u_R} = 150\text{kN/m}^2 / 1.5\text{kN/m}^2 = 100$.

Figure below shows the distribution of \bar{u} at time $t = 0$; note that $\Delta \bar{z} = 2/8 = 0.25$.





Now, $t_R = \frac{z_R^2}{c_v}$ again $\bar{t} = \frac{t}{t_R}$

Hence, $\Delta \bar{t} = \frac{\Delta \bar{t}}{t_R}$, since t_R is constant

So, $\Delta \bar{t} = \frac{\Delta \bar{t}}{z_R^2} c_v$

Let $\Delta t = 5$ days for both layers. So, for layer 1,

$$\Delta \bar{t} = \frac{\Delta \bar{t}}{z_R^2} c_v = 0.0203 \quad \frac{\Delta \bar{t}_{(1)}}{(\Delta \bar{z})^2} = \frac{0.0203}{0.25^2} = 0.325 (< 0.5)$$

For layer 2,

$$\Delta \bar{t}_{(2)} = \frac{C_{v2} \Delta t}{z_R^2} = \frac{0.3}{1}$$

For $t = 5$ days,

At $\bar{z} = 0$,

$$\bar{u}_{0, \bar{z} + \Delta \bar{z}} = 0$$

At $\bar{z} = 0.25$,

$$\begin{aligned} \bar{u}_{0, \bar{z} + \Delta \bar{z}} &= \frac{\Delta \bar{t}_{(1)}}{(\Delta \bar{z})^2} (\bar{u}_{1, \bar{z}} + \bar{u}_{3, \bar{z}} - 2\bar{u}_{0, \bar{z}}) + \bar{u}_{0, \bar{z}} \\ &= 0.325 [0 + 100 - 2(100)] + 100 = 67.5 \end{aligned}$$

$$\begin{aligned}
\bar{u}_{0,\bar{z}+\Delta\bar{z}} &= \frac{1+k_2/k_1}{1+(k_2/k_1)(C_{v1}/C_{v2})} \frac{\Delta\bar{t}_{(1)}}{(\Delta\bar{z})^2} \\
&\quad \times \left(\frac{2k_1}{k_1+k_2} \bar{u}_{1,\bar{z}} + \frac{2k_2}{k_1+k_2} \bar{u}_{3,\bar{z}} - 2\bar{u}_{0,\bar{z}} \right) + \bar{u}_{0,\bar{z}} \\
&= \frac{1+\frac{2}{2.8}}{1+(2 \times 0.26)/(2.8 \times 0.38)} (0.325) \\
&\quad \times \left[\frac{2 \times 2.8}{2+2.8} (100) + \frac{2 \times 2}{2+2.8} (100) - 2(100) \right] + 100
\end{aligned}$$

or

$$\bar{u}_{0,\bar{z}+\Delta\bar{z}} = (1.152)(0.325)(116.67 + 83.33 - 200) + 100 = 100$$

At $\bar{z} = 0.75$,

$$\begin{aligned}
\bar{u}_{0,\bar{z}+\Delta\bar{z}} &= \frac{\Delta\bar{t}_{(2)}}{(\Delta\bar{z})^2} (\bar{u}_{1,\bar{z}} + \bar{u}_{3,\bar{z}} - 2\bar{u}_{0,\bar{z}}) + \bar{u}_{0,\bar{z}} \\
&= 0.475[100 + 0 - 2(100)] + 100 = 52.5
\end{aligned}$$

At $\bar{z} = 1.0$,

$$\bar{u}_{0,\bar{z}+\Delta\bar{z}} = 0$$

For $t = 10$ days,

At $\bar{z} = 0$,

$$\bar{u}_{0,\bar{z}+\Delta\bar{z}} = 0$$

At $\bar{z} = 0.25$,

$$\bar{u}_{0,\bar{z}+\Delta\bar{z}} = 0.325[0 + 100 - 2(67.5)] + 67.5 = 56.13$$

At $\bar{z} = 0.5$,

$$\begin{aligned}
\bar{u}_{0,\bar{z}+\Delta\bar{z}} &= (1.152)(0.325) \left[\frac{2 \times 2.8}{2+2.8} (67.5) + \frac{2 \times 2}{2+2.8} (52.5) - 2(100) \right] + 100 \\
&= (1.152)(0.325)(78.75 + 43.75 - 200) + 100 = 70.98
\end{aligned}$$

At $\bar{z} = 0.75$,

$$\bar{u}_{0,\bar{z}+\Delta\bar{z}} = 0.475[100 + 0 - 2(52.5)] + 52.5 = 50.12$$

At $\bar{z} = 1.0$,

$$\bar{u}_{0,\bar{z}+\Delta\bar{z}} = 0$$

1.19 CONSOLIDATION UNDER TIME-DEPENDENT LOADING

Olson (1977) presented a mathematical solution for one-dimensional consolidation due to a single ramp load. Olson's solution can be explained with the help of Fig.1.20, in which a clay layer is drained at the top and at the bottom (H is the drainage distance). A uniformly distributed load q is applied at the ground surface. Note that q is a function of time, as shown in Fig.1.20b. The expression for the excess pore water pressure for the case where $u_i = u_0$ is given in Eq. 1.112 as

$$u = \sum_{m=0}^{\infty} \frac{2u_0}{M} \sin \frac{Mz}{H} \times \exp(-M^2 T_v) \text{-----} \quad \text{Eq.1.112}$$

$$\text{Where } T_v = \frac{C_v t}{H^2}$$

As stated above, the applied load is a function of time:

$$q = f(t_a) \text{-----} \quad \text{Eq.1.113}$$

where t_a is the time of application of any load.

For a differential load dq applied at time, t_a , the instantaneous pore pressure increase will be found as $du_i = dq$. At time t the remaining excess pore water pressure du at a depth z can be given by the expression

$$du = \sum_{m=0}^{\infty} \frac{2dq}{M} \sin \frac{Mz}{H} \exp \left[\frac{-M^2 C_v (t-t_a)}{H^2} \right] \text{-----} \quad \text{Eq.1.114}$$

$$= \sum_{m=0}^{\infty} \frac{2dq}{M} \sin \frac{Mz}{H} \exp \left[\frac{-M^2 C_v (t-t_a)}{H^2} \right] \text{-----} \quad \text{Eq.1.115}$$

The average degree of consolidation can be defined as

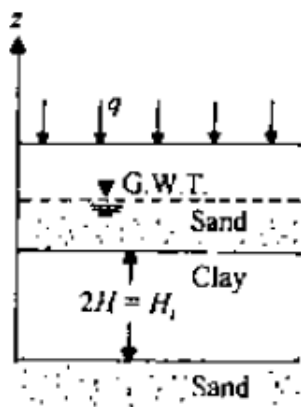
$$u_{av} = \frac{\alpha q_c \frac{1}{Ht} \int_0^H u dz}{q_c} = \frac{\text{settlement at time } t}{\text{settlement at time } t=\infty} \text{-----} \quad \text{Eq.1.116}$$

where, q_c is the total load per unit area applied at the time of the analysis.

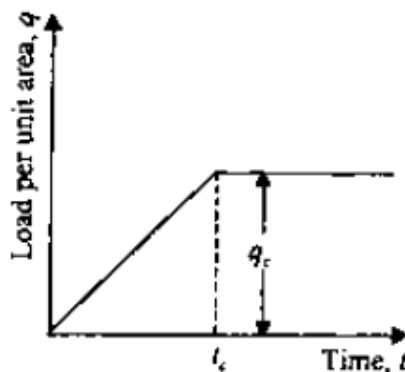
T_a is the time of application of any loading

The settlement at time $t = \infty$ is, of course, the ultimate settlement.

Note that the term q_c in the denominator of Eq. 1.113 is equal to the instantaneous excess pore water pressure $u_i = q_c$ that might have been generated throughout the clay layer had the stress q_c been applied instantaneously.



(a)



(b)

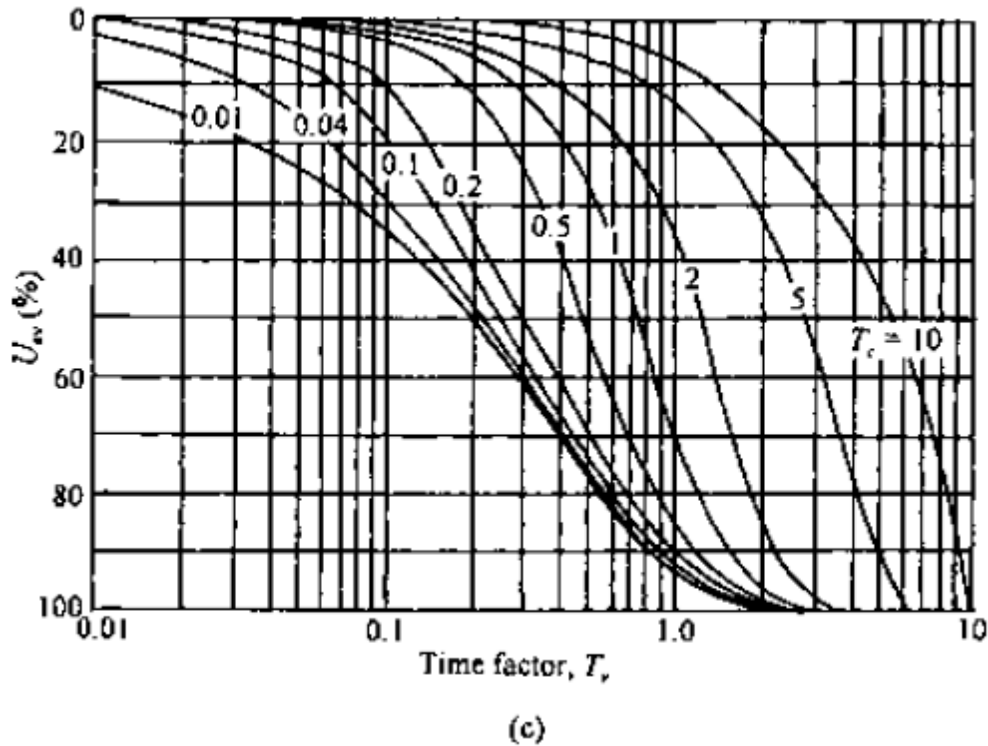


Fig.1.20: One-dimensional consolidation due to single ramp load (after Olson, 1977)

Proper integration of Eqs. 1.115 and 116 gives the following:

For $T_v \leq T_c$

$$u = \int_{m=0}^{m=\infty} \frac{2q_c}{M^3 T_c} \sin \frac{Mz}{H} [1 - \exp(-M^2 T_v)] \dots \dots \dots \text{Eq.1.117}$$

And

$$U_{avg} = \frac{T_v}{T_c} \left\{ 1 - \frac{2}{T_v} \sum_{m=0}^{m=\infty} \frac{1}{M^4} [1 - \exp(-M^2 T_v)] \right\} \dots \dots \dots \text{Eq.1.118}$$

For $T_v \geq T_c$

$$u = \int_{m=0}^{m=\infty} \frac{2q_c}{M^3 T_c} [\exp(M^2 T_v) - 1] \sin \frac{Mz}{H} \exp(-M^2 T_v) \dots \dots \dots \text{Eq.1.119}$$

And

$$U_{avg} = 1 - \frac{2}{T_c} \sum_{m=0}^{m=\infty} \frac{1}{M^4} [\exp(M^2 T_v) - 1] \exp(-M^2 T_v) \dots \dots \dots \text{Eq.1.120}$$

Where $T_c = \frac{c_v t_c}{H^2} \dots \dots \dots \text{Eq.1.121}$

Figure 1.20 c shows the plot of U_{avg} against T_v for various values of T_c .

Example:

Based on one-dimensional consolidation test results on a clay, the coefficient of consolidation for a given pressure range was obtained as $8 \times 10^{-3} \text{ mm}^2/\text{s}$. In the field there is a 2-m-thick layer of the same clay with two-way drainage. Based on the assumption that a uniform surcharge of 70 kN/m^2 was to be applied instantaneously, the total consolidation settlement was estimated to

be 150 mm. However, during the construction, the loading was gradual; the resulting surcharge can be approximated as

$$q \text{ (kN/m}^2\text{)} = \frac{70}{60}t \text{ (days)}$$

for $t \leq 60$ days and

$$q = 70 \text{ kN/m}^2$$

for $t \geq 60$ days. Estimate the settlement at $t = 30$ and 120 days.

SOLUTION

$$T_c = \frac{C_v t_c}{H^2}$$

Now, $t_c = 60$ days $= 60 \times 24 \times 60 \times 60$ s; also, $H_t = 2$ m $= 2H$ (two-way drainage), and so $H = 1$ m $= 1000$ mm. Hence,

$$T_c = \frac{(8 \times 10^{-3})(60 \times 24 \times 60 \times 60)}{(1000)^2} = 0.0414$$

At $t = 30$ days,

$$T_v = \frac{C_v t}{H^2} = \frac{(8 \times 10^{-3})(30 \times 24 \times 60 \times 60)}{(1000)^2} = 0.0207$$

From Figure 1c, for $T_v = 0.0207$ and $T_c = 0.0414$, $U_{av} \approx 5\%$. So,

$$\text{Settlement} = (0.05)(150) = 7.5 \text{ mm}$$

At $t = 120$ days,

$$T_v = \frac{(8 \times 10^{-3})(120 \times 24 \times 60 \times 60)}{(1000)^2} = 0.083$$

From Figure 1c for $T_v = 0.083$ and $T_c = 0.0414$, $U_{av} \approx 27\%$. So,

$$\text{Settlement} = (0.27)(150) = 40.5 \text{ mm}$$

2.0 SHEAR STRENGTH OF SOILS

2.1 Introduction

Shearing Strength' of a soil is perhaps the most important of its engineering properties. This is because all stability analyses in the field of geotechnical engineering, whether they relate to foundation, slopes of cuts or earth dams, involve a basic knowledge of this engineering property of the soil. 'Shearing strength' or merely 'Shear strength' may be defined as the resistance to shearing stresses and a consequent tendency for shear deformation.

Shearing strength of a soil is the most difficult to comprehend in view of the multitude of factors known to affect it. A lot of maturity and skill may be required on the part of the engineer in interpreting the results of the laboratory tests for application to the conditions in the field.

Basically speaking, a soil derives its shearing strength from the following:

- (1) Resistance due to the interlocking of particles.
- (2) Frictional resistance between the individual soil grains, which may be sliding friction, rolling friction, or both.
- (3) Adhesion between soil particles or 'cohesion'.

Granular soils of sands may derive their shear strength from the first two sources, while cohesive soils or clays may derive their shear strength from the second and third sources.

Highly plastic clays, however, may exhibit the third source alone for their shearing strength.

Most natural soil deposits are partly cohesive and partly granular and as such, may fall into the second of the three categories just mentioned, from the point of view of shearing strength. The shear strength of a soil cannot be tabulated in codes of practice since a soil can significantly exhibit different shear strengths under different field and engineering conditions.

2.2 INTERNAL FRICTION WITHIN GRANULAR SOIL MASSES

In granular or cohesionless soil masses, the resistance to sliding on any plane through the point within the mass is similar to that discussed in the previous sub-section; the friction angle in this case is called the 'angle of internal friction'. However, the frictional resistance in granular soil masses is rather more complex than that between solid bodies, since the nature of the resistance is partly sliding friction and partly rolling friction. Further, a phenomenon known as 'interlocking' is also supposed to contribute to the shearing resistance of such soil masses, as part of the frictional resistance.

The angle of internal friction, which is a limiting angle of obliquity and hence the primary criterion for slip or failure to occur on a certain plane, varies appreciably for given sand with the density index, since the degree of interlocking is known to be directly dependent upon the density. This angle also varies somewhat with the normal stress. However, the angle of internal friction is mostly considered constant, since it is almost so for a given sand at a given density.

Since failure or slip within a soil mass cannot be restricted to any specific plane, it is necessary to understand the relationships that exist between the stresses on different planes passing through a point, as a prerequisite for further consideration of shearing strength of soils.

2.3 PRINCIPAL PLANES AND PRINCIPAL STRESSES-MOHR'S CIRCLE

At a point in a stressed material, every plane will be subjected, in general, to a normal or direct stress and a shearing stress. In the field of geotechnical engineering, compressive direct stresses are usually considered positive, while tensile stresses are considered negative. A 'Principal plane' is defined as a plane on which the stress is wholly normal, or one which does not carry shearing stress. From mechanics, it is known that there exists three principal planes at any point in a stressed material. The normal stresses acting on these principal planes are known as the 'principal stresses'. The three principal planes are to be mutually perpendicular. In the order of decreasing magnitude the principal stresses are designated the 'major principal stress', the 'intermediate principal stress' and the 'minor principal stress', the corresponding principal planes being designated exactly in the same manner. It can be engineering by two-dimensional analysis, the intermediate principal stress being commonly ignored.

Let us consider an element of soil whose sides are chosen as the principal planes, the major and the minor, as shown in Fig.2.1. (a):

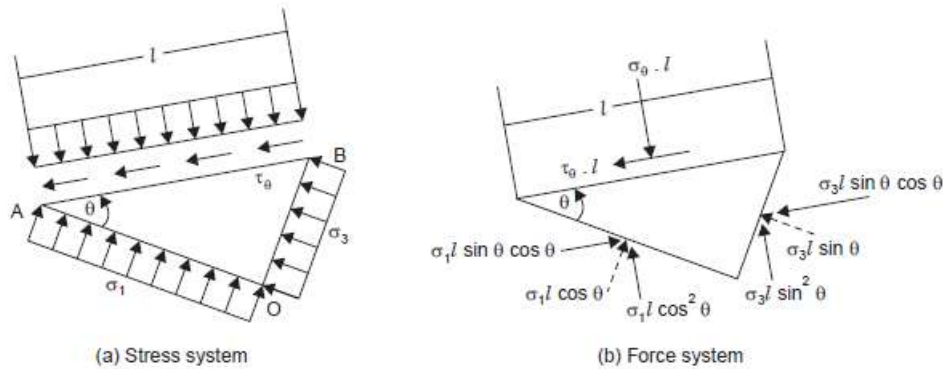


Fig.2.1: Stresses on a plane inclined to the principal planes

Let O be any point in the stressed medium and OA and OB be the major and minor principal planes, with the corresponding principal stresses σ_1 and σ_3 . The plane of the figure is the intermediate principal plane. Let it be required to determine the stress conditions on a plane normal to the figure, and inclined at an angle θ to the major principal plane, considered positive when measured counter-clockwise. If the stress conditions are uniform, the size of the element is immaterial. If the stresses are varying, the element must be infinitesimal in size, so that the variation of stress along a side needed to be considered.

Let us consider the element to be of unit thickness perpendicular to the plane of the figure, AB being l . The forces on the sides of the element are shown dotted and their components parallel and perpendicular to AB are shown by full lines. Considering the equilibrium of the element and resolving all forces in the directions parallel and perpendicular to AB , the following equations may be obtained:

$$\sigma_\theta = \sigma_1 \cos^2 \theta + \sigma_3 \sin^2 \theta = \sigma_3 (\sigma_1 - \sigma_3) \cos^2 \theta$$

$$\sigma_\theta = \frac{\sigma_1 + \sigma_3}{2} + \left(\frac{\sigma_1 - \sigma_3}{2} \right) \cos 2\theta \text{-----} \quad \text{Eq.2.1}$$

$$\tau_\theta = \frac{\sigma_1 - \sigma_3}{2} \sin 2\theta \text{-----} \quad \text{Eq.2.2}$$

Thus it may be noted that the normal and shearing stresses on any plane which is normal to the intermediate principal plane may be expressed in terms of σ_1 , σ_3 , and θ . Otto Mohr (1882) represented these results graphically in a circle diagram, which is called Mohr's circle. Normal stress is represented as abscissa and shear stress as ordinate. If the coordinates, σ_θ and τ_θ represented by Eqs.1 and 2 are plotted for all possible values of θ , the locus is a circle as shown in Fig.2. This circle has its centre on the axis and cuts it at values σ_3 and σ_1 . This circle is known as the Mohr's circle.

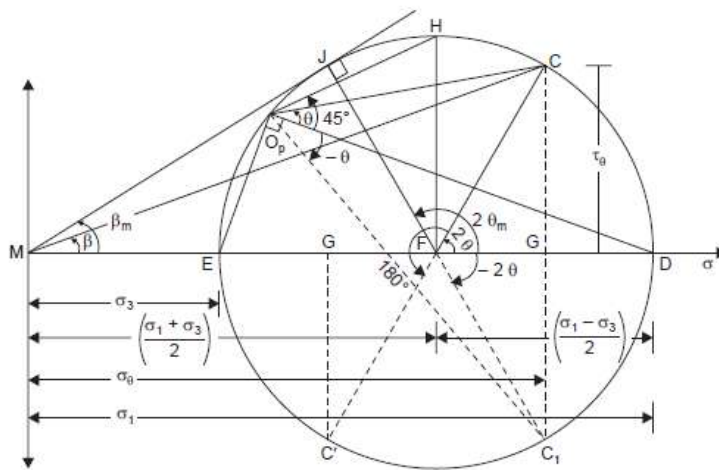


Fig.2.2: Mohr's circle for the stress conditions illustrated in Fig.2 1

The Mohr's circle diagram provides excellent means of visualisation of the orientation of different planes. Let a line be drawn parallel to the major principal plane through D , the coordinate of which is the major principal stress. The intersection of this line with the Mohr's circle, O_p is called the 'Origin of planes'. If a line parallel to the minor principal plane is drawn through E , the co-ordinate of which is the minor principal stress, it will also be observed to pass through O_p ; the angle between these two lines is a right angle from the properties of the circle. Likewise it can be shown that any line through O_p , parallel to any arbitrarily chosen plane, intersects the Mohr's circle at a point the co-ordinates of which represent the normal and shear stresses on that plane. Thus the stresses on the plane represented by AB in Fig.2.1 (a), may be obtained by drawing O_p parallel to AB , that is, at an angle θ with respect to O_pD , the major principal plane, and measuring off the co-ordinates of C , namely σ_θ and τ_θ .

Since angle $CO_pD = \theta$, angle $CFD = 2\theta$, from the properties of the circle. From the geometry of the figure, the co-ordinates of the point C , are established as follows:

$$\sigma_\theta = MG = MF + FG \text{-----} \quad \text{Eq.2.3}$$

$$\frac{\sigma_1 + \sigma_3}{2} + \left(\frac{\sigma_1 - \sigma_3}{2} \right) \cos 2\theta \text{-----} \quad \text{Eq.2.4}$$

And
$$\tau_{\theta} = CG = \frac{\sigma_1 - \sigma_3}{2} \sin 2\theta \text{-----} \quad \text{Eq.2.5}$$

These are the same as in Eqs.2.1 and 2.2, which prove our statement. In the special case where the major and minor principal planes are vertical and horizontal respectively, or vice-versa, the origin of planes will be *D* or *E*, as the case may be. In other words, it will lie on the σ -axis. A few important basic facts and relationships may be directly obtained from the Mohr's circle:

1. The only planes free from shear are the given sides of the element which are the principal planes. The stresses on these are the greatest and smallest normal stresses.
2. The maximum or principal shearing stress is equal to the radius of the Mohr's circle, and it occurs on planes inclined at 45° to the principal planes.

$$\tau_{max} = \frac{\sigma_1 - \sigma_3}{2} \text{-----} \quad \text{Eq.2.6}$$

3. The normal stresses on planes of maximum shear are equal to each other and is equal to half the sum of the principal stresses.

$$\sigma_c = (\sigma_1 + \sigma_3)/2 \text{-----} \quad \text{Eq.2.7}$$

4. Shearing stresses on planes at right angles to each other are numerically equal and are of an opposite sign. These are called conjugate shearing stresses.

5. The sum of the normal stresses on mutually perpendicular planes is a constant ($MG' + MG = 2MF = \sigma_1 + \sigma_3$). If we designate the normal stress on a plane perpendicular to the plane on which it is σ_{θ} as σ'_{θ}

$$\sigma_{\theta} + \sigma'_{\theta} = \sigma_1 + \sigma_3 \text{-----} \quad \text{Eq.2.8}$$

Of the two stresses σ_{θ} and σ'_{θ} the one which makes the smaller angle with σ_1 is the greater of the two.

6. The resultant stress, σ_r , on any plane is

$$\sigma_r = \sqrt{\sigma_{\theta}^2 + \tau_{\theta}^2} \text{-----} \quad \text{Eq.2.9}$$

and has an obliquity, β , which is equal to

$$\beta = \tan^{-1} \left(\frac{\tau_{\theta}}{\sigma_{\theta}} \right) \text{-----} \quad \text{Eq.2.10}$$

7. Stresses on conjugate planes, that is, planes which are equally inclined in different directions with respect to a principal plane are equal. (This is indicated by the co-ordinates of C and C1 in Fig. 2).

8. When the principal stresses are equal to each other, the radius of the Mohr's circle becomes zero, which means that shear stresses vanish on all planes. Such a point is called an isotropic point.

9. The maximum angle of obliquity, β_m , occurs on a plane inclined at

$$\theta_{cr} = \frac{45^\circ + \beta_m}{2} \text{-----} \quad \text{Eq.2.11}$$

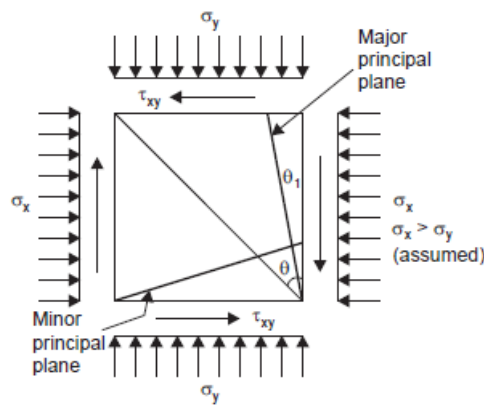
This may be obtained by drawing a line which passes through the origin and is tangential to the Mohr's circle. The co-ordinates of the point of tangency are the stresses on the plane of maximum obliquity; the shear stress on this plane is obviously less than the principal or maximum shear stress. On the plane of principal shear the obliquity is slightly smaller than β_m . It is the plane of maximum obliquity which is most liable to failure and not the plane of maximum

shear, since the criterion of slip is limiting obliquity. When β_m approaches and equals the angle of internal friction, ϕ , of the soil, failure will become incipient. Mohr's circle affords an easy means of obtaining all important relationships. The following are a few such relationships

$$\sin\beta_m = \left(\frac{\sigma_1 - \sigma_3}{\sigma_1 + \sigma_3}\right) \text{-----} \quad \text{Eq.2.12}$$

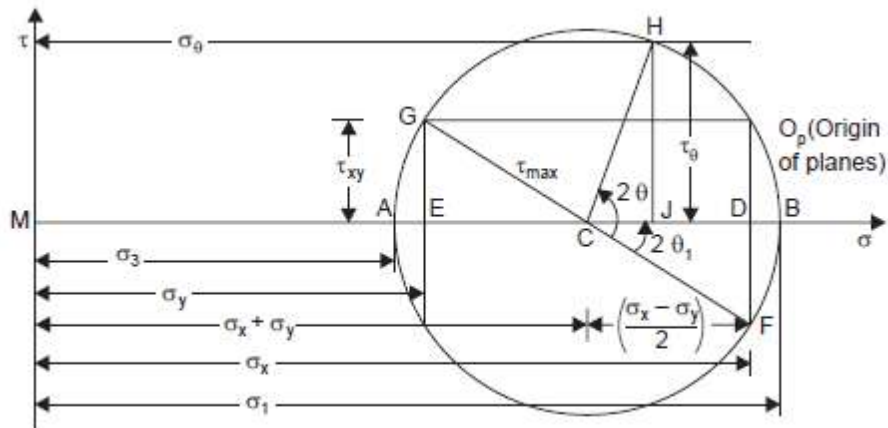
$$\frac{\sigma_1}{\sigma_3} = \left(\frac{1 + \sin\beta_m}{1 - \sin\beta_m}\right) \text{-----} \quad \text{Eq.2.13}$$

In case the normal and shearing stresses on two mutually perpendicular planes are known, the principal planes and principal stresses may be determined with the aid of the Mohr's circle diagram, as shown in Fig.2 3(a). The shearing stresses on two mutually perpendicular planes are equal in magnitude by the principle of complementary shear.



(a) General two-dimensional stress system

(a) General two-dimensional stress system



(b) Mohr's circle for general two-dimensional stress system

(b) Mohr's circle for general two-dimensional stress system

Fig.2 3: Determination of principal planes and principal stresses from Mohr's circle

Figure 2.3 (a) shows an element subjected to a general two-dimensional stress system, normal stresses σ_x and σ_y on mutually perpendicular planes and shear stresses τ_{xy} on these planes, as

indicated. Fig. 2.3 (b) shows the corresponding Mohr's circle, the construction of which is obvious.

From a consideration of the equilibrium of a portion of the element, the normal and shearing stress components, σ_θ and τ_θ , respectively, on a plane inclined at an angle θ , measured counter-clockwise with respect to the plane on which σ_x acts, may be obtained as follows:

$$\sigma_\theta = \frac{\sigma_x + \sigma_y}{2} + \left(\frac{\sigma_x - \sigma_y}{2}\right) \cos 2\theta + \tau_{xy} \sin 2\theta \text{-----} \quad \text{Eq.2.14}$$

$$\tau_\theta = \frac{\sigma_x - \sigma_y}{2} \sin 2\theta - \tau_{xy} \cos \theta \text{-----} \quad \text{Eq.2.15}$$

Squaring and adding these Eqs, we obtain

$$\left[\sigma_\theta - \frac{\sigma_x + \sigma_y}{2}\right]^2 + \tau_\theta^2 = \left(\frac{\sigma_x - \sigma_y}{2}\right)^2 + \tau_{xy}^2 \text{-----} \quad \text{Eq.2.16}$$

This represents a circle with centre $\frac{\sigma_x + \sigma_y}{2}, 0$ and radius $\sqrt{\left(\frac{\sigma_x - \sigma_y}{2}\right)^2 + \tau_{xy}^2}$

Once the Mohr's circle is constructed, the principal stresses σ_1 and σ_3 , and the orientation of the principal planes may be obtained from the diagram. The shearing stress is to be plotted upward or downward according as it is positive or negative. It is common to take a shear stress which tends to rotate the element counter-clockwise, positive.

It may be noted that the same Mohr's circle and hence the same principal stresses are obtained, irrespective of how the shear stresses are plotted. (The centre of the Mohr's circle, C , is the mid-point of DE , with the co-ordinates and 0; the radius of the circle is CG , the co-ordinates of G being σ_y and τ_{xy}).

The following relationships are also easily obtained

$$\sigma_1 = \frac{\sigma_x + \sigma_y}{2} + \frac{1}{2} \sqrt{(\sigma_x - \sigma_y)^2 + 4\tau_{xy}^2} \text{-----} \quad \text{Eq.2.17}$$

$$\sigma_3 = \frac{\sigma_x + \sigma_y}{2} - \frac{1}{2} \sqrt{(\sigma_x - \sigma_y)^2 + 4\tau_{xy}^2} \text{-----} \quad \text{Eq.2.18}$$

$$\tan 2\theta_{1.3} = \frac{2\tau_{xy}}{\sigma_x - \sigma_y} \text{-----} \quad \text{Eq.2.19}$$

$$\tau_{max} = \frac{1}{2} \sqrt{\left(\frac{\sigma_x - \sigma_y}{2}\right)^2 + 4\tau_{xy}^2} \text{-----} \quad \text{Eq.2.20}$$

Invariably, the vertical stress will be the major principal stress and the horizontal one the minor principal stress in geotechnical engineering situations.

2.4 MOHR'S STRENGTH THEORY

We have seen that the shearing stress may be expressed as $\tau = \sigma \tan \beta$ on any plane, where β is the angle of obliquity. If the obliquity angle is the maximum or has limiting value ϕ , the shearing stress is also at its limiting value and it is called the shearing strength, s . For a cohesionless soil the shearing strength may be expressed as:

$$s = \sigma \tan \phi \dots \quad \text{Eq.2.21}$$

If the angle of internal friction ϕ is assumed to be a constant, the shearing strength may be represented by a pair of straight lines at inclinations of $+\phi$ and $-\phi$ with the σ -axis and passing through the origin of the Mohr's circle diagram. A line of this type is called a Mohr envelope.

The Mohr envelopes for a cohesionless soil, as shown in Fig. 2.4, are the straight lines OA and OA' .

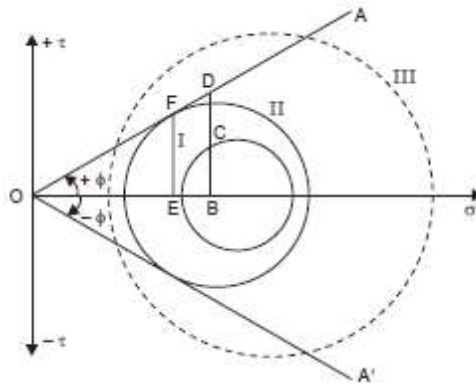


Fig.2.4: Mohr's strength theory—Mohr envelopes for cohesionless soil

If the stress conditions at a point are represented by Mohr's circle I, the shear stress on any plane through the point is less than the shearing strength, as indicated by the line BCD ;

BC represents the shear stress on a plane on which the normal stress is given by OD . BD , representing the shearing strength for this normal stress, is greater than BC .

The stress conditions represented by the Mohr's Circle II, which is tangential to the Mohr's envelope at F , are such that the shearing stress, EF , on the plane of maximum obliquity is equal to the shearing strength. Failure is incipient on this plane and will occur unless the normal stress on the critical plane increases.

It may be noted that it would be impossible to apply the stress conditions represented by Mohr's circle III (dashed) to this soil sample, since failure would have occurred even by the time the shear stress on the critical plane equals the shearing strength available on that plane, thus eliminating the possibility of the shear stress exceeding the shearing strength.

The Mohr's strength theory, or theory of failure or rupture, may thus be stated as follows:

The stress condition given by any Mohr's circle falling within the Mohr's envelope represents a condition of stability, while the condition given by any Mohr's circle tangent to the Mohr's envelope indicates incipient failure on the plane relating to the point of tangency. The Mohr's envelope may be treated to be a property of the material and independent of the imposed stresses. Also, the Mohr's circle of stress depends only upon the imposed stresses and has nothing to do with the nature and properties of the material.

To emphasise that the stresses in Eq.2.21 are those on the plane on which failure is incipient, we add the subscript f to σ , so that it becomes

$$s = \sigma_f \tan \phi \text{-----} \quad \text{Eq.2.22}$$

It is possible to express the strength in terms of normal stress on any plane, with the aid of the Mohr's circle of stress. Some common relationships are

$$\sigma_f = \sigma_3(1 + \sin \phi) = \sigma_1(1 - \sin \phi) \text{-----} \quad \text{Eq.2.23}$$

$$s = \sigma_f \tan \phi = \frac{\sigma_1 - \sigma_3}{2} \cos \phi \text{-----} \quad \text{Eq.2.24}$$

The primary assumptions in the Mohr's strength theory are that the intermediate principal stress has no influence on the strength and that the strength is dependent only upon the normal stress on the plane of maximum obliquity. However, the shearing strength, in fact, does depend to a small extent upon the intermediate principal stress, density speed of application of shear, and so on. But the Mohr theory explains satisfactorily the strength concept in soils and hence is in vogue. It may also be noted that the Mohr envelope will not be a straight line but is actually slightly curved since the angle of internal friction is known to decrease slightly with increase in stress.

2.5 MOHR-COULOMB THEORY

The Mohr-Coulomb theory of shearing strength of a soil, first propounded by Coulomb (1776) and later generalised by Mohr, is the most commonly used concept. The functional relationship between the normal stress on any plane and the shearing strength available on that plane was assumed to be linear by Coulomb; thus the following is usually known as Coulomb's law:

$$s = c + \sigma \tan \phi \text{-----} \quad \text{Eq. 2.25}$$

where c and ϕ are empirical parameters, known as the 'apparent cohesion' and 'angle of shearing resistance' (or angle of internal friction), respectively. These are better visualised as 'parameters' and not as absolute properties of a soil since they are known to vary with water content, conditions of testing such as speed of shear and drainage conditions, and a number of other factors besides the type of soil.

Coulomb's law is merely a mathematical equation of the failure envelope shown in Fig.2.5 (a); Mohr's generalisation of the failure envelope as a curve which becomes flatter with increasing normal stress is shown in Fig.2.5 (b).

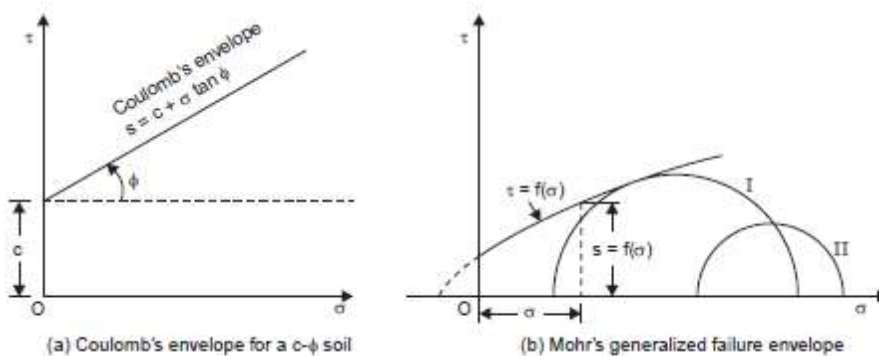


Fig.2.5: Mohr-Coulomb Theory—failure envelopes

The envelopes are called 'strength envelopes' or 'failure envelopes'. The meaning of an envelope has already been given in the previous section; if the normal and shear stress components on a plane plotted on to the failure envelope, failure is supposed to be incipient and

if the stresses plot below the envelope, the condition represents stability. And, it is impossible that these plot above the envelope, since failure should have occurred previously

Coulomb's law is also written as follows to indicate that the stress condition refers to that on the plane of failure:

$$s = c + \sigma_f \tan \phi \text{ -----} \quad \text{Eq.2.26}$$

In a different way, it can be said that the Mohr's circle of stress relating to a given stress condition would represent, incipient failure condition if it just touches or is tangent to the strength or failure envelope (circle I); otherwise, it would wholly lie below the envelopes as shown in circle II, Fig.2 5 (b).

The Coulomb envelope in special cases may take the shapes given in Fig.2.6 (a) and (b); for a purely cohesionless or granular soil or a pure sand, it would be as shown in Fig. 6 (a) and for a purely cohesive soil or a pure clay, it would be as shown in Fig.2. 6 (b).

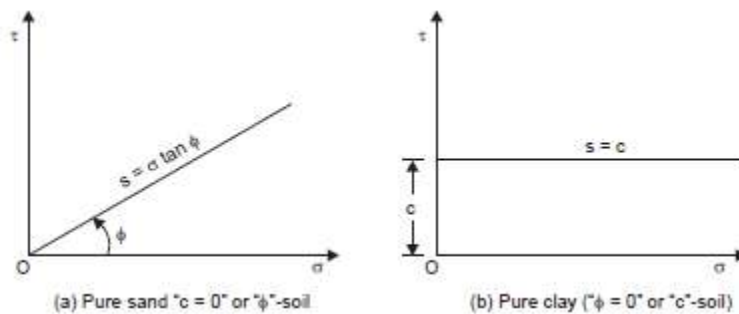


Fig.2.6: Coulomb envelopes for pure sand and for pure clay

2.6 SHEARING STRENGTH—A FUNCTION OF EFFECTIVE STRESS

Equation 2.26 apparently indicates that the shearing strength of a soil is governed by the total normal stress on the failure plane. However, according to Terzaghi, it is the effective stress on the failure plane that governs the shearing strength and not the total stress.

It may be expected intuitively that the denser a soil, the greater the shearing strength. It has been learnt in chapter seven that a soil deposit becomes densest under any given pressure after the occurrence of complete consolidation and consequent dissipation of pore water

Thus, complete consolidation, dependent upon the dissipation of pore water pressure and hence upon the increase in the effective stress, leads to increase in the shearing strength of a soil. In other words, it is the effective stress in the case of a saturated soil and not the total stress which is relevant to the mobilisation of shearing stress.

Further, the density of a soil increase when subjected to shearing action, drainage being allowed simultaneously. Therefore, even if two soils are equally dense on having been consolidated to the same effective stress, they will exhibit different shearing strengths if drainage is permitted during shear for one, while it is not for the other.

These ideas lead to a statement that “the strength of a soil is a unique function of the effective stress acting on the failure plane”.

Equation 8.26 may now be modified to read:

$$s = c' + \sigma_f \tan \phi' \text{-----Eq.2.7}$$

where c' and ϕ' are called the effective cohesion and effective angle of internal friction, respectively, since they are based on the effective normal stress on the failure plane. Collectively, they are called ‘effective stress parameters’, while c and ϕ of Eq. 2.25 are called “total stress parameters”.

2.7 SHEARING STRENGTH TESTS

Determination of shearing strength of a soil involves the plotting of failure envelopes and evaluation of the shear strength parameters for the necessary conditions. The following tests are available for this purpose :

Laboratory Tests

1. Direct Shear Test
2. Triaxial Compression Test
3. Unconfined Compression Test
4. Laboratory Vane Shear Test
5. Torsion Test
6. Ring Shear Tests

Field Tests

1. Vane Shear Test
2. Penetration Test

The first three tests among the laboratory tests are very commonly used, while the fourth is gaining popularity owing to its simplicity. The fifth and sixth are mostly used for research purposes and hence are not dealt with here.

The principle of the field vane test is the same as that of the laboratory vane shear test, except that the apparatus is bigger in size for convenience of field use. The penetration test involves the measurement of resistance of a soil to penetration of a cone or a cylinder, as an indication of the shearing strength. This procedure is indirect and rather empirical in nature although correlations are possible. The field tests are also not considered here. The details of the test procedures are available in the relevant I.S. codes or any book on laboratory testing, such as Lambe (1951).

2.7.1 Direct Shear Test

The direct shear device, also called the ‘shear box apparatus’, essentially consists of a brass box, split horizontally at mid-height of the soil specimen, as shown schematically in Fig. 2.7.

The soil is gripped in perforated metal grilles, behind which porous discs can be placed if required to allow the specimen to drain. For undrained tests, metal plates and solid metal grilles may be used. The usual plan size of the specimen is 60 mm square; but a larger size such as 300 mm square or even more, is employed for testing larger size granular material such as gravel. The minimum thickness or height of the specimen is 20 mm. After the sample to be tested is

placed in the apparatus or shear box, a normal load which is vertical is applied to the top of the sample by means of a loading yoke and weights. Since the shear plane is predetermined as the horizontal plane, this becomes the normal stress on the failure plane, which is kept constant throughout the test. A shearing force is applied to the upper-half of the box, which is zero initially and is increased until the specimen fails.

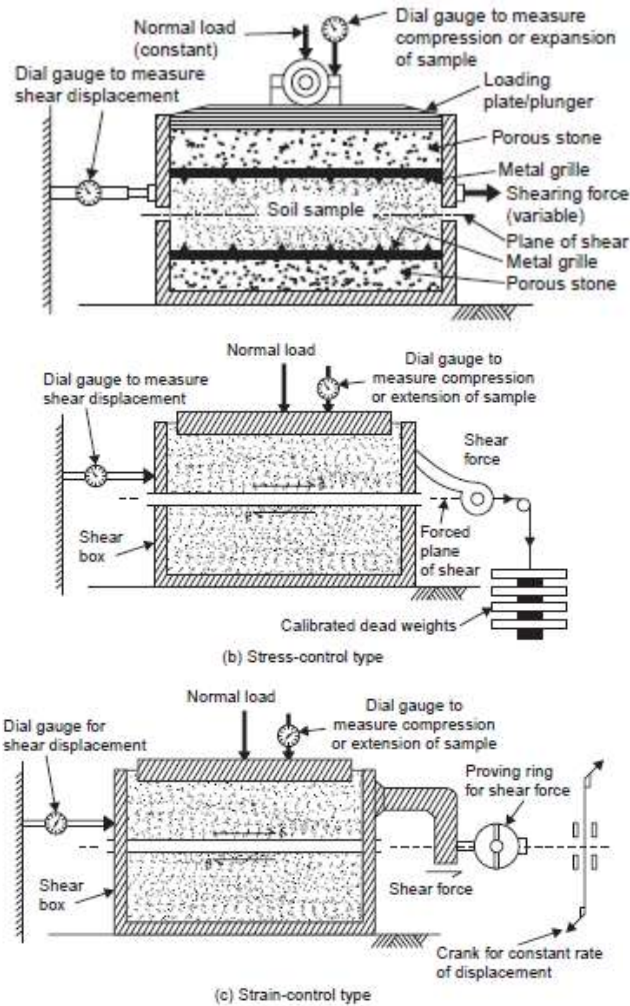


Fig.2.7: Direct Shear Test Device

Two types of application of shear are possible—one in which the shear stress is controlled and the other in which the shear strain is controlled. The principles of these two types of devices are illustrated schematically in Fig. 1 (b) and (c), respectively. In the stress-controlled type, the shear stress, which is the controlled variable, may be applied at a constant rate or more commonly in equal increments by means of calibrated weights hung from a hanger attached to a wire passing over a pulley. Each increment of shearing force is applied and held constant, until the shearing deformation ceases. The shear displacement is measured with the aid of a dial gauge attached to the side of the box. In the strain-controlled type, the shear displacement is applied at a constant

rate by means of a screw operated manually or by motor. With this type of test the shearing force necessary to overcome the resistance within the soil is automatically developed. This shearing force is measured with the aid of a proving ring—a steel ring that has been carefully machined, balanced and calibrated. The deflection of the annular ring is measured with the aid of a dial gauge set inside the ring, the causative force being got for any displacement by means of the calibration chart supplied by the manufacturer.

The shear displacement is measured again with the aid of another dial gauge attached to the side of the box

In both cases, a dial gauge attached to the plunger, through which the normal load is applied, will enable one to determine the changes in the thickness of the soil sample which will help in the computation of volume changes of the sample, if any. The strain-controlled type is very widely used. The strain is taken as the ratio of the shear displacement to the thickness of the sample. The proving ring readings may be taken at fixed displacements or even at fixed intervals of time as the rate of strain is made constant by an electric motor. A sudden drop in the proving ring reading or a leveling-off in successive readings indicates shear failure of the soil specimen.

The shear strain may be plotted against the shear stress; it may be plotted versus the ratio of the shearing stress on normal stress; and it may also be plotted versus volume change.

Each plot may yield information useful in one way or the other. The stresses may be obtained from the forces by dividing them by the area of cross-section of the sample. The stress-conditions on the failure plane and the corresponding Mohr's circle for direct shear test are shown in Fig. 2 (a) and (b) respectively.

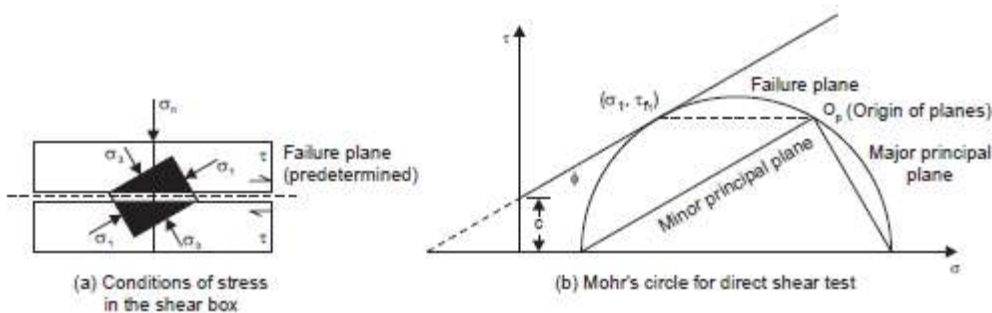


Fig.2.8: Mohr's circle representation of stress condition for Direct shear test results

The failure plane is predetermined as the horizontal plane here. Several specimens are tested under different normal loads and the results plotted to obtain failure envelopes.

The direct shear test is a relatively simple test. Quick drainage, *i.e.*, quick dissipation of pore pressures is possible since the thickness of the specimen is small. However, the test suffers from the following inherent **disadvantages**, which limit its application.

The stress conditions are complex primarily because of the non-uniform distribution of normal and shear stresses on the plane.

2. There is virtually no control of the drainage of the soil specimen as the water content of a saturated soil changes rapidly with stress.

3. The area of the sliding surface at failure will be less than the original area of the soil specimen and strictly speaking, this should be accounted for.
4. The ridges of the metal gratings embedded on the top and bottom of the specimen, causes distortion of the specimen to some degree.
5. The effect of lateral restraint by the side walls of the shear box is likely to affect the results.
6. The failure plane is predetermined and this may not be the weakest plane. In fact, this is the most important limitation of the direct shear test.

2.7.2 Triaxial Shear Test

The triaxial shear test is one of the most reliable methods available for determining shear strength parameters. It is used widely for research and conventional testing. A diagram of the triaxial test layout is shown in Figure 2.9.

In this test, a soil specimen about 36 mm in diameter and 76 mm (3 in.) long generally is used. The specimen is encased by a thin rubber membrane and placed inside a plastic cylindrical chamber that usually is filled with water or glycerine. The specimen is subjected to a confining pressure by compression of the fluid in the chamber. (*Note:* Air is sometimes used as a compression medium.) To cause shear failure in the specimen, one must apply axial stress (sometimes called *deviator stress*) through a vertical loading ram.

This stress can be applied in one of two ways:

1. Application of dead weights or hydraulic pressure in equal increments until the specimen fails.
2. Application of axial deformation at a constant rate by means of a geared or hydraulic loading press. This is a strain-controlled test.

The axial load applied by the loading ram corresponding to a given axial deformation is measured by a proving ring or load cell attached to the ram.

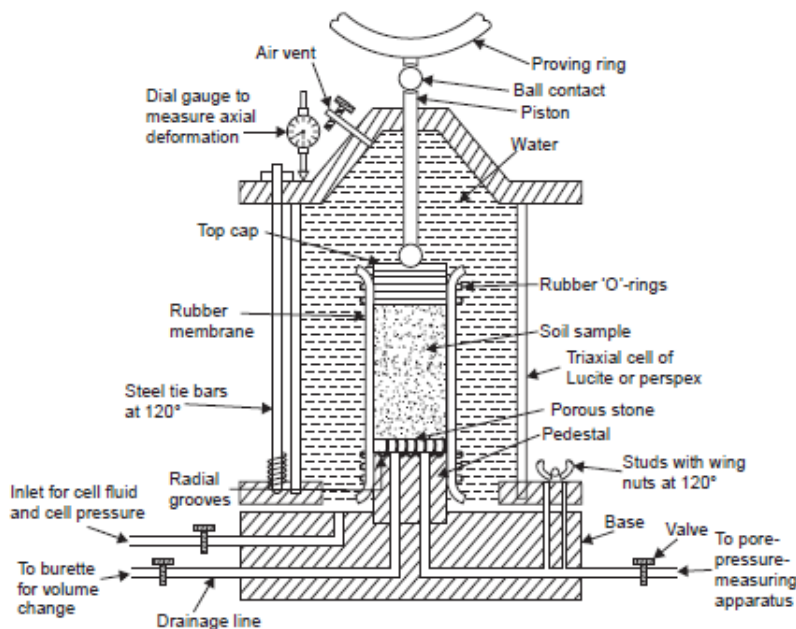


Fig.2.9:Triaxial experimental set up

2.7.2.1: Test Procedure

The essential steps in the conduct of the test are as follows:

- (i) A saturated porous stone is placed on the pedestal and the cylindrical soil specimen is placed on it.
- (ii) The specimen is enveloped by a rubber membrane to isolate it from the water with which the cell is to be filled later; it is sealed with the pedestal and top cap by rubber “O” rings.
- (iii) The cell is filled with water and pressure is applied to the water, which in turn is transmitted to the soil specimen all-round and at top. This pressure is called ‘cell pressure’, ‘chamber pressure’ or ‘confining pressure’.
- (iv) Additional axial stress is applied while keeping the cell pressure constant. This introduces shearing stresses on all planes except the horizontal and vertical planes, on which the major, minor and intermediate principal stresses act, the last two being equal to the cell pressure on account of axial symmetry.
- (v) The additional axial stress is continuously increased until failure of the specimen occurs. (What constitutes failure is often a question of definition and may be different for different kinds of soils. This aspect would be discussed later on).

A number of observations may be made during a triaxial compression test regarding the physical changes occurring in the soil specimen:

- (a) As the cell pressure is applied, pore water pressure develops in the specimen, which can be measured with the help of a pore pressure measuring apparatus, such as Bishop’s pore pressure device (Bishop, 1960), connected to the pore pressure line, after closing the valve of the drainage line.
- (b) If the pore pressure is to be dissipated, the pore water line is closed, the drainage line opened and connected to a burette. The volume decrease of the specimen due to consolidation is indicated by the water drained into the burette.
- (c) The axial strain associated with the application of additional axial stress can be measured by means of a dial gauge, set to record the downward movement of the loading piston.
- (d) Upon application of the additional axial stress, some pore pressure develops. It may be measured with the pore pressure device, after the drainage line is closed. On the other hand, if it is desired that any pore pressure developed be allowed to be dissipated, the pore water line is closed and the drainage line opened as stated previously.
- (e) The cell pressure is measured and kept constant during the course of the test.
- (f) The additional axial stress applied is also measured with the aid of a proving ring and dial gauge.

Thus the entire triaxial test may be visualised in two important stages:

- (i) The specimen is placed in the triaxial cell and cell pressure is applied during the first stage.
- (ii) The additional axial stress is applied and is continuously increased to cause a shear failure, the potential failure plane being that with maximum obliquity during the second stage.

2.7.2.2 Area Correction for the Determination of Additional Axial Stress or Deviatoric Stress

The additional axial load applied at any stage of the test can be determined from the proving ring reading. During the application of the load, the specimen undergoes axial compression and

horizontal expansion to some extent. Little error is expected to creep in if the volume is supposed to remain constant, although the area of cross-section varies as axial strain increases.

The assumption is perfectly valid if the test is conducted under undrained conditions, but, for drained conditions, the exact relationship is somewhat different.

If A_0 , h_0 and V_0 are the initial area of cross-section, height and volume of the soil specimen respectively, and if A , h , and V are the corresponding values at any stage of the test, the corresponding changes in the values being design

$$A(h_0 - \Delta h) = V = V_0 + \Delta V \text{-----} \quad \text{Eq.2.8}$$

$$\text{Hence } A = \frac{V_0 + \Delta V}{h_0 - \Delta h} \text{-----} \quad \text{Eq.2.9}$$

But, for axial compression, Δh is known to be negative.

$$A = \frac{V_0 + \Delta V}{h_0 - \Delta h} = \frac{V_0(1 + \frac{\Delta V}{V_0})}{h_0(1 - \frac{\Delta h}{h_0})} = \frac{A_0(1 + \frac{\Delta V}{V_0})}{1 - \epsilon_a} \text{-----} \quad \text{Eq.2.10}$$

$$\text{since the axial strain, } \epsilon_a = \Delta h/h_0 \text{-----} \quad \text{Eq.2.11}$$

$$\text{For an undrained test, } A = \frac{A_0}{1 - \epsilon_a} \text{-----} \quad \text{Eq.2.12}$$

since $\Delta V = 0$.

This is called the ‘Area correction’ and $\frac{1}{1 - \epsilon_a}$ is the correction factor.

A more accurate expression for the corrected area is given by

$$A = \frac{A_0}{1 - \epsilon_a} = \frac{V_0 + \Delta V}{h_0 - \Delta h} \text{-----} \quad \text{Eq.2.14}$$

Once the corrected area is determined, the additional axial stress or the deviator stress, $\Delta\sigma$, is obtained as

$$\Delta\sigma = \sigma_1 - \sigma_3 = \text{Axial load (from proving ring reading)/Corrected area}$$

The cell pressure or the confining pressure, σ_c , itself being the minor principal stress, σ_3 , this is constant for one test; however, the major principal stress, σ_1 , goes on increasing until failure.

$$\sigma_1 = \sigma_3 + \Delta\sigma \text{-----} \quad \text{Eq.2.15}$$

2.7.2.3 Mohr’s Circle for Triaxial Test

The stress conditions in a triaxial test may be represented by a Mohr’s circle, at any stage of the test, as well as at failure, as shown in Fig. 2.10

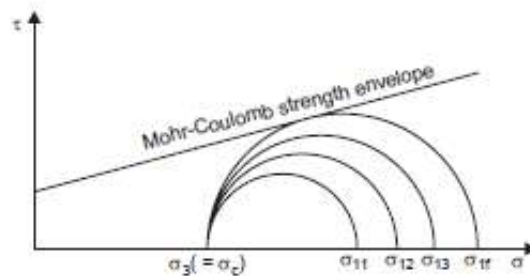


Fig.2.10: Mohr’s circle during Triaxial test

The cell pressure, σ_c which is also the minor principal stress is constant and $\sigma_{11}, \sigma_{12}, \sigma_{13}, \dots, \sigma_{1f}$ are the major principal stresses at different stages of loading and at failure. The Mohr's circle at failure will be tangential to the Mohr-Coulomb strength envelope, while those at intermediate stages will be lying wholly below it. The Mohr's circle at failure for one particular value of cell pressure will be as shown in Fig.2.11.

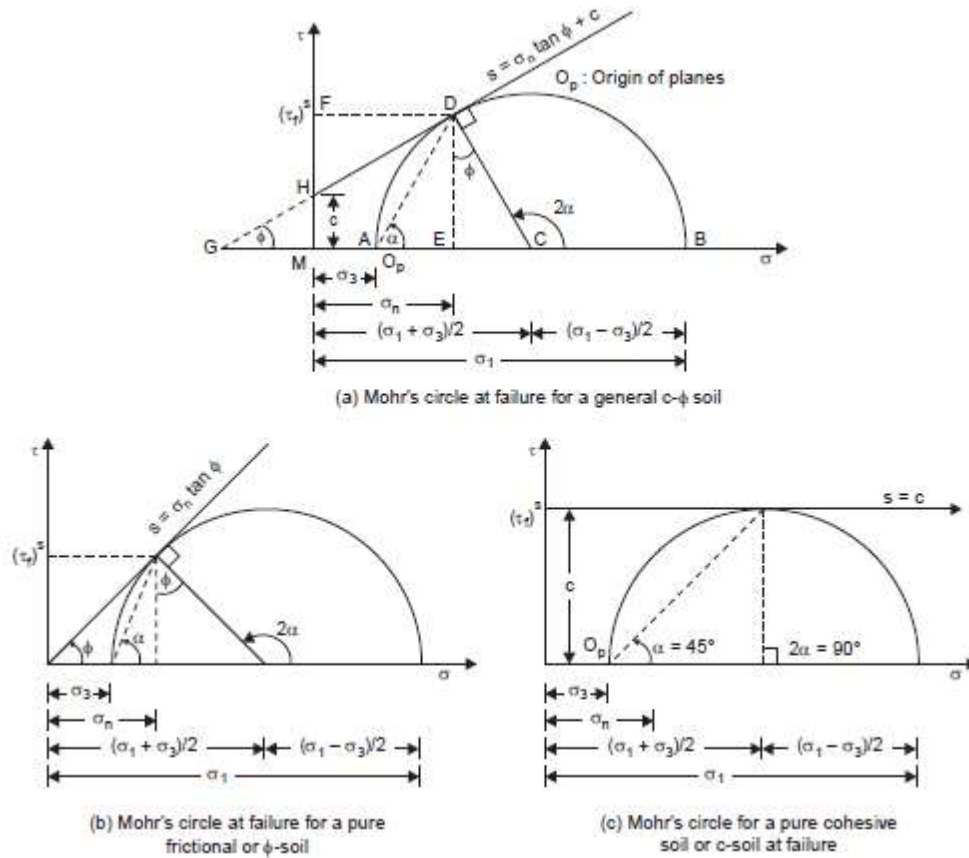


Fig. 2.11: Mohr's circle at failure for a particular cell pressure

The Mohr's circles at failure for one particular cell pressure are shown for the three typical cases of a general $c-\phi$ soil, a ϕ -soil and a c -soil in Figs. 2.11 (a), (b), and (c) respectively.

With reference to Fig. 2.11 (a), the relationship between the major and minor principal stresses at failure may be established from the geometry of the Mohr's circle, as follows:

From $\triangle DCG$, $2\alpha = 90^\circ + \phi$

$$\therefore \alpha = 45^\circ + \phi/2 \text{-----} \text{Eq.2.16}$$

Again from $\triangle DCG$

$$\sin \phi = \frac{DC}{GC} = \frac{DC}{GM+MC} = \frac{\left(\frac{\sigma_1 - \sigma_3}{2}\right)}{c \cot \phi + \frac{\sigma_1 + \sigma_3}{2}} \text{-----} \text{Eq.2.17}$$

$$\sigma_1 - \sigma_3 = 2c \cot \phi + (\sigma_1 + \sigma_3) \sin \phi \text{-----} \text{Eq.2.18}$$

$$\text{Or, } \sigma_1 = \sigma_3 \tan^2 (45^\circ + \phi/2) + 2c \tan (45^\circ + \phi/2) \text{-----} \text{Eq.2.19}$$

$$\text{Or, } \sigma_1 = \sigma_3 \tan^2 \alpha + 2c \tan \alpha \text{-----} \text{Eq.2.20}$$

This is also written as

$$\sigma_1 = \sigma_3 N\phi + 2c N\phi \text{ ----- Eq.2.21}$$

$$\text{where, } N\phi = \tan^2 \alpha = \tan^2(45^\circ + \phi/2) \text{ ----- Eq.2.22}$$

The above equations define the relationship between the principal stresses at failure. This state of stress is defined as ‘Plastic equilibrium condition’, when failure is imminent.

From one test, a set of σ_1 and σ_3 is known; however, it can be seen from that at least two such sets are necessary to evaluate the parameters c and ϕ . conventionally; three or more such sets are used from a corresponding number of tests.

The usual procedure is to plot the Mohr’s circles for a number of tests and take the best common tangent to the circles as the strength envelope. A small curvature occurs in the strength envelope of most soils, but since this effect is slight, the envelope for all practical purposes, may be taken as a straight line. The intercept of the strength envelope on the τ -axis gives the cohesion and the angle of slope of this line with σ -axis gives the angle of internal friction, as shown in Fig. 2.12.

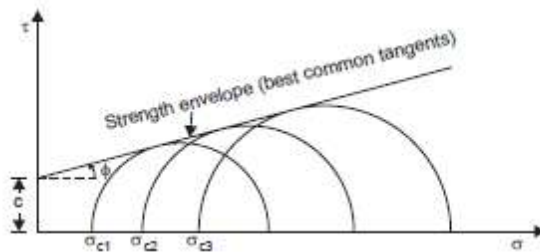


Fig.2.12: Mohr’s circle at failure for different cell pressures

2.7.2.4 Merits of Triaxial Compression Test

The following are the significant points of merit of triaxial compression test:

- (1) Failure occurs along the weakest plane unlike along the predetermined plane in the case of direct shear test.
- (2) The stress distribution on the failure plane is much more uniform than it is in the direct shear test: the failure is not also progressive, but the shear strength is mobilised all at once. Of course, the effect of end restraint for the sample is considered to be a disadvantage; however, this may not have pronounced effect on the results since the conditions are more uniform to the desired degree near the middle of the height of the sample where failure usually occurs.
- (3) Complete control of the drainage conditions is possible with the triaxial compression test; this would enable one to simulate the field conditions better.
- (4) The possibility to vary the cell pressure or confining pressure also affords another means to simulate the field conditions for the sample, so that the results are more meaningfully interpreted.
- (5) Precise measurements of pore water pressure and volume changes during the test are possible.
- (6) The state of stress within the specimen is known on all planes and not only on a predetermined failure plane as it is with direct shear tests.
- (7) The state of stress on any plane is capable of being determined not only at failure but also at any earlier stage.

(8) Special tests such as extension tests are also possible to be conducted with the triaxial testing apparatus.

(9) It provides an ingenious and a symmetrical three-dimensional stress system better suited to simulate field conditions.

2.7.2.5 Types of Shear Tests Based on Drainage Conditions

Before considering various methods of conducting shearing strength tests on a soil, it is necessary to consider the possible drainage conditions before and during the tests since the results is significantly affected by these.

A cohesionless or a coarse-grained soil may be tested for shearing strength either in the dry condition or in the saturated condition. A cohesive or fine-grained soil is usually tested in the saturated condition. Depending upon whether drainage is permitted before and during the test, shear tests on such saturated soils are classified as follows:

2.7.2.6 Unconsolidated Undrained Test

Drainage is not permitted at any stage of the test, that is, either before the test during the application of the normal stress or during the test when the shear stress is applied. Hence no time is allowed for dissipation of pore water pressure and consequent consolidation of the soil; also, no significant volume changes are expected. Usually, 5 to 10 minutes may be adequate for the whole test, because of the shortness of drainage path. However, undrained tests are often performed only on soils of low permeability. This is the most unfavourable condition which might occur in geotechnical engineering practice and hence is simulated in shear testing. Since a relatively small time is allowed for the testing till failure, it is also called the 'Quick test.' It is designated UU , Q , or Qu test.

2.7.2.7 Consolidated Undrained Test

Drainage is permitted fully in this type of test during the application of the normal stress and no drainage is permitted during the application of the shear stress. Thus volume changes do not take place during shear and excess pore pressure develops. Usually, after the soil is consolidated under the applied normal stress to the desired degree, 5 to 10 minutes may be adequate for the test. This test is also called 'consolidated quick test' and is designated CU or Qc test, These conditions are also common in geotechnical engineering practice.

2.7.2.8 Consolidated-Drained Triaxial Test

In the CD test, the saturated specimen first is subjected to an all around confining pressure, σ_3 , by compression of the chamber fluid. As confining pressure is applied, the pore water pressure of the specimen increases by u_c (if drainage is prevented). This increase in the pore water pressure can be expressed as a nondimensional parameter in the form

$$B = \frac{u_c}{\sigma_3} \text{-----} \quad \text{Eq.2.23}$$

Where, B = Skempton's pore pressure parameter (Skempton, 1954).

For saturated soft soils, B is approximately equal to 1; however, for saturated stiff soils, the magnitude of B can be less than 1. Black and Lee (1973) gave the theoretical values of B for various soils at complete saturation.

Now, if the connection to drainage is opened, dissipation of the excess pore water pressure, and thus consolidation, will occur. With time, u_c will become equal to 0. In saturated soil, the change

in the volume of the specimen (ΔV_c) that takes place during consolidation can be obtained from the volume of pore water drained (Fig.2.13 a)

Next, the deviator stress, $\Delta\sigma_d$ on the specimen is increased very slowly (Figure 2.13 b). The drainage connection is kept open, and the slow rate of deviator stress application allows complete dissipation of any pore water pressure that developed as a result ($\Delta u_d=0$)

A typical plot of the variation of deviator stress against strain in loose sand and normally consolidated clay is shown in Figure 2.13 b. and c shows a similar plot for dense sand and over consolidated clay. The volume change, ΔV_d , of specimens that occurs because of the application of deviator stress in various soils is also shown in Figures 2.13 d and 1e.

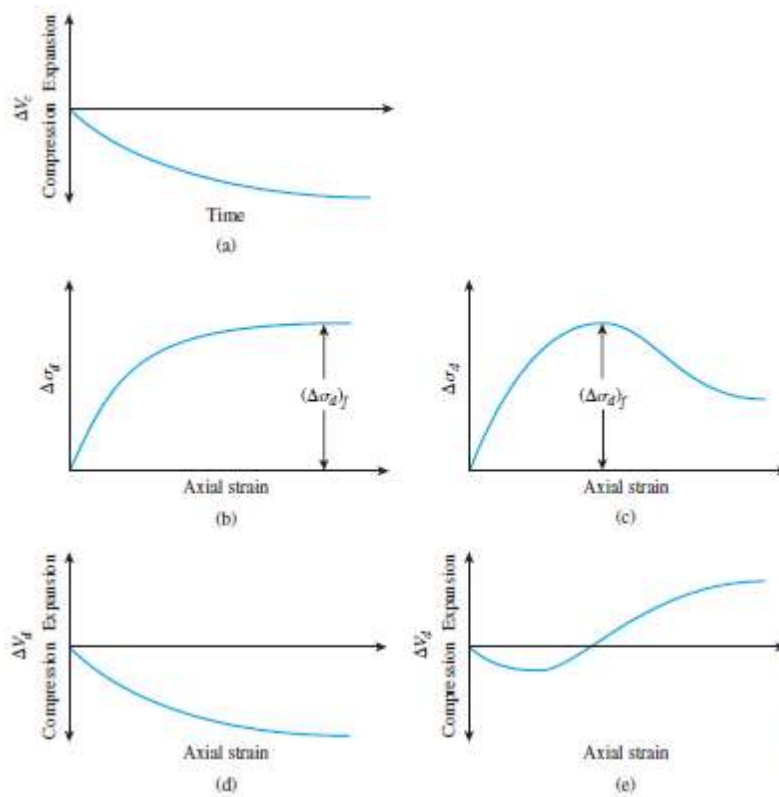


Fig.2.13: Consolidated-drained triaxial test: (a) volume change of specimen caused by chamber-confining pressure; (b) plot of deviator stress against strain in the vertical direction for loose sand and normally consolidated clay; (c) plot of deviator stress against strain in the vertical direction for dense sand and over consolidated clay; (d) volume change in loose sand and normally consolidated clay during deviator stress application; (e) volume change in dense sand and over consolidated clay during deviator stress application

Because the pore water pressure developed during the test is completely dissipated, we have

$$\text{Total and effective confining stress} = \sigma_3 = \sigma'_3$$

$$\text{Total and effective axial stress at failure} = \sigma_3 + \Delta\sigma_{df} = \sigma_1 = \sigma'_1$$

In a triaxial test, σ'_1 is the major principal effective stress at failure and is the minor principal effective stress at failure. Several tests on similar specimens can be conducted by varying the confining pressure. With the major and minor principal stresses at failure for each test the

Mohr's circles can be drawn and the failure envelopes can be obtained. Fig. 2.14 shows the type of effective stress failure envelope obtained for tests on sand and normally consolidated clay.

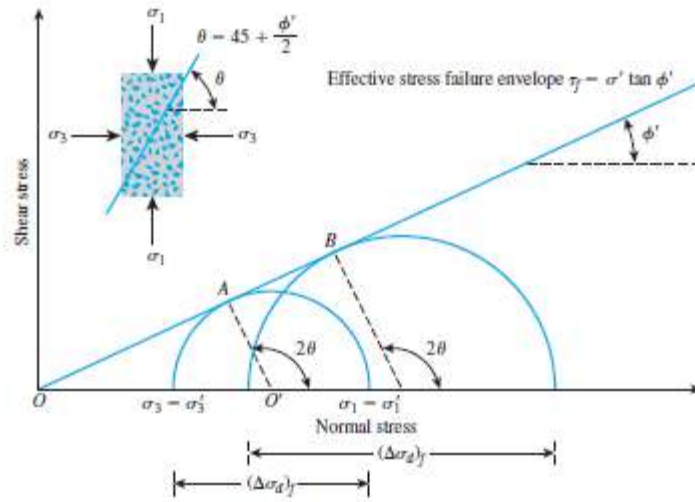


Fig.2.14: Effective stress failure envelope from drained tests on sand and normally consolidated clay

The coordinates of the point of tangency of the failure envelope with a Mohr's circle (that is, point A) give the stresses (normal and shear) on the failure plane of that test specimen.

For normally consolidated clay, referring to Figure 2

$$\sin\phi' = \frac{OA'}{OO'} \text{-----} \quad \text{Eq.2.24}$$

$$\text{OR } \sin\phi' = \frac{\sigma_1' - \sigma_3'}{\sigma_1' + \sigma_3'} \text{-----} \quad \text{Eq.2.25}$$

$$\text{Hence } \phi' = \sin^{-1} \left(\frac{\sigma_1' - \sigma_3'}{\sigma_1' + \sigma_3'} \right) \text{-----} \quad \text{Eq.2.26}$$

Also, the failure plane will be inclined at an angle of $\theta = 45 + \frac{\phi'}{2}$ to the major principal plane, as shown in Figure 2.14.

Over consolidation results when a clay initially is consolidated under an all-around chamber pressure of $\sigma_c = \sigma_c'$ and is allowed to swell by reducing the chamber pressure to $\sigma_3 = \sigma_3'$. The failure envelope obtained from drained triaxial tests of such overconsolidated clay specimens shows two distinct branches (*ab* and *bc* in Figure 2.15). The portion *ab* has a flatter slope with a cohesion intercept, and the shear strength equation for this branch can be written as

$$r_f = c' + \sigma' \tan\phi' \text{-----} \quad \text{Eq.2.27}$$

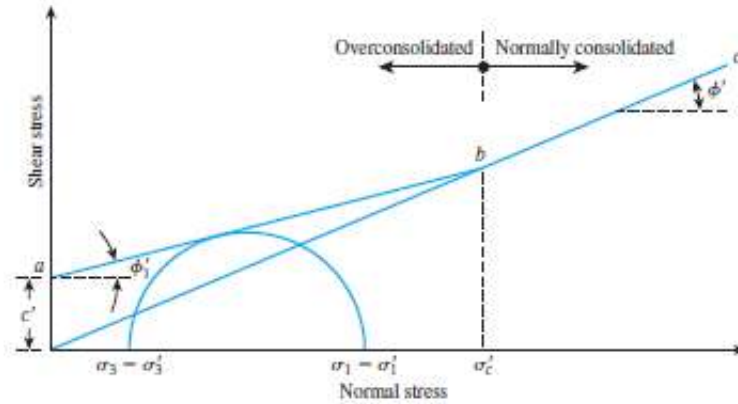


Fig. 2.15 Effective stress failure envelope for over consolidated clay

A consolidated-drained triaxial test on a clayey soil may take several days to complete. This amount of time is required because deviator stress must be applied very slowly to ensure full drainage from the soil specimen. For this reason, the CD type of triaxial test is uncommon.

2.7.2.9 Consolidated-Un-drained Triaxial Test

The consolidated-un-drained test is the most common type of triaxial test. In this test, the saturated soil specimen is first consolidated by an all-around chamber fluid pressure, σ_3 , that results in drainage (Figures 2.16 a & 4b).

After the pore water pressure generated by the application of confining pressure is dissipated, the deviator stress, $\Delta\sigma_d$, on the specimen is increased to cause shear failure (Figure 4c). During this phase of the test, the drainage line from the specimen is kept closed. Because drainage is not permitted, the pore water pressure, Δu_d , will increase.

During the test, simultaneous measurements of $\Delta\sigma_d$, and Δu_d are made. The increase in the pore water pressure, Δu_d can be expressed in a non dimensional form as

$$\bar{A} = \frac{\Delta u_d}{\Delta\sigma_d} \text{-----} \tag{Eq.2.28}$$

where \bar{A} = Skempton's pore pressure parameter (Skempton, 1954).

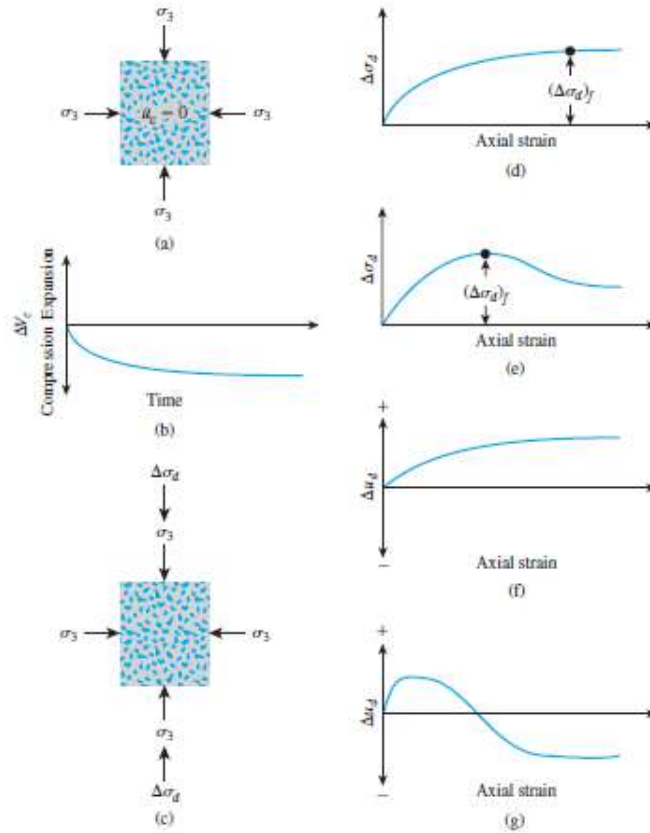


Fig.2.26: Consolidated-undrained test: (a) specimen under chamber-confining pressure; (b) volume change in specimen caused by confining pressure; (c) deviator stress application; (d) deviator stress against axial strain for loose sand and normally consolidated clay; (e) deviator stress against axial strain for dense sand and over consolidated clay; (f) variation of pore water pressure with axial strain for loose sand and normally consolidated clay; (g) variation of pore water pressure with axial strain for dense sand and over consolidated clay

The general patterns of variation of $\Delta\sigma_d$ and Δu_d with axial strain for sand and clay soils are shown in Figures 2.26 d through g. In loose sand and normally consolidated clay, the pore water pressure increases with strain. In dense sand and over consolidated clay, the pore water pressure increases with strain to a certain limit, beyond which it decreases and becomes negative (with respect to the atmospheric pressure). This decrease is because of a tendency of the soil to dilate. Unlike the consolidated-drained test, the total and effective principal stresses are not the same in the consolidated-undrained test. Because the pore water pressure at failure is measured in this test, the principal stresses may be analyzed as follows:

- Major principal stress at failure (total):
- Major principal stress at failure (effective):
- Minor principal stress at failure (total):
- Minor principal stress at failure (effective):

The preceding derivations show that

$$\sigma_1 - \sigma_3 = \sigma'_1 - \sigma'_3 \text{-----} \quad \text{Eq.2.29}$$

Tests on several similar specimens with varying confining pressures may be conducted to determine the shear strength parameters. Figure 2.27 shows the total and effective stress

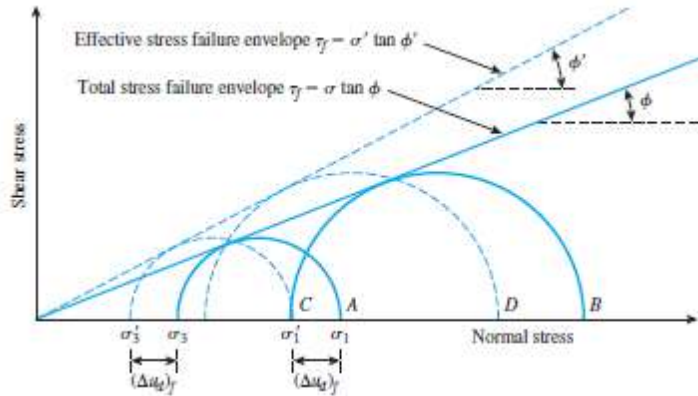


Figure 2.27: Total and effective stress failure envelopes for consolidated undrained triaxial tests

Mohr's circles at failure obtained from consolidated-undrained triaxial tests in sand and normally consolidated clay. Note that A and B are two total stress Mohr's circles obtained from two tests. C and D are the effective stress Mohr's circles corresponding to total stress circles A and B, respectively. The diameters of circles A and C are the same; similarly, the diameters of circles B and D are the same. In Figure 2.27, the total stress failure envelope can be obtained by drawing a line that touches all the total stress Mohr's circles. For sand and normally consolidated clays, this will be approximately a straight line passing through the origin and may be expressed by the equation

$$\tau_f = \sigma \tan \phi \text{-----} \quad \text{Eq.2.30}$$

where σ = total stress

ϕ = the angle that the total stress failure envelope makes with the normal stress axis, also known as the *consolidated-undrained angle of shearing resistance*

For sand and normally consolidated clay, we can write

$$\phi = \sin^{-1} \left(\frac{\sigma_1 - \sigma_3}{\sigma_1 + \sigma_3} \right) \text{-----} \quad \text{Eq.2.31}$$

And

$$\phi' = \sin^{-1} \left(\frac{\sigma_1 - \sigma_3}{\sigma_1 + \sigma_3 - 2(\Delta u_d)} \right) \text{-----} \quad \text{Eq.2.32}$$

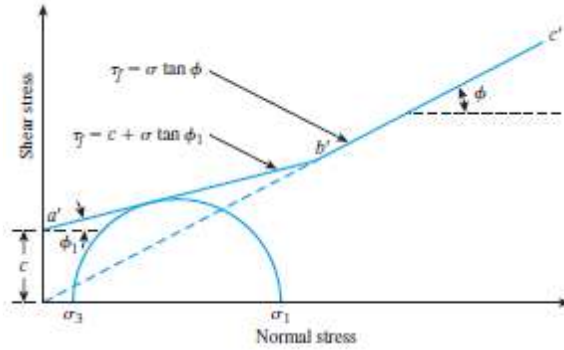


Fig.2.28: Total stress failure envelope obtained from consolidated-undrained tests in over consolidated clay

Again referring to Figure 2.27, we see that the failure envelope that is tangent to all the effective stress Mohr's circles can be represented by the equation

$$\tau_f = \sigma' \tan \phi' \text{-----} \quad \text{Eq.2.33}$$

which is the same as that obtained from consolidated-drained tests. In over consolidated clays, the total stress failure envelope obtained from consolidated un-drained tests will take the shape shown in Figure 6. The straight line is represented by the equation

$$\tau_f = \sigma \tan \phi_1 \text{-----} \quad \text{Eq.2.34}$$

and the straight line follows the relationship given by the above equation. The effective stress failure envelope drawn from the effective stress Mohr's circles will be similar to that shown in Figure 2.14.

Consolidated-drained tests on clay soils take considerable time. For this reason, consolidated-undrained tests can be conducted on such soils with pore pressure measurements to obtain the drained shear strength parameters. Because drainage is not allowed in these tests during the application of deviator stress, they can be performed quickly. Skempton's pore water pressure parameter was defined as follows. At failure, the parameter can be written as

$$\bar{A} = \bar{A}_f = \frac{\Delta u_{df}}{\Delta \sigma_{df}} \text{-----} \quad \text{Eq.2.35}$$

2.7.2.10 Unconsolidated-Undrained Triaxial Test

In unconsolidated-undrained tests, drainage from the soil specimen is not permitted during the application of chamber pressure σ_3 . The test specimen is sheared to failure by the application of deviator stress, $\Delta \sigma_d$, and drainage is prevented. Because drainage is not allowed at any stage, the test can be performed quickly. Because of the application of chamber confining pressure, σ_3 , the pore water pressure in the soil specimen will increase by u_c . A further increase in the pore water pressure ($\Delta \sigma_d$) will occur because of the deviator stress application. Hence, the total pore water pressure u in the specimen at any stage of deviator stress application can be given as

$$u = u_c + \Delta u_d \text{-----} \quad \text{Eq.2.36}$$

But we know that $u_c = B \sigma_3$ and $\Delta u_c = \bar{A} \Delta \sigma_d$

Now substituting above relation, we obtain

$$u = B\sigma_3 + \bar{A}\Delta\sigma_d \text{-----} \text{Eq.2.37}$$

This test usually is conducted on clay specimens and depends on a very important strength concept for cohesive soils if the soil is fully saturated. The added axial stress at failure $\Delta\sigma_{df}$ is practically the same regardless of the chamber confining pressure. This property is shown in Figure 2.29. The failure envelope for the total stress Mohr's circles becomes a horizontal line and hence is called a $\phi = 0$ condition. So we get

$$\tau_f = c = c_u \text{-----} \text{Eq.2.38}$$

where c_u is the un-drained shear strength and is equal to the radius of the Mohr's circles.

Note that the $\phi = 0$ concept is applicable to only saturated clays and silts.

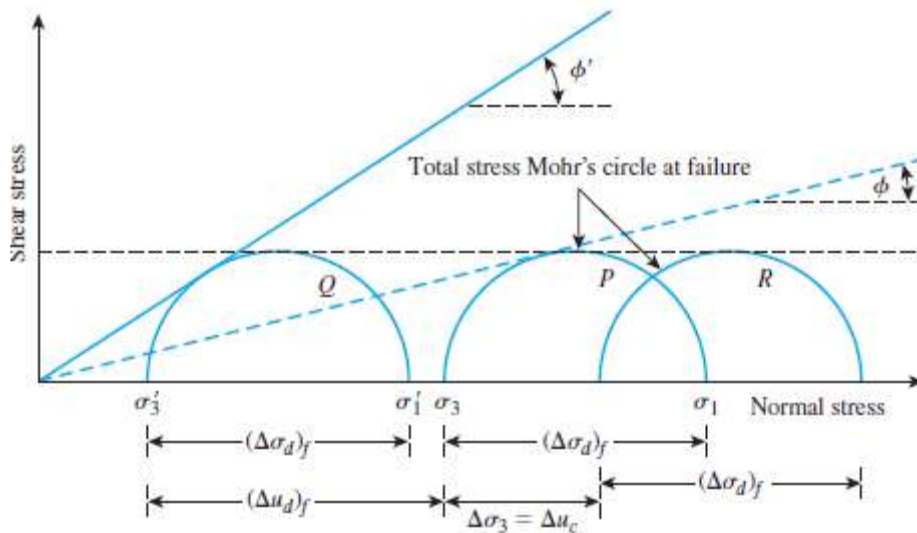


Fig. 2.29: Mohr's circle for total and effective stress and failure envelope, $\phi = 0$

The reason for obtaining the same added axial stress $\Delta\sigma_{df}$ regardless of the confining pressure can be explained as follows. If a clay specimen (No.I) is consolidated at a chamber pressure σ_3 and then sheared to failure without drainage, the total stress conditions at failure can be represented by the Mohr's circle P in Figure 2.29. The pore pressure developed in the specimen at failure is equal to $\Delta\sigma_{df}$. Thus, the major and minor principal effective stresses at failure are, respectively,

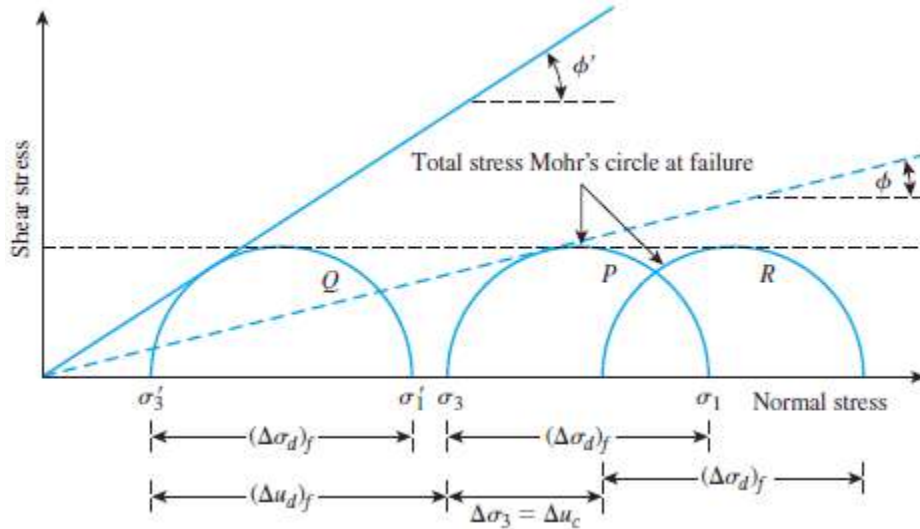


Fig. 2.30: The $\phi = 0$ concept

$$\sigma'_1 = [\sigma_3 + \Delta\sigma_{df}] - \Delta u_{df} = \sigma_1 - (\Delta u_d)_f \text{-----} \text{Eq.2.39}$$

$$\sigma'_3 = \sigma_3 - (\Delta u_d)_f \text{-----} \text{Eq.2.40}$$

Q is the effective stress Mohr's circle drawn with the preceding principal stresses.

Note that the diameters of circles P and Q are the same.

Any value of σ_3 could have been chosen for testing the specimen. In any case, the deviator stress $\Delta\sigma_{df}$ to cause failure would have been the same as long as the soil was fully saturated and fully un-drained during both stages of the test.

2.3 SHEARING CHARACTERISTICS OF SANDS

The shearing strength in sand may be said to consist of two parts, the internal frictional resistance between grains, which is a combination of rolling and sliding friction and another part known as 'interlocking'. Interlocking, which means locking of one particle by the adjacent ones, resisting movements, contributes a large portion of the shearing strength in dense sands, while it does not occur in loose sands. The Mohr strength theory is not invalidated by the occurrence of interlocking. The Mohr envelopes merely show large ordinates and steeper slopes for dense soils than for loose ones. The angle of internal friction is a measure of the resistance of the soil to sliding along a plane. This varies with the density of packing, characterised by density index, particle shape angularity and roughness of particles and also with better gradation. This is influenced to some extent by the normal pressure on the plane of shear and also the rate of application of shear.

The 'angle of repose' is the angle to the horizontal at which a heap of dry sand, poured freely from a small height, will stand without support. It is approximately the same as the angle of friction in the loose state. Some clean sands exhibit slight cohesion under certain conditions of

moisture content, owing to capillary tension in the water contained in the voids. Since this is small and may disappear with change in water content, it should not be relied upon for shear strength. On the other hand, even small percentages of silt and clay in a sand give it cohesive properties which may be sufficiently large so as to merit consideration. Unless drainage is deliberately prevented, a shear test on sand will be a drained one as the high value of permeability makes consolidation and drainage virtually instantaneous. A sand can be tested either in the dry or in the saturated condition. If it is dry, there will be no pore water pressures and if it is saturated, the pore water pressure will be zero due to quick drainage. In either case, the intergranular pressure will be equal to the applied stress. However, there may be certain situations in which significant pore pressures are developed, at least temporarily, in sands. For example, during earth-quakes, heavy blasting and operation of vibratory equipment instantaneous pore pressures are likely to develop due to large shocks or dynamic loads. These may lead to the phenomenon of 'liquefaction' or sudden and total loss of shearing strength, which is a grave situation of lack of stability.

Further discussion of shear characteristics of sands is presented in the following subsections.

2.3.1 *Stress-strain Behaviour of Sands*

The stress-strain behaviour of sands is dependent to a large extent on the initial density of packing, as characterised by the density index. This is represented in Fig. 2.31. It can be observed from Fig. 2.31 (a), the shear stress (in the case of direct shear tests) or deviator stress (in the case of triaxial compression tests) builds up gradually for an initially loose sand, while for an initially dense sand, it reaches a peak value and decreases at greater values of shear/axial strain to an ultimate value comparable to that for an initially loose specimen.

The behaviour of medium-dense sand is intermediate to that of loose sand and dense sand. Intuitively, it should be expected that the denser sand is stronger. The hatched portion represents the additional strength due to the phenomenon of interlocking in the case of dense sands.

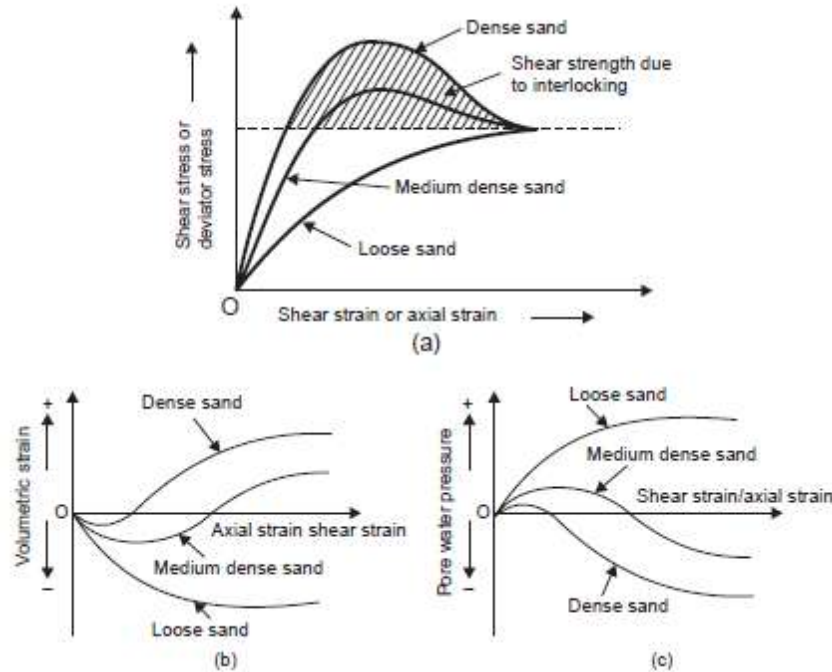


Fig. 2.31: Stress-strain characteristics of sands

The volume change characteristic of sands is another interesting feature, as depicted in Fig. 1(b). An initially dense specimen tends to increase in volume and become loose with increasing values of strain, while an initially loose specimen tends to decrease in volume and become dense. This is explained in terms of the rearrangement of particles during shear.

The changes in pore water pressure during undrained shear, which is rather not very common owing to high permeability of sands, are depicted in Fig. 2.31 (c). Positive pore pressures develop in the case of an initially loose specimen and negative pore pressures develop in the case of an initially dense specimen.

2.3.2 Critical Void Ratio

Volume change characteristics depend upon various factors such as the particle size, particle shape and distribution, principal stresses, previous stress history and significantly on density index. Volume changes, expressed in terms of the void ratio versus shear strain are typically as shown in Fig. 2.

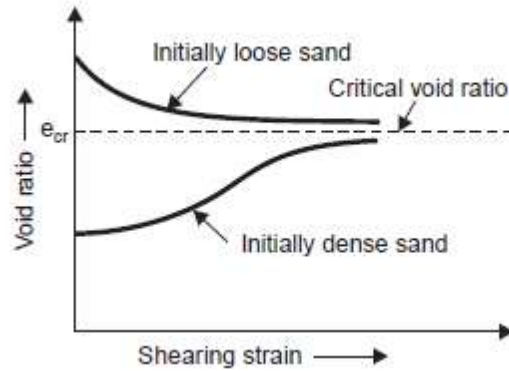


Fig. 2.32: Effect of initial density on changes in void ratio

At large strains both initially loose and initially dense specimens attain nearly the same void ratio, at which further strain will not produce any volume changes. Such a void ratio is usually referred to as the ‘Critical Void Ratio’. Sands with initial void ratio greater than the critical value will tend to decrease in volume during shearing, while sands with initial void ratio less than the critical will tend to increase in volume.

The critical void ratio is dependent upon the cell pressure (in the case of triaxial compression tests) or effective normal pressure (in the case of direct shear tests), besides a few other particle characteristics. It bears a reciprocal relationship with pressure. The value of critical void ratio under a given set of conditions may be determined by plotting the volume changes versus void ratio. The value for which the volume change is zero is the critical one.

2.4 SHEARING STRENGTH OF SANDS

The shearing strength of cohesionless soils has been established to depend primarily upon the angle of internal friction which itself is dependent upon a number of factors including the normal pressure on the failure plane. The nature of the results of the shear tests will be influenced by the type of test—direct shear or triaxial compression, by the fact whether the sand is saturated or dry and also by the nature of stresses considered—total or effective.

Each direct shear test is usually conducted under a certain normal stress. Each stress strain diagram therefore reflects the behaviour of a specimen under a particular normal stress. A number of specimens are tested under different normal stresses. It is to be noted that only the effective normal stress is capable of mobilising shear strength. The results when plotted appear as shown in Fig.2.32.

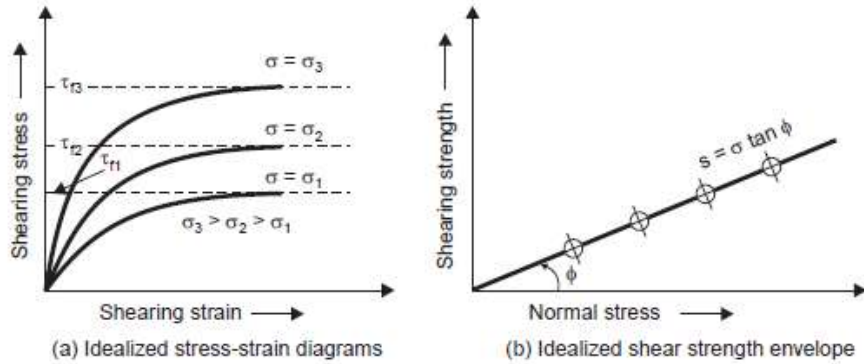


Fig. 2.32: Shear characteristics of sands from direct shear tests

It may be observed from Fig. 2.32 (a) that the greater the effective normal pressure during shear, the greater is the shearing stress at failure or shearing strength. The shear strength plotted against effective normal pressure gives the Coulomb strength envelope as a straight line, passing through the origin and inclined at the angle of internal friction to the normal stress axis. It is shown in Fig.2.32 (b). The failure envelope obtained from ultimate shear strength values is assumed to pass through the origin for dry cohesionless soils. The same is true even for saturated sands if the plot is made in terms of effective stresses. In the case of dense sands, the values of ϕ obtained by plotting peak strength values will be somewhat greater than those from ultimate strength values.

Ultimate values of ϕ may range from 29 to 35° and peak values from 32 to 45° for sands. The values of ϕ selected for use in practical problems should be related to soil strains expected. If soil deformation is limited, using the peak value for ϕ would be justified. If the deformation is relatively large, ultimate value of ϕ should be used

If the sand is moist, the failure envelope does not pass through the origin as shown in Fig. 2.33. The intercept on the shear stress axis is referred to as the ‘apparent cohesion’, attributed to factors such as surface tension of the moisture films on the grains. The extra strength would be lost if the soil were to dry out or to become saturated or submerged. For this reason the extra shear strength attributed to apparent cohesion is neglected in practice.

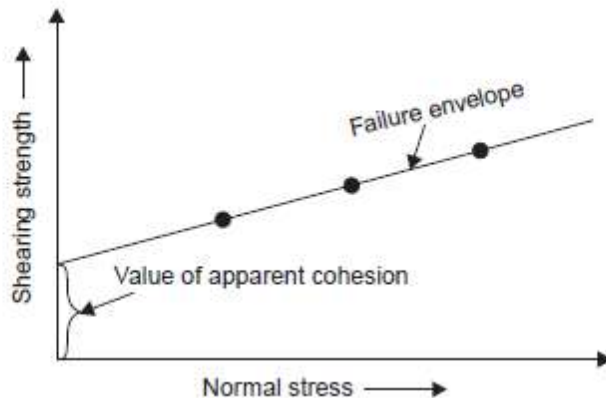


Fig. 2.33: Failure envelope for moist sand indicating apparent cohesion

In the case of triaxial compression tests, different tests with different cell pressure are to be conducted to evaluate the shearing strength and the angle of internal friction. In each test, the axial normal stress is gradually increased keeping the cell pressure constant, until failure occurs. The value of ϕ is obtained by plotting the Mohr Circles and the corresponding Mohr's envelope. The failure envelope obtained from a series of drained triaxial compression tests on saturated sand specimens initially at the same density index is approximately a straight line passing through the origin, as shown in Fig. 2.34.

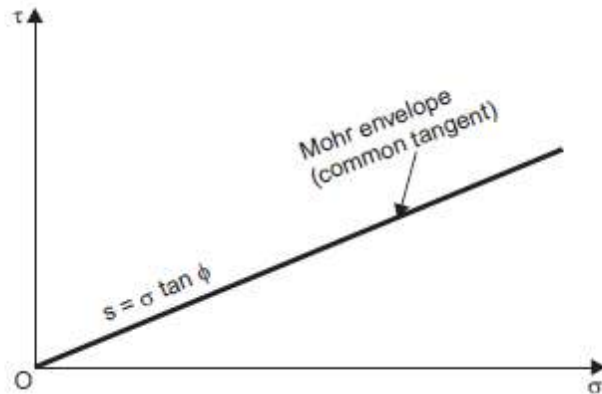


Fig. 2.34: Drained triaxial compression tests on saturated sand

Similar results are obtained when undrained triaxial compression tests are conducted with pore pressure measurements on saturated sand samples and Mohr's circles are plotted in terms of effective stresses. However, if Mohr's circles are plotted in terms of total stresses, the shape of envelopes will be similar to those for a purely cohesive soil. The failure envelope will be approximately horizontal with an intercept on the shearing stress axis, indicating the so called 'apparent cohesion', as shown in Fig. 2.35.

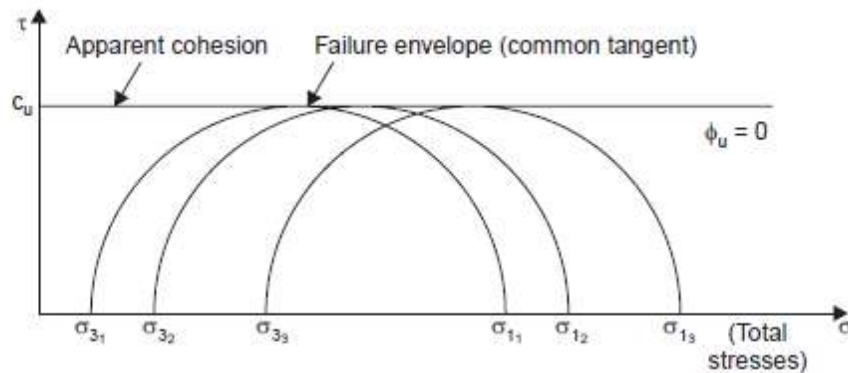


Fig. 2.35: Undrained triaxial compression tests on saturated sands (total stresses)

2.5 SHEARING CHARACTERISTICS OF CLAYS

The understanding of the fundamentals of shearing strength is much more important in the case of cohesive soils or clays in view of their troublesome nature with regard to stability. In fact, the most complex physical property of clays is the shearing strength, as it is dependent on a multitude of inter-related factors. One of the most difficult tasks is to interpret results of laboratory shearing strength tests to the shearing strength of natural clay deposits.

2.5.1 *Source and Nature of Shearing Strength of Clays*

i) Cohesion

This is a characteristic of true clay. This is sometimes referred to as no-load shear strength and is responsible for the strength of unconfined specimens. Cohesion in clays is a property which varies considerably with consistency. Cohesion therefore varies with both the type of clay and condition of clay. It is a kind of surface attraction among particles.

ii) Adhesion

Whereas cohesion is the mutual attraction of two different parts of a clay mass to each other, clay often also exhibits the property of 'adhesion', which is a propensity to adhere to other materials at a common surface. This has no relation to normal pressure. This is of particular interest in relation to the supporting capacity of friction piling in clays and to the lateral pressures on retaining walls.

iii) Viscous Friction

Solid friction effects are of relatively minor importance and the effects of viscous friction are quite pronounced. The laws of viscous friction are, in general, opposite to those of solid friction.

The total frictional resistance is independent of normal force, but varies directly with the contact area. It varies with some power of the relative velocity of adjacent layers of fluid or with the rate of shearing. The well-established fact that the strength of saturated clays varies with consistency also is in accord with the concept that strength is due to viscous rather than solid friction.

iv) Tensile Strength

In varying degrees and for different periods of time, many clays are capable of developing a certain amount of tensile strength. This may affect the magnitude of normal stresses on failure planes.

2.5.2 *Shearing Strength of Clays*

Shear behaviour of clays is influenced by the fact whether the clay is normally consolidated or over consolidated, by the fact whether it is undisturbed or remoulded, by the drainage conditions during testing, consistency of the clay, by certain structural effects, by the type of test and by the

type and rate of strain. The following discussion relates to the shearing strength of saturated clays which are in a normally consolidated state; the modifications that may be expected in case the clay is in an over consolidated state are indicated at the appropriate places.

2.5.3 Unconsolidated Undrained Tests

It is difficult, if not impossible, to utilise the concept of effective stress in connection with the shearing strength of saturated clays. It is difficult to imagine that any substantial part of the normal stress is transmitted through particle contacts when grain-to-grain contacts are relatively infrequent or when the solid phase is weak in itself. For this reason, it is common practice to consider only total stresses in the case of saturated clays. The results of unconsolidated undrained tests in direct shear are indicated in Fig.2.36.

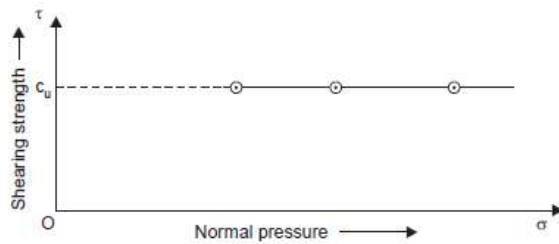


Fig. 2.36: Unconsolidated undrained tests in direct shear on saturated clays

It is seen that the total normal pressure does not influence the shearing strength of saturated clay from undrained tests; the intercept of the horizontal plot on the shear strength axis gives the cohesion c_u . The strength of clay is often reported simply in terms of unit cohesion, regardless of the overburden pressure. The results of such tests in triaxial compression are indicated in Fig. 2.37.

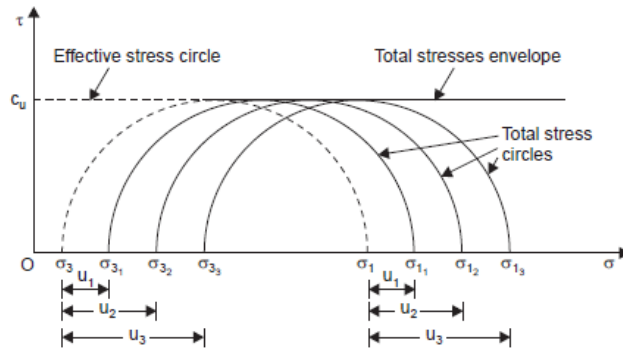


Fig. 2.36: Unconsolidated undrained tests in triaxial compression on saturated clays

Since drainage is not permitted both during the application of cell pressure and during the application of deviator stress (or additional axial stress), the increase in cell pressure or axial stress automatically increases the pore water pressure by an equal magnitude, the effective stress

remaining constant. In view of this, the diameter of the effective stress circle will be the same as that of the total stress circles with mere lateral shifts. The total stress envelope is thus a horizontal line, the intercept on the shearing strength axis being cohesion C_u and Q_u being zero. It may also be easily understood that the effective stress envelope cannot be obtained from these tests since only one circle will be obtained for all tests. Consolidated undrained or drained tests may be used for this purpose. Pore pressure measurements are not usually made in the unconsolidated undrained tests as they are not useful. It is common knowledge that the shear strength of clay varies widely with its consistency, the shear strength being negligible when the water content is at liquid limit. This is reflected in Fig. 2.36.

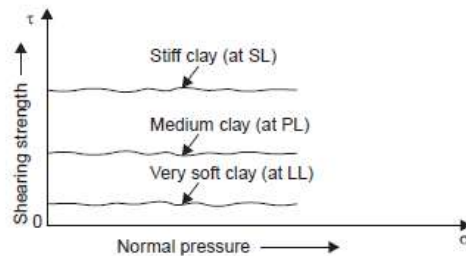


Fig.2.36: Variation of shearing strength with consistency of saturated clays
 The shearing strength of partially saturated clays is a more complex phenomenon and, hence, is considered outside the scope of the present work.

2.5.4 Consolidated Undrained Tests

If consolidated undrained tests are conducted in direct shear on remoulded, saturated and normally consolidated clay specimens with the same initial void ratio, but consolidated under different normal pressures, and sheared under the normal pressure of consolidation, without permitting drainage during shear, results as indicated in Fig. 2.37 are obtained.

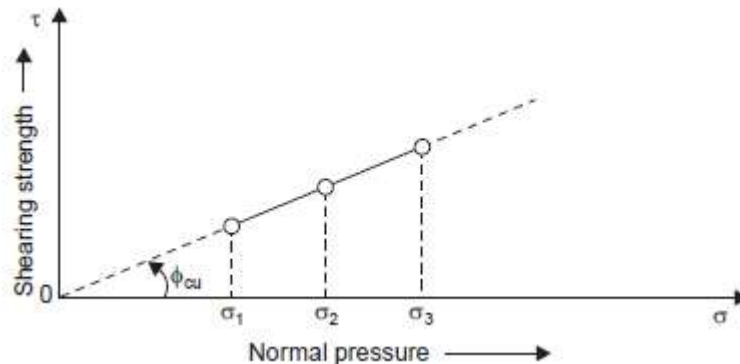


Fig. 2.37 Consolidated undrained tests in direct shear on remoulded, saturated, and normally consolidated clay (consolidated and sheared under normal pressures σ_1 , σ_2 , and σ_3)

It is observed that the shear strength is proportional to the normal pressure. The strength envelope passes through the origin, giving an angle of shearing resistance ϕ_{cu} . However, it is fallacious to assume that the shear strength is related to the normal pressure during the application of shear. This may be demonstrated by consolidating all the samples under one particular pressure and testing them in shear under a different pressure. In such a case the results will appear somewhat as shown in Fig.2.38.

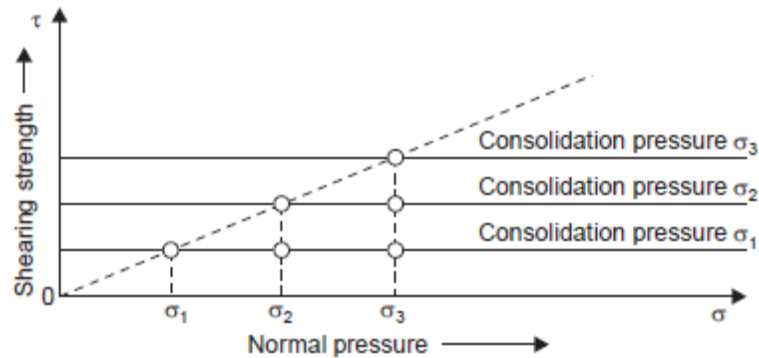


Fig. 2.38: Consolidated undrained tests in direct shear on remoulded, saturated, and normally consolidated clay (consolidated under normal pressures σ_1 , σ_2 , and σ_3 , and sheared under different normal pressures)

It is observed that the shearing strength is independent of the normal pressure during shear but is dependent only on the normal pressure during consolidation or consolidation pressure. The process of pre consolidation may thus be viewed simply as a method of changing the consistency of the clay, the strength at a given consistency being practically independent of normal pressure during shear.

Similarly, consolidated undrained tests may be conducted in triaxial compression by either of the following procedures:

- (i) The specimens of saturated, remoulded, and normally consolidated clay are consolidated under different cell pressures and sheared, without permitting drainage, under a cell pressure equal to the consolidation pressure. This approach is more commonly used.
- (ii) The specimens are consolidated under the same cell pressure σ_c , and then sheared under undrained conditions with different cell pressures by increasing the axial stress; different series of these tests may be performed with different values of cell pressure for consolidation, which will be constant for any one series, as stated above.

The results from the first method appear somewhat as shown in Fig. 6; total stress envelopes as well as effective stress envelopes are shown.

The failure envelopes pass through the origin, giving $c_{cu} = c_{cu}' = 0$, and values of ϕ_{cu} and ϕ_{cu}' such that $\phi_{cu}' > \phi_{cu}$. If the tests are conducted starting with a very low consolidation pressure, the initial portion of the envelope is usually curved and shows a cohesion intercept. The straight portion when extended passes through the origin.

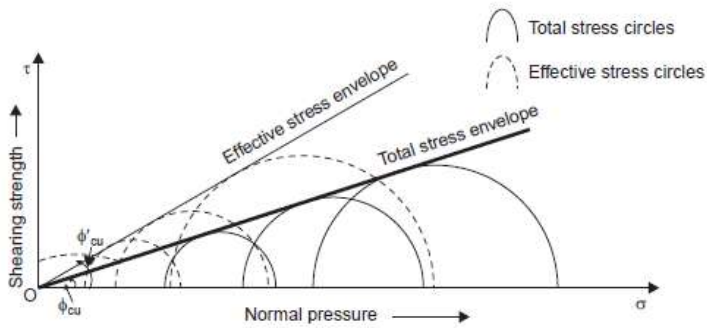


Fig.2.39: Consolidated undrained tests in triaxial compression on remoulded, saturated, and normally consolidated clay (consolidated under different cell pressures and sheared undrained under the same cell pressures)

An over consolidated clay shows an apparent cohesion; the equation for shear strength Here, σ_c is the consolidation pressure and σ is the applied normal pressure. The envelope is generally curved up to the pre consolidation pressure and shows a cohesion intercept. The corresponding equations for shear strength in terms of effective stresses are written with primes.

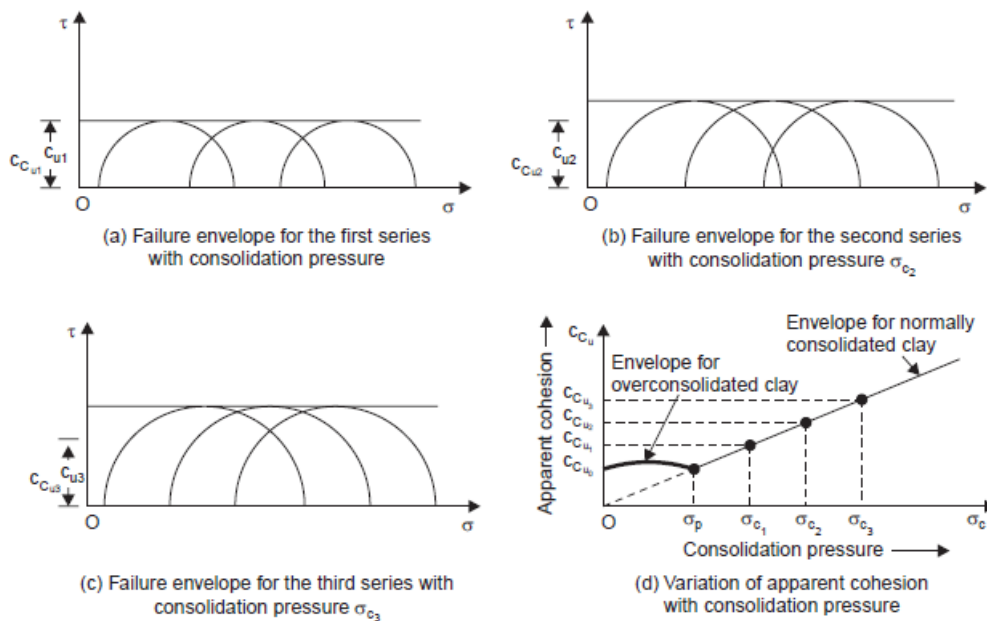


Fig.2.40: Consolidated undrained tests in triaxial compression on remoulded, saturated, and normally consolidated clay consolidated under a particular cell pressure and sheared undrained under cell pressures different from consolidated pressures

The effect of pre consolidation is to reduce the value of A-parameter and thus cause higher strength. At higher values of over-consolidation ratio, A-factor may be even negative; the effective stress circles will then get shifted to the right of the total stress circles instead of to the

left. This gives lower value of effective apparent cohesion and higher value of effective angle of shearing resistance than those of total stress values.

The results from the second method appear somewhat as shown in Fig.2.40. The results indicate that, for a particular series, the deviator stress at failure is independent of the cell pressure. The failure envelope will be horizontal for each series, the apparent cohesion c_u being different for different series; the angle ϕ_u is zero, as indicated by Fig. 2.40 (a), (b) and (c). The greater the effective consolidation pressure, the greater is the apparent cohesion. This is indicated in Fig. 2.40 (d). If the clay is over-consolidated, the consolidation pressure versus apparent cohesion curve will show a discontinuity at the pressure corresponding to the pre consolidation pressure; below this pressure, the relationship is non-linear and will show an intercept at zero pressure and, above this pressure, it is linear. If the clay is normally consolidated for all the consolidation pressures used in the tests, this relationship will be a straight line, which, when produced backwards, will pass through the-origin.

2.5.5 Drained Tests

The specimen is first consolidated under a certain cell pressure and is then sheared sufficiently slowly so that no pore pressures are allowed to develop at any stage. The effective stresses will be the same as the total stresses. The results will be similar to those obtained from the consolidated undrained tests, with the same modifications as for a clay in an over consolidated condition, as shown in Fig. 2.41.

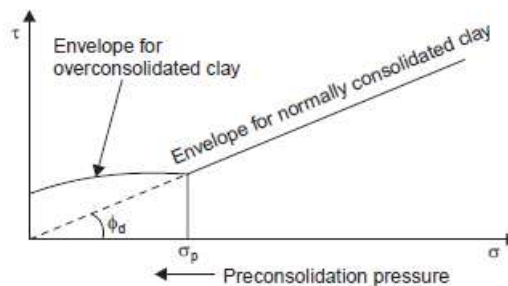


Fig.2.41: Drained tests in triaxial compression on a remoulded saturated clay sheared under cell pressure equal to the consolidation pressure

2.5.6 Stress-strain Behaviour of Clays

The stress-strain behaviour of clays is primarily dependent upon whether the clay is in a normally consolidated state or in an over consolidated state. The stress-strain relationships for a normally consolidated clay and those for an over consolidated clay are shown in Figs. 2.42 and 2.43 respectively.

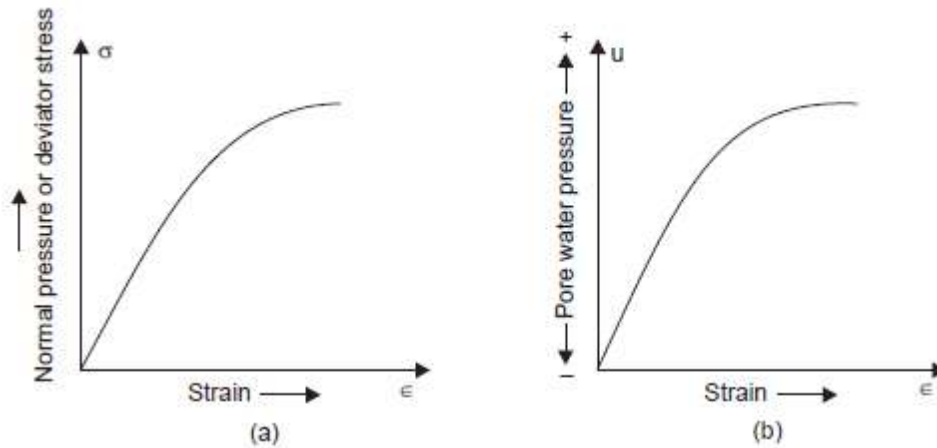


Fig. 2.42: Stress-strain relationships for normally consolidated clay

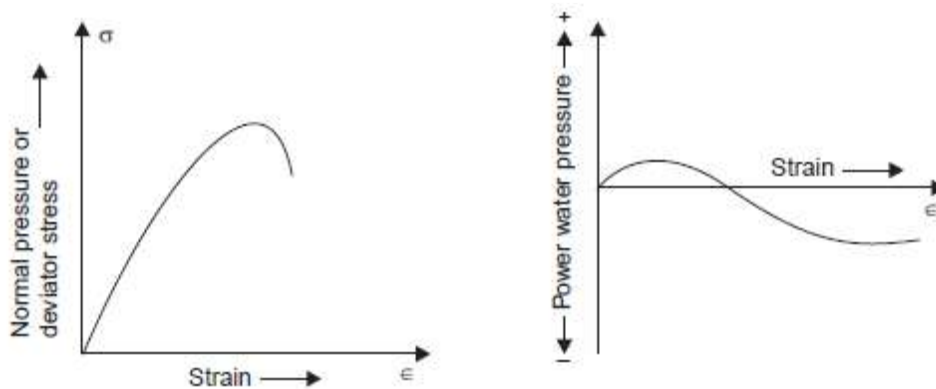


Fig.2.43: Stress-strain relationships for an over consolidated clay

The behaviour of a normally consolidated clay is somewhat similar to that of a loose sand and that of an over consolidated clay is similar to that of a dense sand. In the case of plastic nature of stress-strain relationship with no specific failure point, an arbitrary strain of 15 to 20% is considered to be representative of failure condition.

2.5.7 Effect of Rate and Nature of Shear Strain

Clays are often sensitive to the rate and manner of shearing. Usually standard rates of shearing are adopted for proper comparison. A strain of about 0.10 to 0.15 cm/min., is considered standard in strain-controlled direct shear. However, it is not common that strain is controlled in nature or in construction operations.

It is observed that shear strength increases somewhat with increased rates of strain. If the loading is not at a uniform rate but is effected in increments, much greater shearing resistance is developed; however, the failure in such a case is observed to occur rather suddenly. The increase in shear strength could be as much as 25% with increase in rate of strain from a very slow rate; this increase would be as high as 100% or more if the loading is by increments.

If there is interruption of strain, the shear stress could decrease steadily by a creep in saturated clays; but in the case of sands, this will not have any significant effect on shearing stress. Also, greater shearing displacements are associated with smaller rates of shearing strain and vice versa. This is also in contrast to the behaviour of sand for which these factor do not appear to materially affect the results.

Example 1: The stresses at failure on the failure plane in a cohesionless soil mass were:

Shear stress = 4 kN/m²; normal stress = 10 kN/m². Determine the resultant stress on the failure plane, the angle of internal friction of the soil and the angle of inclination of the failure plane to the major principal plane.

Sol: Resultant stress = $\sqrt{\sigma^2 + \tau^2}$
 $= \sqrt{100 + 16} = 10.77 \text{ kN/m}^2$

$\tan\phi = 4/10 = 0.4$

$\phi = 21^\circ 48'$

$\theta = 45^\circ + 21^\circ 48'/2$

$= 55^\circ 54'$

Graphical solution (Fig. 1):

The procedure is first to draw the σ - and τ -axes from an origin O and then, to a suitable scale, set-off point D with coordinates (10,4). Joining O to D , the strength envelope is got. The Mohr Circle should be tangential to OD to D . DC is drawn perpendicular to OD to cut OX in C , which is the centre of the circle. With C as the centre and CD as radius, the circle is completed to cut OX in A and B .

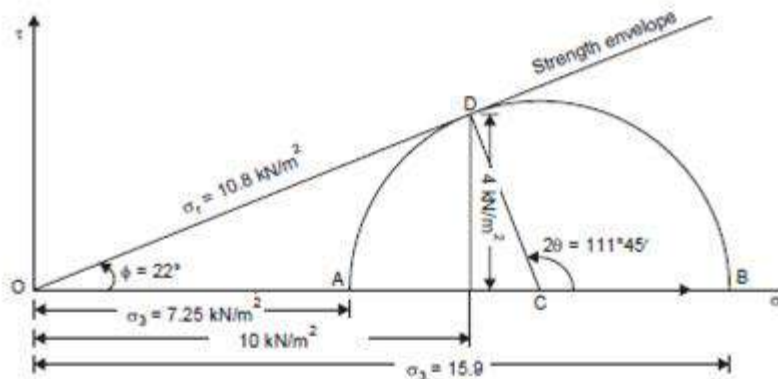


Fig.1

By scaling, the resultant stress = $OD = 10.8 \text{ kN/m}^2$.

With protractor, $\phi = 22^\circ$ and $\theta = 55^\circ 53'$

We also observe that $\sigma_3 = OA = 7.25 \text{ kN/m}^2$ and $\sigma_1 = OB = 15.9 \text{ kN/m}^2$.

Example 2 : Calculate the potential shear strength on a horizontal plane at a depth of 3 m below the surface in a formation of cohesionless soil when the water table is at a depth of 3.5 m. The degree of saturation may be taken as 0.5 on the average. Void ratio = 0.50; grain specific gravity = 2.70; angle of internal friction = 30°. What will be the modified value of shear strength if the water table reaches the ground surface ?

$$\begin{aligned} \text{Effective unit weight } \gamma &= \frac{(G - 1)}{(1 + e)} \cdot \gamma_w \\ &= \frac{(2.70 - 1)}{(1 + 0.5)} \times 10 = 11.33 \text{ kN/m}^3 \end{aligned}$$

Unit weight, γ , at 50% saturation

$$= \frac{(G + S \cdot e)}{(1 + e)} \cdot \gamma_w = \frac{(2.70 + 0.5 \times 0.5)}{(1 + 0.5)} \times 10 = 19.667 \text{ kN/m}^3$$

(a) When the water table is at 3.5 m below the surface:

Normal stress at 3 m depth, $\sigma = 19.67 \times 3 = 59 \text{ kN/m}^2$

Shear strength, $s = \sigma \tan \phi$ for a sand
 $= 59 \tan 30^\circ = 34 \text{ kN/m}^2$ (nearly).

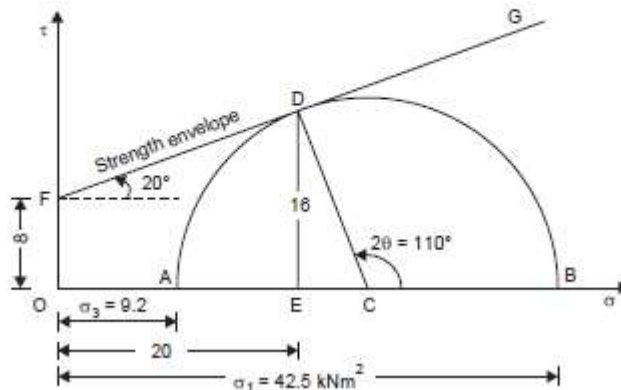
(b) When water table reaches the ground surface:

Effective Normal stress at 3 m depth

$$\bar{\sigma} = \gamma' \cdot h = 11.33 \times 3 = 34 \text{ kN/m}^2$$

Shear strength, $s = \bar{\sigma} \tan \phi$
 $= 34 \tan 30^\circ$
 $= 19.6 \text{ kN/m}^2$ (nearly).

Example 3 : The following data were obtained in a direct shear test. Normal pressure = 20 kN/m², tangential pressure = 16 kN/m². Angle of internal friction = 20°, cohesion = 8 kN/m². Represent the data by Mohr's Circle and compute the principal stresses and the direction of the principal planes.



The strength envelope FG is located since both c and ϕ are given. Point D is set-off with co-ordinates (20, 16) with respect to the origin O ; it should fall on the envelope. (In this case, there appears to be slight discrepancy in the data). DC is drawn perpendicular to FD to meet the σ -axis in C . With C as centre and CD as radius, the Mohr's circle is completed. The principal stresses σ_3 (OA) and σ_1 (OB) are scaled off and found to be 9.2 kN/m² and 42.5 kN/m². Angle BCD is measured and found to be 110°. Hence the major principal plane is inclined at 55° (clockwise) and the minor principal plane at 35° (counter clockwise) to the plane of shear

Analytical solution:

$$\begin{aligned} \sigma_1 &= \sigma_3 N_\phi + 2c \sqrt{N_\phi} \\ N_\phi &= \tan^2 (45^\circ + \phi/2) = \tan^2 55^\circ = 2.04 \\ \sigma_1 &= 2.04 \sigma_3 + 2 \times 8 \times \tan 55^\circ = 2.04 \sigma_3 + 22.88 \end{aligned} \quad \dots(1)$$

$$\begin{aligned} \sigma_n &= \sigma_1 \cos^2 55^\circ + \sigma_3 \sin^2 55^\circ = 20 \\ 0.33 \sigma_1 + 0.67 \sigma_3 &= 20 \end{aligned} \quad \dots(2)$$

Solving, $\sigma_1 = 42.5 \text{ kN/m}^2$ and $\sigma_3 = 9.2 \text{ kN/m}^2$, as obtained graphically.

Example 4 : A series of shear tests were performed on a soil. Each test was carried out until the sample sheared and the principal stresses for each test were :

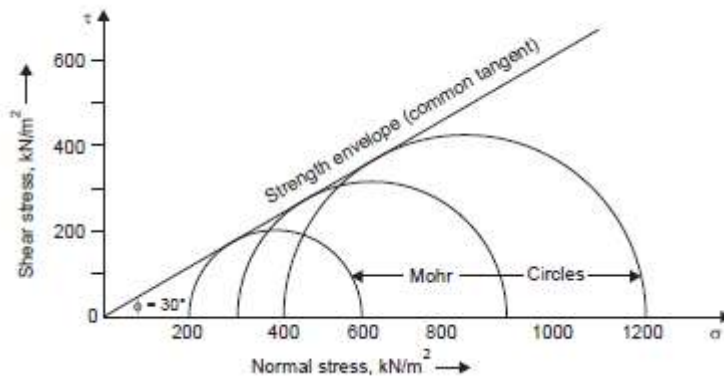
Test No.	(kN/m ²)	(kN/m ²)
1	200	600
2	300	900
3	400	1200

Plot the Mohr's circles and hence determine the strength envelope and angle of internal friction of the soil.

Sol:

The data indicate that the tests are triaxial compression tests; the Mohr's circles are plotted with $(\sigma_1 - \sigma_3)$ as diameter and the strength envelope is obtained as the common tangent.

The angle of internal friction of found to be 30° , by measurement with a protractor from



Example 5 : A particular soil failed under a major principal stress of 300 kN/m^2 with a corresponding minor principal stress of 100 kN/m^2 . If, for the same soil, the minor principal stress had been 200 kN/m^2 , determine what the major principal stress would have been if

- (a) $\phi = 30^\circ$ and (b) $\phi = 0^\circ$.

The Mohr circle of stress is drawn to which the strength envelope will be tangential; the envelopes for $\phi = 0^\circ$ and $\phi = 30^\circ$ are drawn. Two stress circles, each starting at a minor principal stress value of 200 kN/m^2 , one tangential to $\phi = 0^\circ$ envelope, and the other tangential to $\phi = 30^\circ$ envelope are drawn.

The corresponding major principal stresses are scaled off as 400 kN/m^2 and 600 kN/m^2 .

Analytical solution:

- (a) $\phi = 30^\circ$;

$$\sigma_3 = 100 \text{ kN/m}^2, \sigma_1 = 300 \text{ kN/m}^2$$

$$\frac{\sigma_3}{\sigma_1} = \frac{1 - \sin \phi}{1 + \sin \phi} = \frac{1 - \sin 30^\circ}{1 + \sin 30^\circ} = 1/3$$

The given stress circle will be tangential to the strength envelope with $\phi = 30^\circ$.

With $\sigma_3 = 200 \text{ kN/m}^2$, $\sigma_1 = 3 \times 200 = 600 \text{ kN/m}^2$,

if the circle is to be tangential to the strength envelope $\phi = 30^\circ$ passing through the origin.

- (b) $\phi = 0^\circ$;

If the given stress circle has to be tangential to the strength envelope $\phi = 0^\circ$, the envelope has to be drawn with $c = \tau = 100 \text{ kN/m}^2$. The deviator stress will then be 200 kN/m^2 , irrespective of the minor principal stress.

Hence $\sigma_1 = 200 + 200 = 400 \text{ kN/m}^2$ for $\sigma_3 = 200 \text{ kN/m}^2$.

Example 6 In a triaxial shear test conducted on a soil sample having a cohesion of 12 kN/m^2 and angle of shearing resistance of 36° , the cell pressure was 200 kN/m^2 . Determine the value of the deviator stress at failure.

Sol:

Analytical solution:

$$c = 12 \text{ kN/m}^2$$

$$\phi = 36^\circ$$

$$\sigma_3 = 200 \text{ kN/m}^2$$

$$\sigma_1 = \sigma_3 N_\phi + 2c\sqrt{N_\phi}$$

where $N_\phi = \tan^2(45^\circ + \phi/2)$.

$$N_\phi = \tan^2(45^\circ + 18^\circ) = \tan^2 63^\circ = 3.8518$$

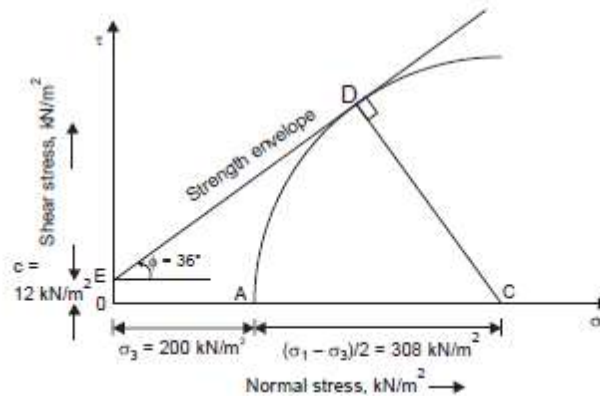
$$\sqrt{N_\phi} = \tan 63^\circ = 1.9626$$

$$\therefore \sigma_1 = 200 \times 3.8518 + 2 \times 12 \times 1.9626 = 817.5 \text{ kN/m}^2$$

$$\text{Deviator stress} = \sigma_1 - \sigma_3 = (817.5 - 200) \text{ kN/m}^2 = 617.5 \text{ kN/m}^2$$

Graphical Sol:

The strength envelope is drawn through E on the τ -axis, OE being equal to $C = 12 \text{ kN/m}^2$ to a convenient scale, at an angle $\phi = 36^\circ$ with the σ -axis. The cell pressure, $\sigma_3 = 200 \text{ kN/m}^2$ is plotted as OA . With centre on the σ -axis, a circle is drawn to pass through A and be tangential to the envelope, by trial and error. AC is scaled-off, C being the centre of the Mohr's circle, which is $(\sigma_1 - \sigma_3)/2$. The deviator stress is double this value. In this case the result is 616 kN/m^2 . (Fig. 8.54).



Example 7 : The shearing resistance of a soil is determined by the equation $s = c' + \sigma' \tan \phi'$. Two drained triaxial tests are performed on the material. In the first test the all-round pressure is 200 kN/m^2 and failure occurs at an added axial stress of 600 kN/m^2 . In the second test all-round pressure is 350 kN/m^2 and failure occurs at an added axial stress of 1050 kN/m^2 . What values of c' and ϕ' correspond to these results?

Sol:

Analytical method:

Since the tests are drained tests, we may assume $c' = 0$. On this basis, we may obtain N_ϕ .

$$\text{From both tests, } N_\phi = \sigma_1/\sigma_3 = 4$$

$$\therefore \sqrt{N_\phi} = \tan(45^\circ + \phi'/2) = 2$$

$$\text{or } 45^\circ + \phi'/2 = 63^\circ 25', \phi'/2 = 18^\circ 25'$$

$$\therefore \phi' = 36^\circ 50'$$

Graphical method:

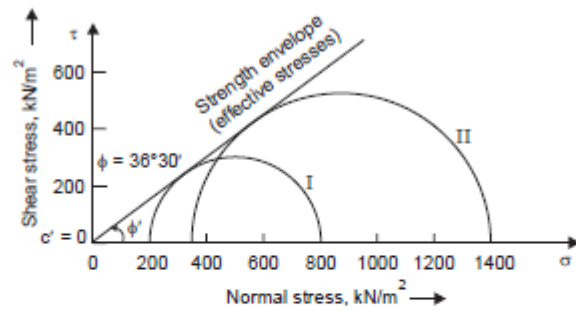


Fig. 8.58 Mohr's circle for effective stress (Ex. 8.15)

Since the cell pressures (σ_3) and the added axial stresses ($\sigma_1 - \sigma_3$) are known, σ_1 -values are also obtained by addition. The Mohr's circles for the two tests are drawn. The common tangent to the two circles is seen to pass very nearly through the origin and is sketched. The inclination of this line, which is the strength envelope in terms of effective stresses, with the σ -axis is the effective friction angle. The value of c' is zero; and the value of ϕ' , as measured with a protractor, is $36^{\circ}30'$.

3.0 STRESS PATH

Results of triaxial tests can be represented by diagrams called *stress paths*. A stress path is a line connecting a series of points, each point representing a successive stress state experienced by a soil specimen during the progress of a test. There are several ways in which the stress path can be drawn, two of which are discussed below.

Rendulic plot

A Rendulic plot is a plot representing the stress path for triaxial tests originally suggested by Rendulic (1937) and later developed by Henkel (1960). It is a plot of the state of stress during triaxial tests on a plane $Oabc$, as shown in Figure 3.1.

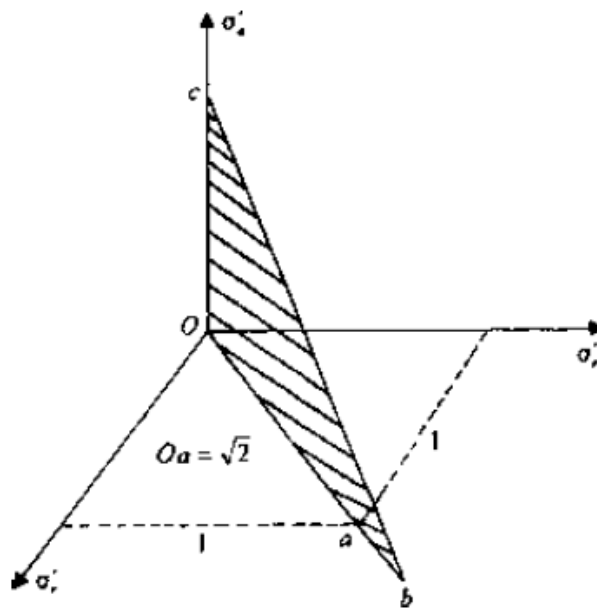


Fig.3.1: Rendulic plot

Along Oa , we plot $\sqrt{2}\sigma'_r$, and along Oc , we plot σ'_a (σ'_r is the effective radial stress and σ'_a the effective axial stress). Line Od in Figure 3.2 represents the isotropic stress line.

The direction cosines of this line are $1/\sqrt{3}, 1/\sqrt{3}, 1/\sqrt{3}$. Line Od in Figure 3.2 will have a slope of 1 vertical to $\sqrt{2}$ horizontal. Note that the trace of the octahedral plane $\sigma'_1 + \sigma'_2 + \sigma'_3 = \text{constant}$ will be at right angles to the line Od .

In triaxial equipment, if a soil specimen is hydrostatically consolidated (i.e., $\sigma'_a = \sigma'_r$), it may be represented by point 1 on the line Od . If this specimen is subjected to a drained axial compression test by increasing σ'_a and keeping σ'_r constant, the stress path can be represented by the line 1–2.

Point 2 represents the state of stress at failure. Similarly,

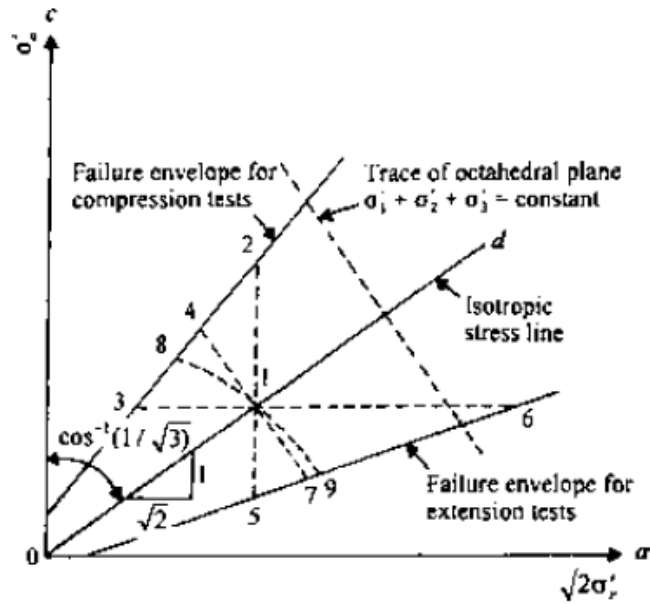


Fig.3.2: Rendulic diagram with Isotropic line

Line 1–3 will represent a drained axial compression test conducted by keeping σ'_a constant and reducing σ'_r .

Line 1–4 will represent a drained axial compression test where the mean principal stress (or $J = \sigma'_1 + \sigma'_2 + \sigma'_3$) is kept constant.

Line 1–5 will represent a drained axial extension test conducted by keeping σ'_r constant and reducing σ'_a .

Line 1–6 will represent a drained axial extension test conducted by keeping σ'_a constant and increasing σ'_r .

Line 1–7 will represent a drained axial extension test with $J = \sigma'_1 + \sigma'_2 + \sigma'_3$ constant (i.e., $J = \sigma'_a + 2\sigma'_r$ constant).

Curve 1–8 will represent an undrained compression test.

Curve 1–9 will represent an undrained extension test.

Curves 1–8 and 1–9 are independent of the total stress combination, since the pore water pressure is adjusted to follow the stress path shown.

If we are given the effective stress path from a triaxial test in which failure of the specimen was caused by loading in an undrained condition, the pore water pressure at a given state during the loading can be easily determined.

This can be explained with the aid of Figure 3.3.

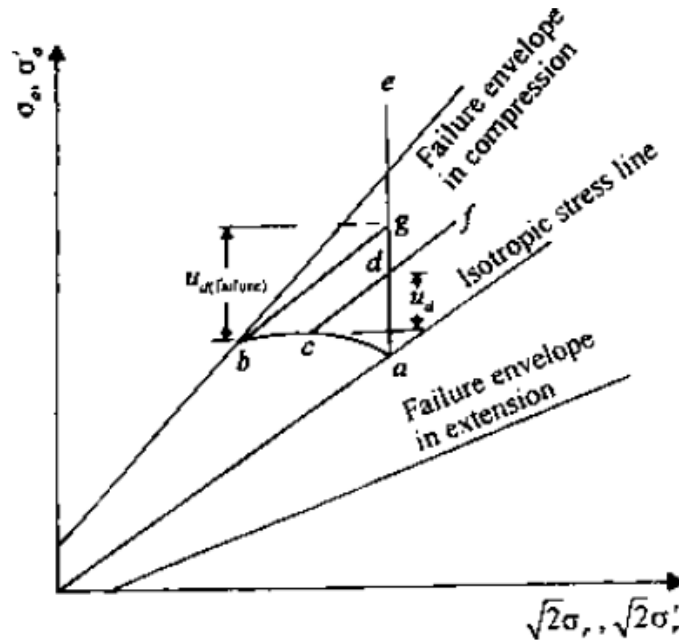


Fig.3.3: Determination of pore water pressure in a Rendulic plot

Consider a soil specimen consolidated with an encompassing pressure σ'_r and with failure caused in the undrained condition by increasing the axial stress σ'_a . Let acb be the effective stress path for this test. We are required to find the excess pore water pressures that were generated at points c and b (i.e., at failure). For this type of triaxial test, we know that the *total stress path* will follow a vertical line such as ae . To find the excess pore water pressure at c , we draw a line cf parallel to the isotropic stress line. Line cf intersects line ae at d . The pore water pressure u_d at c is the *vertical distance* between points c and d . The pore water pressure $u_{d\text{failure}}$ at b can similarly be found by drawing bg parallel to the isotropic stress line and measuring the vertical distance between points b and g .

3.1 LAMBE'S STRESS PATH

Lambe (1964) suggested another type of stress path in which are plotted the successive effective normal and shear stresses on a plane making an angle of 45° to the major principal plane. To understand what a stress path is, consider a normally consolidated clay specimen subjected to a consolidated drained triaxial test (Figure 3.4a).

At any time during the test, the stress condition in the specimen can be represented by Mohr's circle (Figure 4b). Note here that, in a drained test, total stress is equal to effective stress. So

$$\sigma_3 = \sigma'_3 \text{ (minor principal stress)} \text{-----} \text{Eq.3.1}$$

$$\sigma_1 = \sigma_3 + \Delta\sigma = \sigma'_1 \text{ (Major Principal Stress)} \text{-----} \quad \text{Eq.3.2}$$

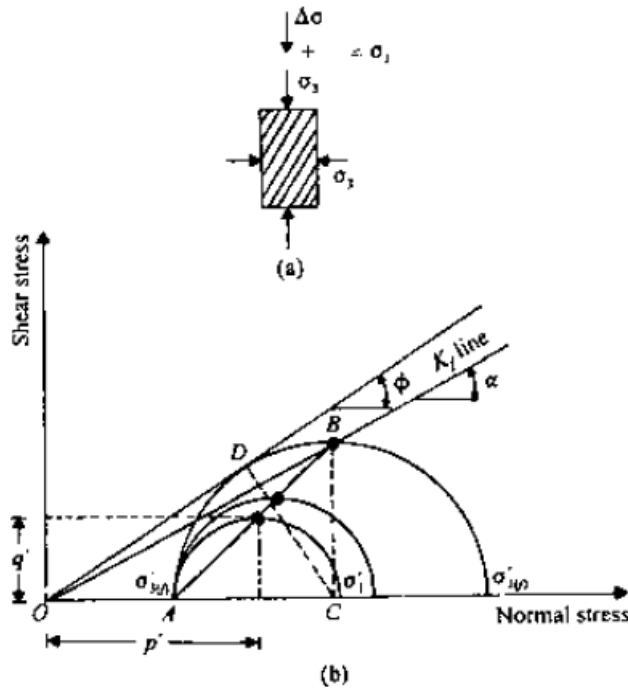


Fig.3.4: Definition of stress path

At failure, Mohr's circle will touch a line that is the Mohr–Coulomb failure envelope; this makes an angle ϕ with the normal stress axis (ϕ is the soil friction angle).

We now consider the effective normal and shear stresses on a plane making an angle of 45° with the major principal plane. Thus

$$\text{Effective normal stress, } p' = \frac{\sigma'_1 + \sigma'_3}{2} \text{-----} \quad \text{Eq.3.3}$$

$$\text{Shear stress, } q' = \frac{\sigma'_1 - \sigma'_3}{2} \text{-----} \quad \text{Eq.3.4}$$

The points on Mohr's circle having coordinates p and q are shown in Figure 4 *b*. If the points with p' and q' coordinates of all Mohr's circles are joined, this will result in the line *AB*. This line is called a stress path.

The straight line joining the origin and point *B* will be defined here as **the K_f line**. The K_f line makes an angle α with the normal stress axis. Now

$$\tan\alpha = \frac{BC}{OC} = \frac{\sigma'_{1f} - \sigma'_{3f}}{\sigma'_{1f} + \sigma'_{3f}} \text{-----} \quad \text{Eq.3.5}$$

Where, σ'_{1f} and σ'_{3f} are the effective major and minor principal stress at failure.

Similarly

$$\sin\phi = \frac{DC}{OC} = \frac{\sigma'_{1f} - \sigma'_{3f}}{\sigma'_{1f} + \sigma'_{3f}} \text{-----} \quad \text{Eq.3.6}$$

$$\text{Thus, } \tan\alpha = \sin\phi \text{-----} \quad \text{Eq.3.7}$$

For a consolidated un-drained test, consider a clay specimen consolidated under an isotropic stress $\sigma_3 = \sigma'_3$ in a triaxial test. When a deviator stress $\Delta\sigma$ is applied on the specimen and drainage is not permitted, there will be an increase in the pore water pressure, Δu (Figure 3.5 a) $\Delta u = A\Delta\sigma$, where A is the pore water pressure parameter.

At this time the effective major and minor principal stresses can be given as

$$\text{Major effective principal stress, } \sigma'_1 = \sigma_1 - \Delta u \text{-----} \quad \text{Eq.3.8}$$

$$\text{Minor effective principal stress, } \sigma'_3 = \sigma_3 - \Delta u \text{-----} \quad \text{Eq.3.9}$$

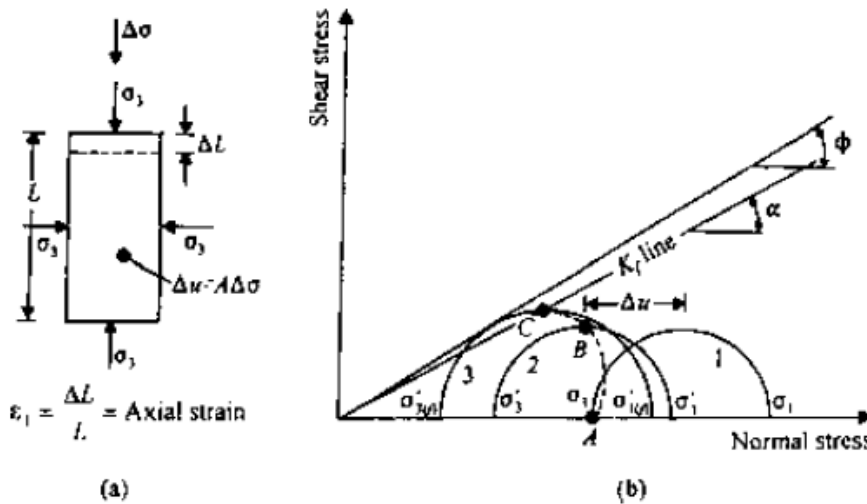


Fig.3.5: Stress Path for Consolidated Un-drained Triaxial Test

Mohr's circles for the total and effective stress at any time of deviator stress application are shown in Figure 3.5 b. (Mohr's circle no. 1 is for total stress and no. 2 for effective stress.) Point B on the effective-stress Mohr's circle has the coordinates p' and q' . If the deviator stress is increased until failure occurs, the effective-stress Mohr's circle at failure will be represented by circle no. 3, as shown in Figure 3.5 b, and the effective-stress path will be represented by the curve ABC .

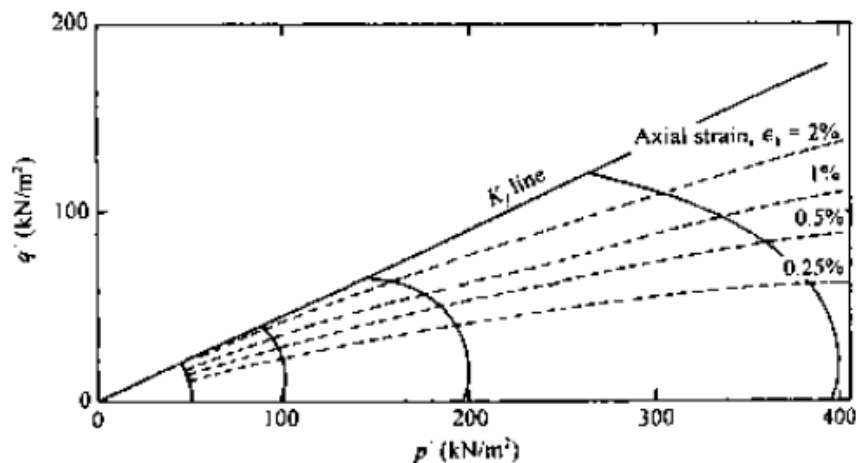


Fig.3.6: Stress Path for Lagunilla Clay (after Lambe, 1964)

The general nature of effective-stress path will depend on the value of A . Figure 3.6 shows the stress path in p' versus q' plot for Lagunilla clay (Lambe, 1964). In any particular problem, if a stress path is given in p' versus q' plot, we should be able to determine the values of the major and minor effective principal stresses for any given point on the stress path. This is demonstrated in Figure 3.7, in which ABC is an effective stress path.

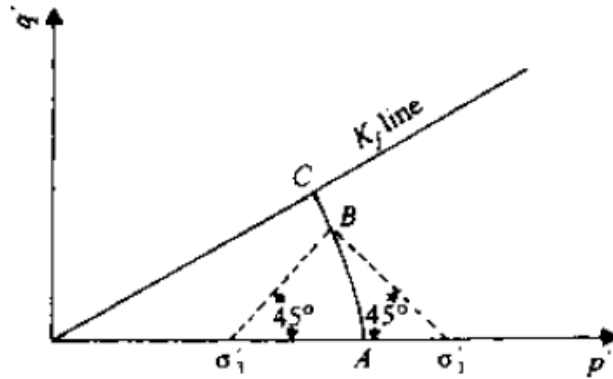


Fig.3.7: Determination of major and minor principal stresses for a point on a stress path

From the Figure 3.6, two important aspects of effective stress path can be summarized as follows:

1. The stress paths for a given normally consolidated soil are geometrically similar.
2. The axial strain in a CU test may be defined as $\epsilon_1 = L/L$ as shown in Figure 3.5a. For a given soil, if the points representing equal strain in a number of stress paths are joined, they will be approximately straight lines passing through the origin. This is also shown in Figure 3.6.

Example 1

For a saturated clay soil, the following are the results of some consolidated, drained triaxial tests at failure:

Test no.	$p' = \frac{\sigma'_1 + \sigma'_3}{2} \text{ (kN/m}^2\text{)}$	$q' = \frac{\sigma'_1 - \sigma'_3}{2} \text{ (kN/m}^2\text{)}$
1	420	179.2
2	630	255.5
3	770	308.0
4	1260	467.0

Draw a p' versus q' diagram, and from that, determine c and ϕ for the soil.

SOLUTION The diagram of q' versus p' is shown in Figure 8 this is a straight line, and the equation of it may be written in the form

$$q' = m + p' \tan \alpha \quad \text{Eq.1}$$

Also,

$$\frac{\sigma'_1 - \sigma'_3}{2} = c \cos \phi + \frac{\sigma'_1 + \sigma'_3}{2} \sin \phi \quad \text{Eq.2}$$

Comparing Eqs. we find $m = c \cos \phi$ or $c = m / \cos \phi$ and $\tan \alpha = \sin \phi$. From Figure 8, $m = 23.8 \text{ kN/m}^2$ and $\alpha = 20^\circ$. So

$$\phi = \sin^{-1}(\tan 20^\circ) = 21.34^\circ$$

and

$$c = \frac{m}{\cos \alpha} = \frac{23.8}{\cos 21.34^\circ} = 25.55 \text{ kN/m}^2$$

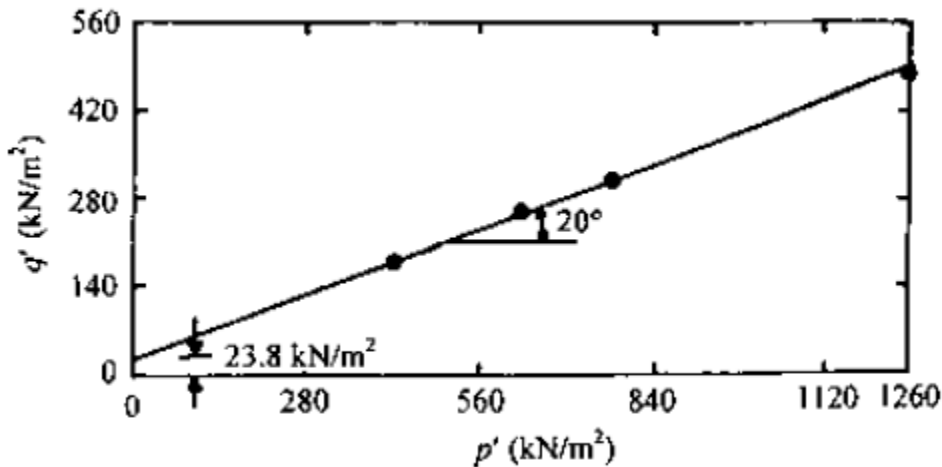


Figure 3.8 Plot of q' versus p'

Example: 2

Two cylindrical specimens of a soil, A and B, were loaded as follows. Both specimens were isotropically loaded by a stress of 200 kPa under drained conditions. Subsequently, the radial stress applied on specimen A was held constant and the axial stress was incrementally increased to 440 kPa under undrained conditions. The axial stress on specimen B was held constant and the radial stress incrementally reduced to 50 kPa under drained conditions. Plot the total and effective stress paths for each specimen, assuming the soil is a linear, isotropic, elastic material. Calculate the maximum excess porewater pressure in specimen A.

Solution:

Step 1: Determine loading condition.

Loading is axisymmetric, and both drained and undrained conditions are specified.

Step 2: Calculate initial stress invariants for isotropic loading path.

For axisymmetric, isotropic loading under drained conditions, $\Delta u = 0$,

$$\Delta p' = \frac{\Delta \sigma'_a + 2\Delta \sigma'_r}{3} = \frac{\Delta \sigma'_l + 2\Delta \sigma'_l}{3} = \Delta \sigma'_l = 200 \text{ kPa}$$

$p_o = p'_o = 200 \text{ kPa}$, since the soil specimens were loaded from a stress-free state under drained conditions.

$$q_o = q'_o = 0$$

Step 3: Set up a graph and plot initial stress points.

Create a graph with axes p' and p as the abscissa and q as the ordinate and plot the isotropic stress path with coordinates $(0, 0)$ and $(200, 0)$, as shown by OA in Figure 1

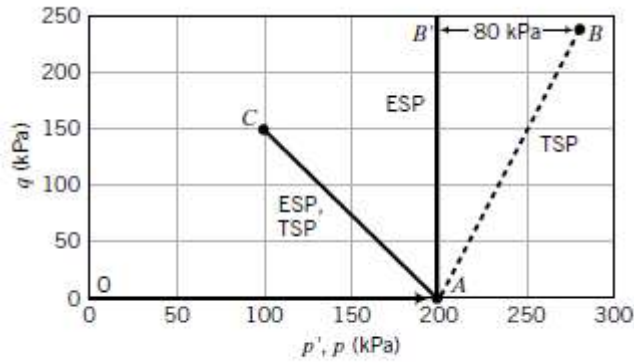


FIGURE 1

Step 4: Determine the increases in stresses.

Specimen A

We have (1) an undrained condition, Δu is not zero, and (2) no change in the radial stress, but the axial stress is increased to 440 kPa. Therefore,

$$\Delta\sigma_3 = 0, \quad \Delta\sigma_1 = 440 - 200 = 240 \text{ kPa}$$

Specimen B

Drained loading ($\Delta u = 0$); therefore, TSP = ESP.

Axial stress held constant, $\Delta\sigma_1 = \Delta\sigma'_1 = 0$; radial stress decreases to 50 kPa; that is,

$$\Delta\sigma_3 = \Delta\sigma'_3 = 50 - 200 = -150 \text{ kPa}$$

Step 5: Calculate the increases in stress invariants.

Specimen A

$$\Delta p = \frac{\Delta\sigma_1 + 2\Delta\sigma_3}{3} = \frac{240 + 2 \times 0}{3} = 80 \text{ kPa}$$

$$\Delta q = \Delta\sigma_1 - \Delta\sigma_3 = 240 - 0 = 240 \text{ kPa}$$

$$\text{Slope of total stress path} = \frac{\Delta q}{\Delta p} = \frac{240}{80} = 3$$

Specimen B

$$\Delta p = \Delta p' = \frac{\Delta\sigma'_1 + 2\Delta\sigma'_3}{3} = \frac{0 + 2 \times (-150)}{3} = -100 \text{ kPa}$$

$$\Delta q = \Delta\sigma_1 - \Delta\sigma_3 = 0 - (-150) = 150 \text{ kPa}$$

$$\text{Slope of ESP (or TSP)} = \frac{\Delta q}{\Delta p'} = \frac{150}{-100} = -1.5$$

Step 6: Calculate the current stress invariants.

Specimen A

$$p = p_o + \Delta p = 200 + 80 = 280 \text{ kPa}, \quad q = q' = q_o + \Delta q = 0 + 240 = 240 \text{ kPa}$$

$$p' = p_o + \Delta p' = 200 + 0 = 200 \text{ kPa (elastic soil)}$$

Specimen B

$$p = p' = p_o + \Delta p = 200 - 100 = 100 \text{ kPa}$$

$$q = q_o + \Delta q' = 0 + 150 = 150 \text{ kPa}$$

Step 7: Plot the current stress invariants.

Specimen A

Plot point B as (280, 240); plot point B' as (200, 240).

Specimen B

Plot point C as (100, 150).

Step 8: Connect the stress points.

Specimen A

AB in Figure 1 shows the total stress path and *AB'* shows the effective stress path.

Specimen B

AC in Figure 1 shows the ESP and TSP.

Step 9: Determine the excess porewater pressure.

Specimen A

BB' shows the maximum excess porewater pressure. The mean stress difference is $280 - 200 = 80 \text{ kPa}$.

Example: 3

Stress path in (p,q) and (s,t) space for soil element next to an excavation

A long excavation is required in a stiff saturated soil for the construction of a building. Consider two soil elements. One, element A, is directly at the bottom of the excavation along the center line and the other, element B, is at the open face (Figure 2).

- (a) Plot the stress paths in (p, q) and (s, t) spaces for elements A and B.
- (b) If the soil is an isotropic, linear elastic material, predict the excess porewater pressures.

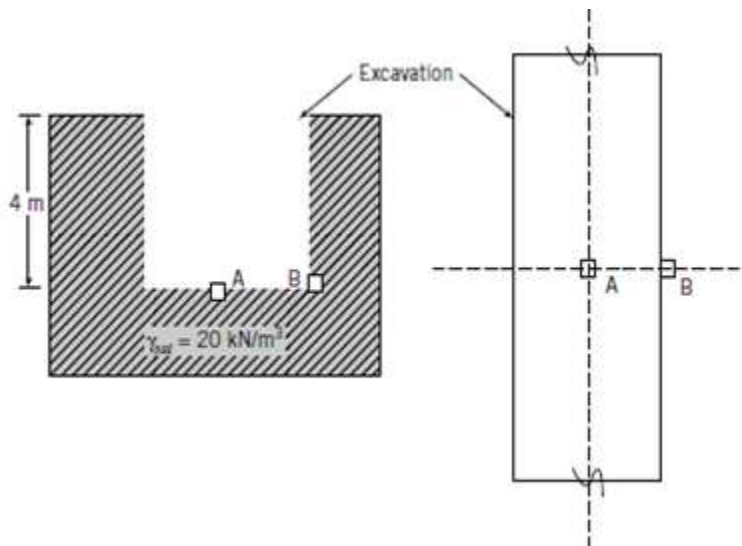


Figure: 2

Solution:

Step 1: Determine loading condition.

Element A is under axisymmetric condition and will be subjected to reduction in vertical and lateral stresses. The increases in lateral stresses are much lower than the increases in vertical stresses. Element B is under plane strain condition and will be subjected to reduction in lateral stresses with no change in vertical stresses.

Step 2: Calculate initial stresses.

Elements A and B have the same initial stresses.

Note: All stresses are principal stresses.

$$p_o = p'_o = \frac{\sigma_x + \sigma_y + \sigma_z}{3} = \frac{80 + 48 + 48}{3} = 58.7 \text{ kPa}$$

$$q_o = \sigma_z - \sigma_x = (80 - 48) = 32 \text{ kPa}$$

$$s_o = s'_o = \frac{\sigma_z + \sigma_x}{2} = \frac{80 + 48}{2} = 64 \text{ kPa}$$

$$t_o = \frac{\sigma_z - \sigma_x}{2} = \frac{80 - 48}{2} = 16 \text{ kPa}$$

Step 3: Determine the changes in stresses.

Element A: The vertical total stress decreases and, as a first approximation, the changes in lateral stress are small and can be neglected.

$$\Delta p = \frac{\Delta\sigma_x + \Delta\sigma_y + \Delta\sigma_z}{3} = \frac{0 + 0 + (-\Delta\sigma_z)}{3} = \frac{-\Delta\sigma_z}{3} = \frac{-80}{3} \text{ kPa}$$

$$\Delta q = (-\Delta\sigma_z) - \Delta\sigma_x = -\Delta\sigma_z - 0 = -\Delta\sigma_z = -80 \text{ kPa}$$

$$\text{slope} = \frac{\Delta q}{\Delta p} = \frac{-\Delta\sigma_z}{\frac{-\Delta\sigma_z}{3}} = 3$$

$$\Delta s = \frac{(-\Delta\sigma_z) + \Delta\sigma_x}{2} = \frac{-\Delta\sigma_z + 0}{2} = \frac{-\Delta\sigma_z}{2} = -40 \text{ kPa}$$

$$\Delta t = \frac{\Delta\sigma_z - \Delta\sigma_x}{2} = \frac{-\Delta\sigma_z - 0}{2} = \frac{-\Delta\sigma_z}{2} = -40 \text{ kPa}$$

$$\text{slope} = \frac{\Delta t}{\Delta s} = \frac{\frac{-\Delta\sigma_z}{2}}{\frac{-\Delta\sigma_z}{2}} = 1$$

Element B: The vertical total stress remains constant, but the lateral stress in the X direction decreases. The change in lateral stress in the Y direction is small and can be neglected.

$$\Delta p = \frac{\Delta\sigma_x + \Delta\sigma_y + \Delta\sigma_z}{3} = \frac{(-\Delta\sigma_x) + 0 + 0}{3} = \frac{-\Delta\sigma_x}{3} = \frac{-48}{3} = -16 \text{ kPa}$$

$$\Delta q = \Delta\sigma_z - (-\Delta\sigma_x) = 0 + \Delta\sigma_x = \Delta\sigma_x = 48 \text{ kPa}$$

$$\text{slope} = \frac{\Delta q}{\Delta p} = \frac{\Delta\sigma_x}{\frac{-\Delta\sigma_x}{3}} = -3$$

$$\Delta s = \frac{\Delta\sigma_z + (-\Delta\sigma_x)}{2} = \frac{0 - \Delta\sigma_x}{2} = \frac{-\Delta\sigma_x}{2} = -24 \text{ kPa}$$

$$\Delta t = \frac{\Delta\sigma_z - \Delta\sigma_x}{2} = \frac{0 - (-\Delta\sigma_x)}{2} = \frac{\Delta\sigma_x}{2} = 24 \text{ kPa}$$

$$\text{slope} = \frac{\Delta t}{\Delta s} = \frac{\frac{\Delta\sigma_x}{2}}{\frac{-\Delta\sigma_x}{2}} = -1$$

Step 4: Plot stress paths.

See Figure 3

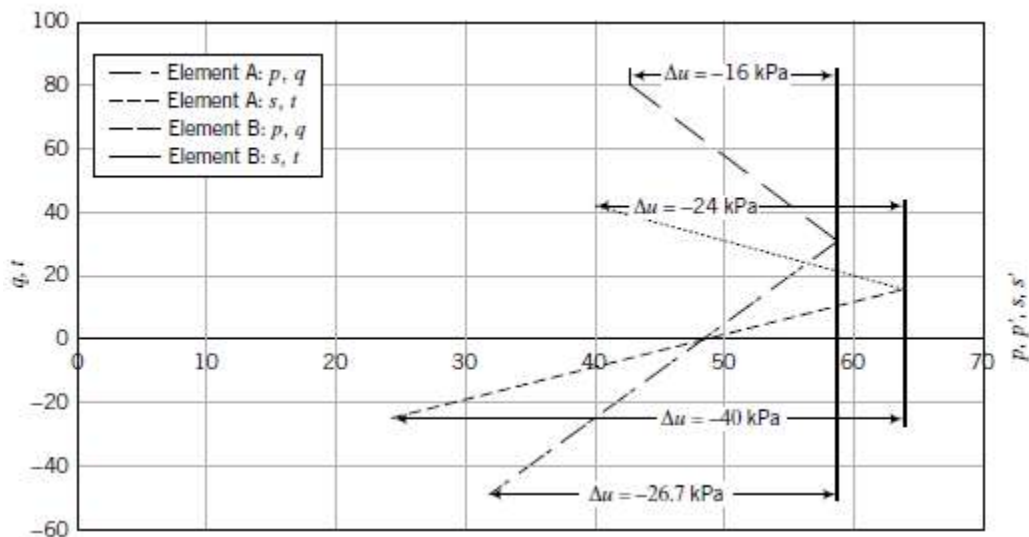


Figure: 3

Step 5: Summarize results.

Element	Space	Slope	u (kPa)
A	p, q	3	-26.7
A	s, t	1	-40
B	p, q	-3	-16
B	s, t	-1	-24

Both elements A and B are unloaded. Element A is unloaded by removing the initial vertical stress, while element B is unloaded by removing the lateral stress. The changes in deviatoric stress for element A are negative, indicating extension, i.e., the lateral stress changes are greater than the vertical stress changes. This is similar to laterally squeezing a pop can. The changes in deviatoric stress for element B are positive values, indicating compression, i.e., the vertical stress changes are greater than the lateral stress changes. This is similar to compressing a pop can vertically and causing lateral bulging (radial extension). The negative porewater pressures (suction) are due to these extensions.

4.0 YIELD CRITERION

A condition that defines the limit of elasticity and the beginning of plastic deformation under any possible combination of stresses is known as the **yield condition** or **yield criterion**. In the elastic region, all the deformation will be recovered once the applied stress is removed (i.e. unloading of stress to zero). However once the yield condition is reached, some of the deformation will be permanent in the sense that it cannot be recovered even after the stress is removed completely. This part of the deformation is known as plastic deformation and the remaining deformation is recoverable upon removal of the stress and is known as elastic deformation. For the simple case of one-dimensional loading, the yield criterion is defined by a stress value beyond which plastic deformation will occur. In other words, the criterion of yield is graphically represented by a *point*. For the case of two dimensional loading, the yielding will occur when the combination of stresses applied in the two loading directions touches a *curve*. In the same way, for the case of three dimensional loading, plastic deformation will occur once the combination of the stresses applied in the three directions touches a *surface* (often known as a yield surface). In short, the yield criterion is generally represented by a surface in stress space. When the stress state is within the yield surface, material behavior is said to be elastic.

Once the stress state is on the yield surface, plastic deformation will be produced. Mathematically, a general form of yield criterion (or surface) can be expressed in terms of either the stress tensor or the three stress invariants as follows:

$$f(\sigma_{ij}) = f(I_1, I_2, I_3) = k \text{-----} \quad \text{Eq.4.1}$$

4.1 YIELD SURFACES FOR METALS

The first yield criterion for metal was suggested by the French engineer H. Tresca in 1864. His experiments suggested that plastic behaviour would commence when the maximum shear stress reached a critical value. Recalling Mohr's circle, we see that the maximum shear stress will always be half the difference between the major and minor principal stresses. One can easily discover the critical stress by performing a simple tension test on a bar of the metal. If we denote the tensile stress at failure (i.e. the onset of plastic behaviour) by σ_T , then the maximum shear stress is exactly half of σ_T . Therefore if we consider the case where $\sigma_1 \geq \sigma_2 \geq \sigma_3$ the yield function f in (Eq.1) becomes $(\sigma_1 - \sigma_3)/2$ and the constant k is $\sigma_T/2$. The yield criterion can be written as:

$$(\sigma_1 - \sigma_3) = \sigma_T \text{-----} \quad \text{Eq. 4.2}$$

Note that the surface defined by (Eq.2) does not depend on the mean stress p . The function f depends only on the diameter of the Mohr circle. This implies that the yield surface image in the π -plane will be independent of the position on the space diagonal.

When we consider the various possibilities, such as

$$\sigma_1 \geq \sigma_3 \geq \sigma_2,$$

$\sigma_2 \geq \sigma_1 \geq \sigma_3$, and so on. The complete yield surface has the shape of a regular hexagon. Its intersection with the π -plane is shown in Figure 4.1.

In principal stress space we see an infinitely long prism. Its cross-section is a hexagon and its central axis is the space diagonal.

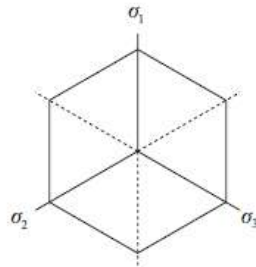


Fig.4.1: The Tresca yield surface

The volume enclosed, by definition, represents the set of all stress states for which the material will be elastic. If the stress point touches the surface, then yielding will occur.

The second yield criterion of general interest for metals was suggested by R. von Mises in 1913. He suggested that yield will occur when the value of the deviatoric stress q reaches a critical value. We write the von Mises yield condition as $q=k$

We see that yield will occur when, in the π -plane, the radial distance from the origin to the stress point reaches the value $\sqrt{2/3} k$. As with Tresca's criterion, we can determine the value of k from a simple tension test. If we set $\sigma_1 = \sigma_T$, the tensile yield stress, and we let $\sigma_2 = \sigma_3 = 0$, then we find that q is exactly σ_T and therefore so is k . The intersection of the von Mises surface with the π -plane is a circle passing through the vertices of the Tresca hexagon (Figure 4.2). The complete surface is an infinitely long cylinder whose central axis coincides with the space diagonal.

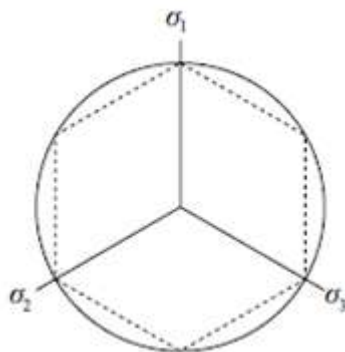


Fig.4.2: The Von Mises yield surface

Both metals and soils often exhibit localisation of deformation within relatively narrow regions or bands when failure is imminent. On a microscopic level, dislocations in the atomic lattice of a metal bear at least a vague similarity to the fracture and rearrangement of particles in a yielding soil. Workers in geotechnical engineering have often attempted to adapt aspects of metal plasticity theories for use in soil mechanics. The reverse, however, is also true since the very first practical yield criterion was derived specifically for soil. It was the work of the great French engineer Charles Augustus Coulomb.

4.2 THE COULOMB YIELD CRITERION

He began by observing that all the materials derived strength from two sources: cohesion and friction. His observations of real soils suggested that failure will usually be associated with a surface of rupture within the soil mass. Restricting attention to this surface he wrote his failure criterion as

$$\tau = c + \sigma \tan \phi \text{-----} \text{Eq.4.3}$$

Where, τ and σ represent the shearing stress and normal stress on the physical plane through which material failure occurs. The constant c is called the cohesion. It has dimensions of stress. The quantity $\tan \phi$ is similar to a coefficient of friction. The angle ϕ is referred to as the angle of internal friction. Coulomb did not write the criterion exactly as we have done here, but his words clearly expressed the meaning we associate with the present equation form.

The intersection of the yield surface with the π -plane will be a straight line of course the straight line will only apply over one of the 60° segments, exactly the same as for the Tresca yield surface. Here, however, there are two important differences with respect to the Tresca surface.

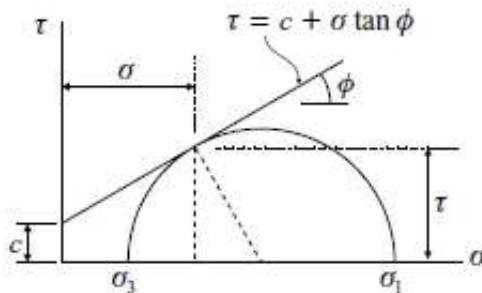


Fig.4.3: The Coulomb failure criterion

The first is that the relative slopes of the surface in the various 60° segments are different. We will see this more clearly in a moment. The second and more important difference is this: the size of the surface depends upon the mean stress p .

Graphically the yield surface for all six of the 60° segments results in the irregular hexagonal shape is shown in Figure 4. 4. For the purposes of constructing this figure we have taken ϕ to be 30° . Each of the vertices of the hexagon has a particular physical meaning. All vertices occur on the lines of symmetry where two of the principal stresses are equal. The uppermost vertex corresponds to the condition where $\sigma_1 > \sigma_2 = \sigma_3$

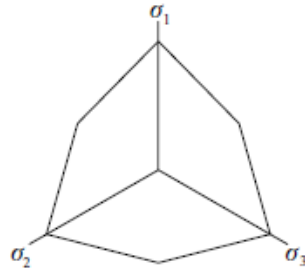


Fig.4.4: Cross-section through the Coulomb yield surface

The resemblance between the Coulomb and Tresca surfaces is more than a passing one. Note that if we set $\varphi = 0$ in (Eq. 3), Coulomb's criterion is essentially the same as Tresca's, namely that failure occurs when the greatest shear stress reaches a critical value. If we set $\varphi = 0$ in (Eq.4.3), provided we set $2c = \sigma_T$. The difference between the yield surface shapes in the π -plane stems solely from φ . But this is not the most important difference. That distinction belongs to the dependence of Coulomb's criterion on the mean stress p . Because of this, the size of the yield surface grows as the mean stress increases. Whereas Tresca's surface was an infinitely long uniform hexagonal prism, Coulomb's surface has an expanding pyramid shape as shown in Figure 4.5.

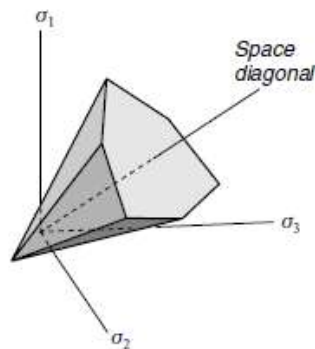


Fig.4.5: Perspective view of the Coulomb yield surface

4.3 MODIFICATIONS TO COULOMB'S CRITERION

There are three modified forms of the Coulomb criterion that we will consider. The first was proposed in 1952 by two of the most prominent researchers from the field of both metal and soil

plasticity: D.C. Drucker and W. Prager. They suggested that the von Mises yield criterion could be modified easily by introducing a dependence on the mean stress p ,

$$q - \xi p = k \text{-----} \tag{Eq.4.4}$$

Here the additional term ξp will change the von Mises yield surface from an infinitely long cylinder to a cone. We can select the values of the constants ξ and k in such a way that the cone will agree with the Coulomb surface at the major vertices. First, recall that

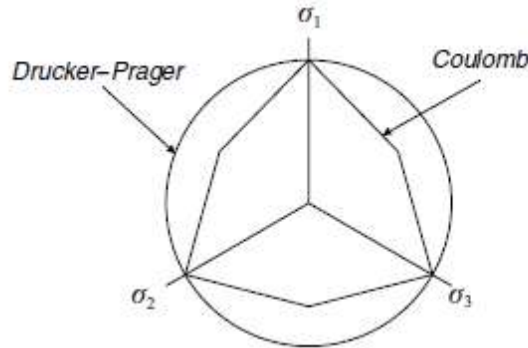


Fig.4.6: The Drucker–Prager and Coulomb yield surfaces

The graph of Drucker and Prager’s yield surface in the π -plane is a circle that touches the Coulomb hexagon as shown in Figure 6. Thinking again about real soil response, tests show that the Drucker–Prager surface is not as accurate a representation as the Coulomb hexagon. Even the relatively common triaxial extension test gives results that lie far closer to the minor vertex of the hexagon than to the circle. Nevertheless, the Drucker–Prager criterion possesses the significant virtue of simplicity, and because of this it is an important addition to the repertoire of the soil plastician.

The second modified form of Coulomb’s surface was developed in 1975 by P.V. Lade and J.M. Duncan. Their yield criterion was proposed expressly for cohesionless soils. It can be written in the form

$$\sigma_1 \sigma_2 \sigma_3 = k p^3 \text{-----} \tag{Eq.4.5}$$

where κ is a constant. On the left-hand side of this equation we see the product of all three principal stresses, which we know to be the third principal stress invariant.

The third modification of the Coulomb criterion was derived by H. Matsuoka and T. Nakai in 1974. Their yield equation can be written as

$$\sigma_1 \sigma_2 \sigma_3 = \xi p (\sigma_1 \sigma_2 + \sigma_2 \sigma_3 + \sigma_3 \sigma_1) \text{-----} \tag{Eq.4.6}$$

Where, ξ is a constant. This equation is also restricted to cohesionless soils. Remarkably, it agrees with the Coulomb hexagon at both major and minor vertices, provided the appropriate value for ξ is used. Figure 4.7 shows the Lade–Duncan and Matsuoka–Nakai yield surfaces compared with the Coulomb yield surface.

The graph of the yield locus in the π -plane can be constructed in the same way as the Lade–Duncan surface was. Both the Lade–Duncan surface and the Matsuoka–Nakai surface provide good agreement with the available cubical triaxial test data.

4.4 STRAIN HARDENING AND PERFECT PLASTICITY

In contrast to perfect plasticity, 'work hardening' implies the yield surface may change in some way once initial yielding has occurred. Usually the way the yield surface changes is related to the amount of plastic strain or to the amount of plastic work that has accumulated. The response of a work hardening material in simple tension might look something like that shown in Figure 4.8

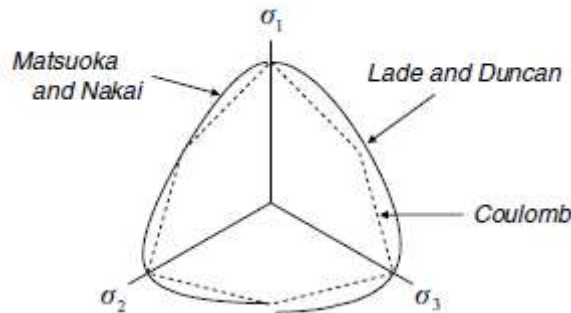


Fig.4.7 Lade–Duncan and Matsuoka–Nakai yield surfaces compared with the Coulomb yield surface

Here the stress and strain may have a one-to-one functional relationship both before and after yield.

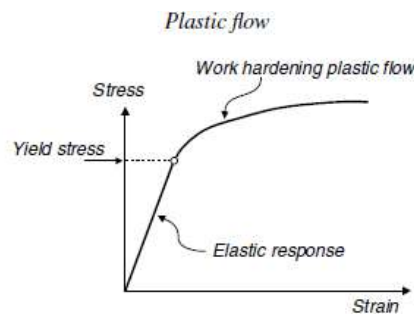


Fig. 4.8: Stress strain response for a work hardening plastic material

Plastic deformation leads to the hardening of a material and the increase of its elastic limit (i.e. the stress limit under which only elastic deformation occurs). In other words, the yield surface will generally not be fixed in stress space; rather it will expand or contract depending on previous plastic deformation and loading history.

Let us for the present consider the case when plastic deformation only changes the size of the yield surface equally in all directions but not its shape (which is known as isotropic hardening). If the yield surface is expanding in size, the material is said to be hardening (i.e. making it more difficult to yield). On the other hand, if the yield surface is contracting in size, then the material

is said to be undergoing softening (i.e. making it easier to yield). The change of the size of the yield surface is often related to some measure or integral of plastic strain rates. The most common measures include the total plastic work per unit volume, the accumulated plastic strain (Hill, 1950), the volumetric plastic strain rate (Schofield and Wroth, 1968; Yu, 1998), or a combination of volumetric and shear plastic strain rates (Wilde, 1977; Yu *et al.*, 2005). The yield surface for a strain-hardening or softening material is also called *the loading surface*. Mathematically, the loading surface, which changes with plastic deformation, may be expressed by

$$f(\sigma_{ij}, \varepsilon_{ij}^p) = 0 \text{-----} \quad \text{Eq.4.7}$$

Where, ε_{ij}^p denotes the plastic strain tensor

If the yield surface does not change with stress history (i.e. fixed), the material is known a perfectly plastic solid. This is a special case of strain-hardening materials. For a perfectly plastic material, the behaviour is elastic when the stress state lies inside the yield surface. Plastic strains will occur as long as the stress state lies on or travels along the yield surface. The complete stress conditions for plastic and elastic behaviour may be stated as

$$\text{Elastic if } f(\sigma_{ij}) < 0 \text{ or } df = \frac{\partial f}{\partial \sigma_{ij}} d\sigma_{ij} < 0 \text{-----} \quad \text{Eq.4.8}$$

$$\text{Plastic if } f(\sigma_{ij}) = 0 \text{ or } df = \frac{\partial f}{\partial \sigma_{ij}} d\sigma_{ij} = 0 \text{-----} \quad \text{Eq.4.9}$$

The elastic behaviour of a strain-hardening solid is the same as that of a perfectly plastic one. Therefore the conditions for initial yield must be the same. Indeed, the difference between the two concerns only the mechanism for continuing plastic flow, plus the fact that the conditions for current yielding will depend on the plastic history of the material. The complete stress conditions for plastic and elastic behavior for a strain-hardening material are

$$\text{Elastic if } f(\sigma_{ij}, \varepsilon_{ij}^p) < 0 \text{ or } df = \frac{\partial f}{\partial \sigma_{ij}} d\sigma_{ij} \leq 0 \text{-----} \quad \text{Eq.4.10}$$

$$\text{Plastic if } f(\sigma_{ij}, \varepsilon_{ij}^p) = 0 \text{ or } df = \frac{\partial f}{\partial \sigma_{ij}} d\sigma_{ij} > 0 \text{-----} \quad \text{Eq.4.11}$$

For solving boundary value problems involving elastic-plastic behaviour, it is essential to clearly determine what behaviour will result from a further stress increment when the stress state is already on the yield surface. Three possible conditions exist and they are

$$\text{Unloading, } f(\sigma_{ij}, \varepsilon_{ij}^p) = 0 \text{ or } df = \frac{\partial f}{\partial \sigma_{ij}} d\sigma_{ij} < 0 \text{-----} \quad \text{Eq.4.12}$$

$$\text{Neutral loading, } f(\sigma_{ij}, \varepsilon_{ij}^p) = 0 \text{ or } df = \frac{\partial f}{\partial \sigma_{ij}} d\sigma_{ij} = 0 \text{-----} \quad \text{Eq.4.13}$$

$$\text{Loading, } f(\sigma_{ij}, \varepsilon_{ij}^p) = 0 \text{ or } df = \frac{\partial f}{\partial \sigma_{ij}} d\sigma_{ij} > 0 \text{-----} \quad \text{Eq.4.14}$$

It is commonly assumed that for both unloading and neutral loading, material behaviour is purely elastic. Plastic behaviour occurs only when the loading condition is satisfied.

4.5 ISOTROPIC AND KINEMATIC HARDENING

Hardening in the theory of plasticity means that the yield surface changes in size or location or even in shape, along with the loading history (often measured by some form of plastic deformation). When the initial yield condition exists and is identified, the rule of hardening defines its modification during the process of plastic flow. Most plasticity models currently in use assume that the shape of the yield surface remains unchanged, although it may change in size or location. This restriction is largely based on mathematical convenience, rather than upon any physical principle or experimental evidence. The two most widely used rules of hardening are known as isotropic hardening and kinematic (or anisotropic) hardening.

4.5.1 Isotropic hardening

The rule of isotropic hardening assumes that the yield surface maintains its shape, centre and orientation, but expands or contracts uniformly about the centre of the yield surface. Isotropic hardening with uniform expansion of the yield surface is shown in Figure 4.9

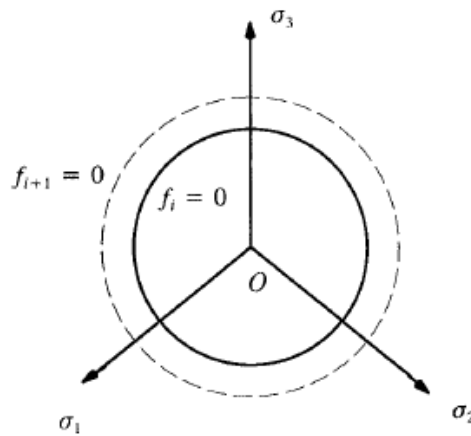


Fig. 4.9: Isotropic hardening with uniform expansion of the yield surface

A yield surface with its centre at the origin may be generally described by the following function $f = f(\sigma_{ij}) - R(\alpha) = 0$ ----- Eq.4.15

where R represents the size of the yield surface, depending on plastic strains through the hardening parameter α . As shown in Hill (1950), the two earliest and most widely used hardening parameters are the accumulated equivalent plastic strain,

$$\alpha = \int \sqrt{\frac{2}{3}} (d\varepsilon_{ij}^p)^{1/2} \text{-----} \text{Eq.4.16}$$

and the plastic work

$$\alpha = \int \sigma_{ij} d\varepsilon_{ij}^p \text{-----} \text{Eq.4.17}$$

4.5.2 Kinematic hardening

The term *kinematic hardening* was introduced by Prager (1955) to construct the first kinematic hardening model. In this first model, it was assumed that during plastic flow, the yield surface

translates in the stress space and its shape and size remain unchanged. This is consistent with the Bauschinger effect observed in the uniaxial tension-compression.

Assume that the initial yield surface can be described by

$$f = f(\sigma_{ij} - \alpha_{ij}) - R_0 = 0 \text{-----} \tag{Eq.4.18}$$

where α_{ij} represents the coordinates of the centre of the yield surface, which is also known as the back stress. R_0 is a material constant representing the size of the original yield surface. It can be seen that as the back stress σ_{ij} changes due to plastic flow, the yield surface translates in the stress space while maintaining its initial shape and size.

The first simple kinematic hardening model was proposed by Prager (1955). This classical model Assumes that the yield surface keeps its original shape and size and move in the direction of plastic strain rate tensor (see Figure 4.10).

Mathematically it can be expressed by the following linear evolution rule

$$d\alpha_{ij} = c d\varepsilon_{ij}^p \text{-----} \tag{Eq.4.19}$$

where c is a material constant.

Whilst Prager's model is reasonable for one-dimensional problems, it does not seem to give consistent predictions for two- and three-dimensional cases (Ziegler, 1959). The reason is that the yield function takes different forms for one-, two- and three-dimensional cases. To overcome this limitation, Ziegler (1959) suggested that the yield surface should move in the direction as determined by the vector $\sigma_{ij} - \alpha_{ij}$, see Figure 4.10.

Mathematically Ziegler's model can be expressed as follow

$$d\alpha_{ij} = d\mu(\sigma_{ij} - \alpha_{ij}) \text{-----} \tag{Eq.4.20}$$

where $d\mu$ is a material constant.

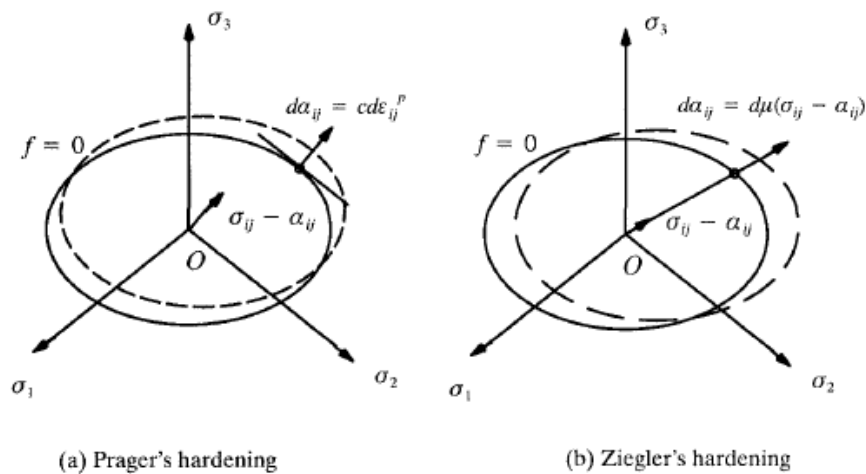


Fig.4.10: Pager's and Ziegler's Kinematic hardening

Mathematically it can be expressed by the following linear evolution rule

$$d\alpha_{ij} = c d\varepsilon_{ij}^p \text{-----} \tag{Eq.4.21}$$

where c is a material constant.

Whilst Prager's model is reasonable for one-dimensional problems, it does not seem to give consistent predictions for two- and three-dimensional cases (Ziegler, 1959). The reason is that the yield function takes different forms for one-, two- and three-dimensional cases. To overcome this limitation, Ziegler (1959) suggested that the yield surface should move in the direction as determined by the vector $\sigma_{ij} - \alpha_{ij}$, see Figure 3. Mathematically Ziegler's model can be expressed as follow

$$d\alpha_{ij} = d\mu(\sigma_{ij} - \alpha_{ij}) \text{-----} \tag{Eq.4.22}$$

where $d\mu$ is a material constant.

4.6 PLASTIC FLOW

It is important to explore what may happen if the stress point arrives at the yield surface. We intuitively expect that yielding will be accompanied by some form of increased deformation, over and above the elastic deformation that has gone on while the stress point has been inside the yield surface. We expect plastic behaviour to be softer than elastic behaviour, with the result that strains will accumulate more quickly. The term *plastic flow* is used to describe the deformation following yield.

One of the main differences between plastic response and elastic response is that plastic flow will be irreversible. While the material is elastic we can increase the stress with a consequent increase in strain, and then completely recover those strains by simply returning the stress state to its initial value. However this will not be possible if yield occurs. Plastic deformation will not be recoverable from simple unloading. If we do reduce the stress to its initial value we will recover whatever elastic strain that has occurred in getting to the yield state, but the plastic strain will be locked within the body. In order to describe plastic flow we might attempt to derive a constitutive relationship linking plastic strain to the current stress state. But this will immediately lead to difficulties owing precisely to the irreversibility mentioned above. There can clearly be no unique one-to-one relationship between plastic strain and stress since there may be an unknown amount of plastic deformation already locked within the body at the start of any loading episode. As a result we choose to seek a relationship between stress and *plastic strain rate*. By looking at the rate of change of plastic strain rather than the total amount we avoid the problem of irreversibility. Of course, if the plastic strain rate is known throughout some loading process, then a simple integration will give the total amount of plastic strain that has accumulated during that process. Obviously, it may be convenient to differentiate between plastic and elastic strain. We do this by using superscripts. The superscript *e* denotes elastic strain while *p* denotes plastic strain. The total strain is the sum of the elastic and plastic parts.

$$\epsilon_{xx} = \epsilon_{xx}^e + \epsilon_{xx}^p \text{-----} \tag{Eq.4.23}$$

4.7 NORMALITY

Our ultimate aim will be to formulate a functional relationship between the components of the plastic strain rate and the components of stress. It is reasonable to assume that the components of

the plastic strain rate can be arranged into a square matrix exactly as for the elastic strains. We will denote this matrix by $\dot{\epsilon}^p$. We expect $\dot{\epsilon}^p$ to be symmetric and to have the principal values.

An important assumption concerning plastic strains relates to Saint-Venant's hypothesis. This assumes that the principal directions of both the stress matrix σ and the plastic strain rate matrix $\dot{\epsilon}_p$ are aligned. If the material is isotropic, and if $\dot{\epsilon}_p$ depends only on σ , then Saint-Venant's hypothesis is no longer an assumption but is required by the rules of linear algebra. In many cases we may be happy to assume that our material is isotropic, but it may be that $\dot{\epsilon}_p$ possesses a functional dependence on more than just the components of the stress matrix.

A consequence of Saint-Venant's hypothesis is that we can relate stresses and plastic strain rates spatially by plotting them on the same graph. For example, in the π -plane we can plot both the principal stresses and the principal components of the plastic strain rate matrix on the same graph. The axes for σ_1 and ϵ_1^p fall on the same line, and a similar result applies for the intermediate and minor principal values of both matrices. Of course, the scales of the respective axes are different and we are not directly comparing stresses with strain rates, but the ability to plot both together will be useful in visualising some parts of our development.

4.8 THE YIELD CONDITION AND THE FLOW RULE

The Mohr-Coulomb yield condition: The methods described in this chapter may be applied to any *perfectly plastic* model soil. For such models, the yield and failure conditions are identical. The methods cannot however be applied to those soil models, such as the critical state model, which take account of strain hardening or strain softening. The Mohr-Coulomb model is most commonly used. The yield (and failure) condition may be stated in the form in terms of total stress as

$$\tau_f = c + \sigma_n \tan \phi \text{-----} \tag{Eq.4.24}$$

in terms of effective stress.

$$\tau_f = c' + (\sigma_n - u) \tan \phi \text{-----} \tag{Eq.4.25}$$

Both the equilibrium and yield conditions may be expressed in similar forms in terms of either total or effective stress. In the remainder of this chapter, the primes denoting effective stress have, for convenience, been omitted, but the methods used and the expressions derived are equally applicable to analysis in terms of total or effective stress.

4.8.1 Strain rate and velocity

A consequence of our assumption of perfect plasticity is that any stress state satisfying the yield condition will, if maintained, because unlimited plastic strain. There is, therefore, no direct relationship between yield stress and plastic strain. We therefore need to define, not the strain, but the *strain rate-that* is, the rate at which the strain is increasing with respect to time. The absolute value of the strain rate is not determinate, since, in designing the soil models, we have not specified any property (such as viscosity) which would control it. This turns out to be not very important as we are concerned only with the *relative* magnitudes of the strain rate

components. These define the directions of the strain rate vectors, and the shape of the deformed body.

Knowing the strains everywhere within a body, we may determine the relative displacements of different points within it. In a similar way, knowing the strain rates, we may determine the *velocities-that is*, the rates of displacement. As in the case of the strain rates, the absolute magnitudes of the velocities are not determinate. Our concern is with the *relative* magnitudes of the velocity components, since these define the directions of the velocity vectors and hence the directions of motion. A pattern of velocity vectors, defining the motion everywhere within the plastic zone is called a **velocity field**.

4.8.2 The Flow Rule and the Plastic Potential

In a linearly elastic body, Hooke's law defines the relation between the components of stress and strain. Similarly, in a perfectly plastic body, the *flow rule* defines the relation between the components of the yield stress (for example, σ_n, τ_f) and the corresponding plastic strain rates (e.g. $\dot{\epsilon}_n^p, \dot{\gamma}^p$, normal strain and shear strain rates)

Von Mises, suggested that the flow rule might be expressed in terms of a *plastic potential function* (f) which may be defined, for a Mohr-Coulomb material, by the equation

$$\frac{\dot{\gamma}^p}{\dot{\epsilon}_n^p} = \frac{\partial f / \partial \tau}{\partial f / \partial \sigma_n} \text{-----} \quad \text{Eq.4.26}$$

Von Mises also suggested that it may often be useful to assume that the potential function is identical with the yield condition. For a Mohr-Coulomb material, where yield and failure conditions are identical

$$f = \tau - c - \sigma_n \tan \phi \leq 0 \text{-----} \quad \text{Eq.4.27}$$

For all stress states on the yield locus, $\tau = \tau_f$ and $f = 0$. A flow rule defined in this way by the yield condition is said to be *associated*.

An associated flow rule makes sense in studies of metal plasticity, since it implies that (a) for isotropic materials, the directions of principal stress and principal strain rate coincide, and (b) for frictionless materials, there is no volumetric strain during plastic yield. Certain problems arise if an associated flow rule is applied to a frictional material. These are discussed in below.

4.8.3 Normality of the Strain Rate Vector

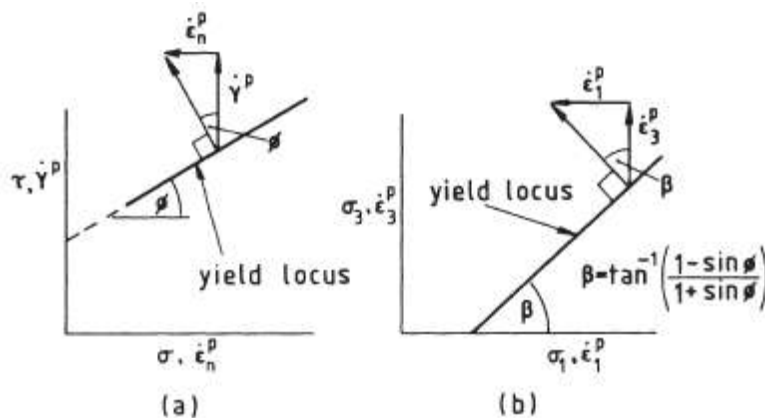


Fig.4.11 Normality of strain rate vector

The Mohr-Coulomb yield condition may be expressed as

$$\tau_f = c + \sigma_n \tan \phi \text{-----} \quad \text{Eq.4.28}$$

The associated flow rule is defined by

$$\frac{\dot{\gamma}^p}{\dot{\epsilon}_n^p} = \frac{\partial f / \partial \tau}{\partial f / \partial \sigma_n} \text{-----} \quad \text{Eq.4.29}$$

Where

$$f = \tau - c - \sigma_n \tan \phi \text{-----} \quad \text{Eq.4.30}$$

So that

$$\frac{\dot{\gamma}^p}{\dot{\epsilon}_n^p} = -\frac{1}{\tan \phi} \text{-----} \quad \text{Eq.4.31}$$

Thus, if the yield stress components are plotted, and are superimposed on a similar plot of the corresponding strain rate components (as shown in Fig. 4.11(a)), it will be seen that *the strain rate vector is normal to the yield locus.*

Similarly, the yield condition may be expressed in the form

$$\sigma_1(1 - \sin \phi) = \sigma_3(1 + \sin \phi) + 2c \cos \phi \text{-----} \quad \text{Eq.4.32}$$

The associated flow rule is defined by

$$\frac{\dot{\epsilon}_3^p}{\dot{\epsilon}_1^p} = \frac{\partial f / \partial \sigma_3}{\partial f / \partial \sigma_1} \text{-----} \quad \text{Eq.4.33}$$

Where

$$f = \sigma_3(1 + \sin \phi) - \sigma_1(1 - \sin \phi) + 2c \cos \phi \text{-----} \quad \text{Eq.4.34}$$

Then

$$\frac{\dot{\epsilon}_3^p}{\dot{\epsilon}_1^p} = \frac{1 + \sin \phi}{1 - \sin \phi} \text{-----} \quad \text{Eq.4.35}$$

But the slope of the yield locus is given by

$$\frac{d\sigma_3}{d\sigma_1} = \frac{1 - \sin \phi}{1 + \sin \phi} \text{-----} \quad \text{Eq.4.36}$$

Showing again (Fig. 4.11(b)) that the strain rate vector is normal to the yield locus. This *normality condition* can be shown to be a general consequence of adopting an associated flow rule.

4.8.4 Associated flow rules

An easy way to introduce the normality condition is to define a *flow rule* of the form

$$\dot{\epsilon}^p = \lambda \frac{\partial f}{\partial \sigma} \text{-----} \quad \text{Eq.4.37}$$

Here f denotes the yield condition as a general function of the components of the stress matrix σ .

The partial derivative $\partial f / \partial \sigma$ imply the derivative with respect to any stress component from which an expression for the corresponding component of the plastic strain rate matrix $\dot{\epsilon}^p$ is obtained. The magnitudes of the components of the strain rate will be undetermined to within λ , which can be regarded as being similar to the Lagrange multiplier. The only constraint we place on λ is that it must be positive. Equation (4.37) ensures that $\dot{\epsilon}^p$ will be normal to the yield

surface f . If our coordinate system aligns with the principal directions of σ , then (Eq.4.37) can be written as

$$\epsilon^p = \lambda \frac{\partial f}{\partial \sigma_k}, k=1,2,3 \text{-----} \quad \text{Eq.4.38}$$

where, k are the principal plastic strain rates and σ_k denote the corresponding principal stresses. Equations 4.37 & 38 are called *associated* flow rules. The adjective refers to the fact the plastic strains are associated directly with the yield surface.

It is possible to introduce non-associated flow rules where f in either of the equations is replaced by some other function, say g . Non-associated flow rules will generally negate many of the advantages of the normality condition, but they may be desirable for certain types of materials or more advanced theories.

Note that, because of the undetermined nature of λ , equations (15) and (16) do not specify directly the magnitude of the plastic strain rates. This is a deliberate move. In many cases the magnitude of the plastic strain rate will not be known unless more information can be supplied. In a general sense we can consider two cases.

Case 1: Perfect Plasticity

We say that a material is ‘perfectly plastic’ if, on yielding, the plastic strains can grow without bound given that no further change in stress occurs and no outside constraints are present. The stress–strain response in simple tension for a perfectly plastic material is illustrated in Figure 4.12.

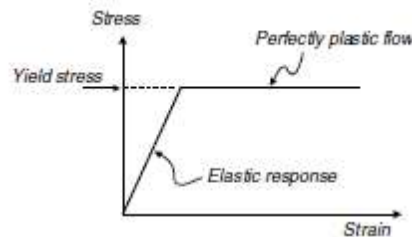


Fig.4.12 Stress–strain response for a perfectly plastic material

We see linear elastic behaviour until the stress reaches its yield value. After yielding there is no further change in stress as plastic strains continue to accumulate. The flat response characterises perfect plasticity. The functional relationship between plastic strain and stress is multiple-valued, and knowledge of the stress does not imply that we know the magnitude of the strain. If the strain is specified, then the stress is known, but not vice versa.

Case 2: Work Hardening Plasticity

In contrast to perfect plasticity, ‘work hardening’ implies the yield surface may change in some way once initial yielding has occurred. Usually the way the yield surface changes is related to the amount of plastic strain or to the amount of plastic work that has accumulated. This introduces an extra parameter into the description of the yield surface. The response of a work hardening

material in simple tension might look something like that shown in Figure 4.13. Here the stress and strain may have a one-to-one functional relationship both before and after yield.

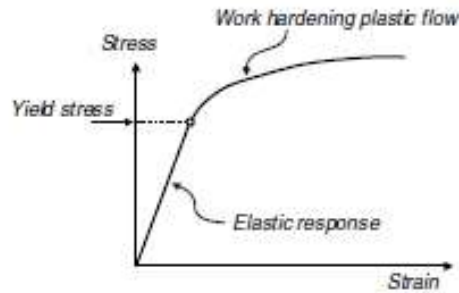


Fig.4.13: Stress–strain response for a work hardening plastic material

In case 2 it will generally be possible to say how large the plastic strains are at any time after yield has occurred, but the same cannot be said for case 1. Often, for a perfectly plastic material, we will not be able to calculate the amount of plastic straining (although in some problems geometric constraints may permit us to do so). Nevertheless perfect plasticity may be profitably used since it permits us to take advantage of certain powerful theorems. There is a place for both perfect plasticity and work hardening plasticity in the repertoire of any geotechnical engineer. We will spend the remainder of the book dealing with one or the other. We begin with a relatively simple example using perfect plasticity

4.8.5 Non-associated flow

For many soils, shearing is accompanied by compaction rather than dilation. For other soils no volumetric strain is evident during shearing. Even for dilating soils, the rate of dilation is usually not large enough. We can look for a solution to this problem in two places. First, we recognise that the pressure dependence of the Coulomb criterion is partly responsible. For compacting soils we would wish the yield surface to grow smaller with increasing mean stress rather than the opposite. For soils that exhibit no volumetric strain we would want the yield surface to neither grow nor shrink.

For dilating soils we require an expanding yield surface. While this may appear to be an impossible wish-list, in fact all three types of behaviour can be accommodated with the Cam Clay and Modified Cam Clay yield surfaces. The resulting theory of critical state soil mechanics will be discussed in subsequent chapter.

The second way to attempt to solve the problem of excessive dilation is to abandon the normality condition. We consider this possibility now. Non-associated flow rules are mathematically similar to Eq.4.37&4.38 with the essential difference being that the yield function f is replaced with another function, $g = g(\sigma)$ for example. The function g is referred to as the *plastic potential* function. In one sense we can write in special cases of the more general flow rule as

$$\epsilon^p = \lambda \frac{\partial g}{\partial \sigma} \text{-----} \quad \text{Eq.4.39}$$

with $g = f$. *Non-associated flow* occurs when g is different from f . Then the flow rule (As expressed by Eq.4.39) gives plastic strain rates that will not be normal to the yield surface. There

are disadvantages to dropping the normality condition, especially with regard to application of certain important theorems, but the problems of excessive plastic dilation can be rectified.

4.9 FAILURE THEORIES

4.9.1 Coulomb's Failure Criterion

Soils, in particular granular soils, are endowed by nature with slip planes. Each contact of one soil particle with another is a potential micro slip plane. Loadings can cause a number of these micro slip planes to align in the direction of least resistance. Thus, we can speculate that a possible mode of soil failure is slip on a plane of least resistance. Recall from your courses in statics or physics that impending slip between two rigid bodies was the basis for Coulomb's frictional law. For example, if a wooden block is pushed horizontally across a table (Figure 4.14 a), the horizontal force (H) required to initiate movement, according to Coulomb's frictional law, is

$$H = \mu W \text{-----} \quad \text{Eq.4.40}$$

where μ is the coefficient of static sliding friction between the block and the table and W is the weight of the block. The angle between the resultant force and the normal force is called the friction angle, $\varphi = \tan^{-1}\mu$

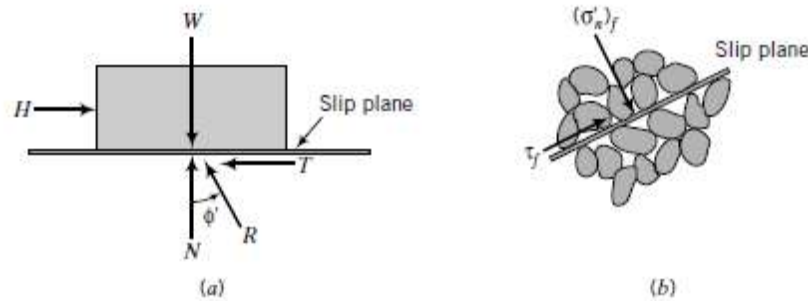


Fig.4.14: (a) Slip of a wooden block (b) A slip plane in a soil mass

Coulomb's law requires the existence or the development of a critical sliding plane, also called slip plane. In the case of the wooden block on the table, the slip plane is the horizontal plane at the interface between the wooden block and the table. Unlike the wooden block, we do not know where the sliding plane is located in soils.

In terms of stresses, Coulomb's law is expressed as

$$\tau_f = \sigma_{n_f} \tan \varphi' \text{-----} \quad \text{Eq.4.41}$$

where $\tau_f = T/A$, where T is the shear force at impending slip and A is the area of the plane parallel to T is the shear stress when slip is initiated, and σ_{n_f} is the normal effective stress on the plane on which slip is initiated. The subscript f denotes failure, which, according to Coulomb's law, occurs when rigid body movement of one body relative to another is initiated. Failure does not necessarily mean collapse, but is the impending movement of one rigid body relative to another.

If we plot Coulomb's equation (2) on a graph of shear stress, τ_f versus normal effective stress, σ_{n_f} we get a straight line similar to OA (Figure 4.15) if $\varphi' = \varphi'_{cs}$. Thus, Coulomb's law may be used to model soil behavior at critical state.

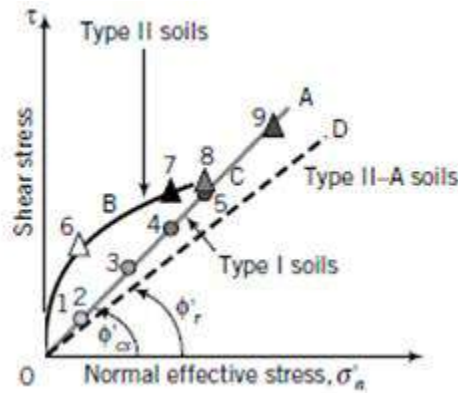


Fig.4.15: Effects of increasing normal effective stresses on the response of soils.

The geometry of soil grains and their structural arrangements are much more complex than our loose and dense assembly. In real soils, the particles are randomly distributed and often irregular. Shearing of a given volume of soil would cause impending slip of some particles to occur up the plane while others occur down the plane. The general form of equation is then

$$\tau_f = \sigma_{n_f} \tan(\varphi' \pm \alpha) \text{-----} \quad \text{Eq.4.42}$$

where the positive sign refers to soils in which the net movement of the particles is initiated up the plane and the negative sign refers to net particle movement down the plane.

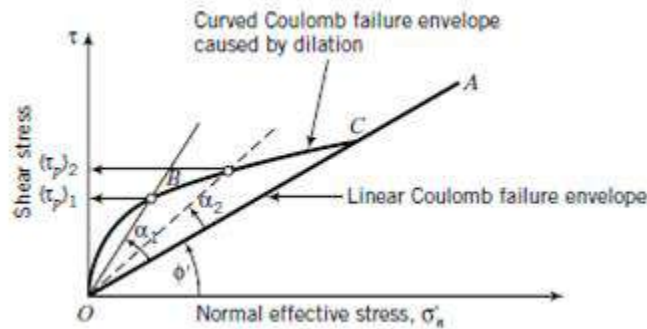


Fig.4.16 Effects of dilation on Coulomb's failure envelope

We will call the angle, as the dilation angle. It is a measure of the change in volumetric strain with respect to the change in shear strain. Soils that have positive values of expand during shearing, while soils with negative values of a contract during shearing. In Mohr's circle of strain (Figure 4.17), the dilation angle is

$$\alpha = \sin^{-1} \left(\frac{\Delta\epsilon_1 + \Delta\epsilon_3}{\Delta\epsilon_1 - \Delta\epsilon_3} \right) = \sin^{-1} \left[\frac{\Delta\epsilon_1 + \Delta\epsilon_3}{\Delta\gamma_{cs}} \right] \text{-----} \quad \text{Eq.4.43}$$

where Δ denotes change. The negative sign is used because we want α to be positive when the soil is expanding. We should recall that compression is taken as positive in soil mechanics. If a soil mass is constrained in the lateral directions, the dilation angle is represented (Figure 4.16) as

$$\alpha = \tan^{-1}\left(\frac{\Delta z}{\Delta x}\right) \text{-----}$$

Eq.4.44

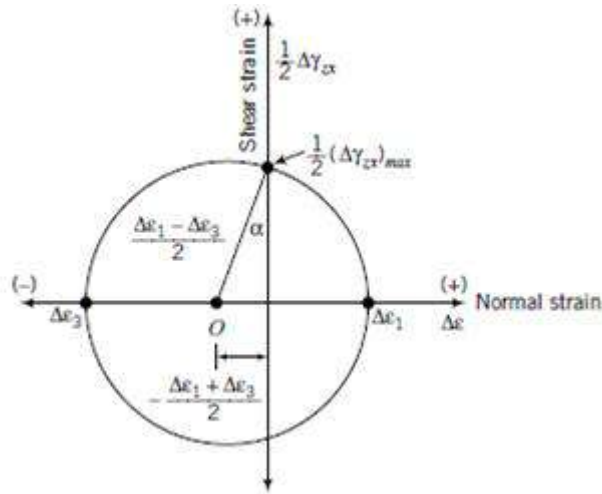


Fig. 4.17 Mohr's circle of strain and dilation angle

Dilation is not a peculiarity of soils, but occurs in many other materials, for example, rice and wheat. Dilation can be seen in action at a beach. If you place your foot on beach sand just following a receding wave, you will notice that the initially wet, saturated sand around your foot momentarily appears to be dry (whitish color). This occurs because the sand mass around your foot dilates, sucking water up into the voids. This water is released, showing up as surface water, when you lift up your foot.

Coulomb's model applies strictly to soil failures that occur along a slip plane, such as a joint or the interface of two soils or the interface between a structure and a soil. Stratified soil deposits such as the over consolidated varved clays (regular layered soils that depict seasonal variations in deposition) and fissured clays are likely candidates for failure following Coulomb's model, especially if the direction of shearing is parallel to the direction of the bedding plane.

4.9.2 Taylor's Failure Criterion

Taylor (1948) used an energy method to derive a simple soil model. He assumed that the shear strength of soil is due to sliding friction from shearing and the interlocking of soil particles. Consider a rectangular soil element that is sheared by a shear stress t under a constant vertical effective stress σ'_z (Figure 4.18). Let us assume that the increment of shear strain is $d\gamma$ and the increment of vertical strain is $d\epsilon_z$

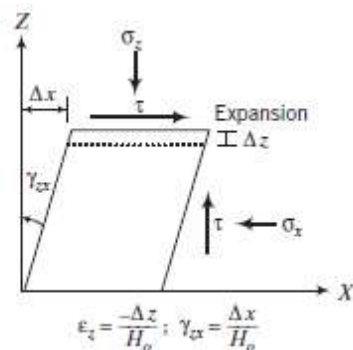


Fig.4.18: Simple shear deformation of soil

The external energy (force x distance moved in the direction of the force or stress x compatible strain) is $\tau d\gamma$. The internal energy is the work done by friction, $\mu_f \sigma'_z d\gamma$. Where μ_f is the static, sliding friction coefficient and the work done by the movement of the soil against the vertical effective stress, $\pm \sigma'_z d\epsilon_z$

The negative sign indicates the vertical strain is in the opposite direction (expansion) to the direction of the vertical effective stress. The energy $\pm \sigma'_z d\epsilon_z$ is the interlocking energy due to the arrangement of the soil particles or soil fabric.

For equilibrium,

$$\tau d\gamma = \mu_f \sigma'_z d\gamma \pm \sigma'_z d\epsilon_z \text{-----} \quad \text{Eq.4.45}$$

Dividing by $\sigma'_z d\gamma$, we get

$$\frac{\tau}{\sigma'_z} = \mu_f \pm \frac{d\epsilon_z}{d\gamma} \text{-----} \quad \text{Eq.4.46}$$

At critical state, $\mu_f = \tan \phi'_{cs}$ and $\lambda = \frac{d\epsilon_z}{d\gamma} = 0$

$$\text{Therefore, } \left(\frac{\tau}{\sigma'_z}\right)_{cs} = \tan \phi'_{cs} \text{-----} \quad \text{Eq.4.47}$$

$$\text{At peak shear strength, } \frac{d\epsilon_z}{d\gamma} = \tan \lambda_p \text{----} \quad \text{Eq.4.48}$$

Therefore,

$$\left(\frac{\tau}{\sigma'_z}\right)_p = \tan \phi'_{cs} + \tan \lambda_p \text{-----} \quad \text{Eq.4.49}$$

Where, the subscripts, c_s and p , denote critical state and peak, respectively. Unlike Coulomb failure criterion, Taylor failure criterion does not require the assumption of any physical mechanism of failure, such as a plane of sliding. It can be applied at every stage of loading for soils that are homogeneous and deform under plane strain conditions similar to simple shear. This failure criterion would not apply to soils that fail along a joint or an interface between two soils. Taylor failure criterion gives a higher peak dilation angle than Coulomb failure criterion.

Equation (4.47) applies to two-dimensional stress systems. Neither Taylor nor Coulomb failure criterion explicitly considers the rotation of the soil particles during shearing.

4.9.3 Mohr–Coulomb Failure Criterion

Coulomb's frictional law for finding the shear strength of soils requires that we know the friction angle and the normal effective stress on the slip plane. Both of these are not readily known because soils are usually subjected to a variety of stresses. We know that Mohr's circle can be used to determine the stress state within a soil mass. By combining Mohr's circle for finding stress states with Coulomb's frictional law, we can develop a generalized failure criterion.

Let us draw a Coulomb frictional failure line, as illustrated by AB in Figure 4.19, and subject a cylindrical sample of soil to principal effective stresses so that Mohr's circle touches the Coulomb failure line. Of course, several circles can share AB as the common tangent, but we will show only one for simplicity.

The point of tangency is at $B [\tau_f, \sigma'_{nf}]$ and the center of the circle is at O . We are going to discuss mostly the top half of the circle; the bottom half is a reflection of the top half. The major

and minor principal effective stresses at failure are σ'_{1f} and σ'_{3f} . Our objective is to find a relationship between the principal effective stresses and ϕ' at failure.

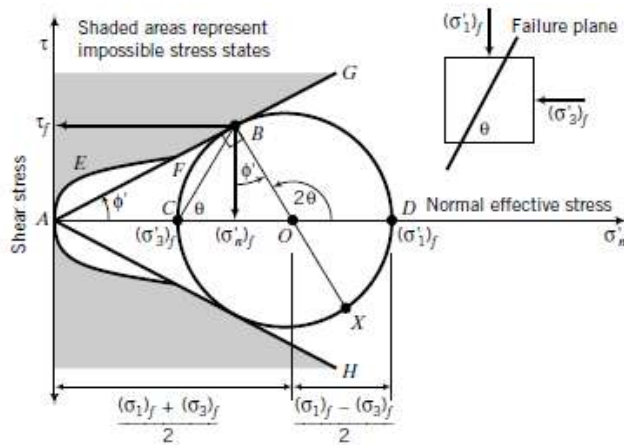


Fig.4.19: Coulomb frictional failure line

From the geometry of Mohr's circle,

$$\sin\phi' = \frac{(\sigma'_{1f} - \sigma'_{3f})/2}{(\sigma'_{1f} + \sigma'_{3f})/2} \quad \text{Eq.4.50}$$

This reduces to

$$\sin\phi' = \frac{(\sigma'_{1f} - \sigma'_{3f})}{(\sigma'_{1f} + \sigma'_{3f})} \quad \text{Eq.4.51}$$

Rearranging Equation (12) gives

$$\frac{\sigma'_{1f}}{\sigma'_{3f}} = \frac{1 + \sin\phi'}{1 - \sin\phi'} = \tan^2\left(45^\circ + \frac{\phi'}{2}\right) = K_p \quad \text{Eq.4.52}$$

Or

$$\frac{\sigma'_{3f}}{\sigma'_{1f}} = \frac{1 - \sin\phi'}{1 + \sin\phi'} = \tan^2\left(45^\circ - \frac{\phi'}{2}\right) = K_a \quad \text{Eq.4.53}$$

Where, K_p and K_a are called the passive and active earth pressure coefficients. K_p and K_a are used in connection with the analysis of earth-retaining walls. The angle $BCO = \theta$ represents the inclination of the failure plane (BC) or slip plane to the plane on which the major principal effective stress acts in Mohr's circle. Let us find a relationship between θ and ϕ' . From the geometry of Mohr's circle (Figure 4.19),

$$\angle BOC = 90 - \phi' \text{ and } \angle BOD = 2\theta = 90 + \phi'$$

$$\theta = 45^\circ + \frac{\phi'}{2} \quad \text{Eq.4.54}$$

The failure stresses (the stresses on the plane BC) are

$$\sigma'_{nf} = \frac{\sigma'_1 + \sigma'_3}{2} = \frac{\sigma'_1 - \sigma'_3}{2} \sin\phi' \quad \text{Eq.4.55}$$

$$\tau_f = \frac{\sigma'_1 - \sigma'_3}{2} \cos\phi' \quad \text{Eq.4.56}$$

The Mohr-Coulomb (MC) failure criterion is a limiting stress criterion, which requires that stresses in the soil mass cannot lie within the shaded region shown in Figure 4.19. That is, the

soil cannot have stress states greater than the failure stress state. The shaded areas are called regions of impossible stress states. For dilating soils, the bounding curve for possible stress states is the failure envelope, $AEFB$. For non-dilating soils, the bounding curve is the linear line AFB . The MC failure criterion derived here is independent of the intermediate principal effective stress σ_2' , and does not consider the strains at which failure occurs. Because MC is a limiting stress criterion, the failure lines AG and AH (Figure 4.17) are fixed lines in $[\tau, \sigma_n]$ space. The line AG is the failure line for compression, while the line AH is the failure line for extension (soil elongates; the lateral effective stress is greater than the vertical effective stress). The shear strength in compression and in extension from interpreting soil strength using the MC failure criterion is identical. In reality, this is not so.

When the stresses on a plane within the soil mass reach the failure line (plane), they must remain there under further loading. For example, point B (Figure 4.17) is on the MC failure line, AG , but point X is not on the failure line, AH . When additional loading is applied, point B must remain on the failure line, AG . The Mohr circle must then gradually rotate clockwise until point X lies on the failure line, AH . In this way, stresses on more planes reach failure. We could have the reverse, whereby point X is on the failure line, AH , and point B is not on the failure line, AG . For certain geotechnical projects, such as in open excavations in soft soils this may be the case. In practice, our main concern is when failure is first achieved, point B in Figure 6, rather than with the post failure behavior.

Traditionally, failure criteria are defined in terms of stresses. Strains are considered at working stresses (stresses below the failure stresses) using stress–strain relationships (also called constitutive relationships) such as Hooke’s law. Strains are important because although the stress or load imposed on a soil may not cause it to fail, the resulting strains or displacements may be intolerable.

If we normalize (make the quantity a number, i.e., no units) Equation (4.51) by dividing the numerator and denominator by σ_3' , we get

$$\sin\phi' = \frac{(\frac{\sigma_1'}{\sigma_3'})^{f-1}}{(\frac{\sigma_1'}{\sigma_3'})^{f+1}} \text{-----} \quad \text{Eq.4.57}$$

The implication of this equation is that the MC failure criterion defines failure when the maximum principal effective stress ratio, called maximum effective stress obliquity, $\frac{\sigma_1'}{\sigma_3'}$, is achieved and not when the maximum shear stress, $[(\sigma_1' - \sigma_3')/2]_{max}$, is achieved. The failure shear stress is then less than the maximum shear stress.

4.9.4 Tresca Failure Criterion

The shear strength of a fine-grained soil under un-drained condition is called the un-drained shear strength, s_u . We use the Tresca failure criterion—shear stress at failure is one-half the principal stress difference—to interpret the un-drained shear strength. The un-drained shear strength, s_u , is the radius of the Mohr total stress circle; that is,

$$s_u = \frac{\sigma_{1f} - \sigma_{3f}}{2} \text{-----} \quad \text{Eq.4.58}$$

as shown in Figure 4.20 a.

The shear strength under un-drained loading depends only on the initial void ratio or the initial water content. An increase in initial normal effective stress, sometimes called confining pressure, causes a decrease in initial void ratio and a larger change in excess porewater pressure when a soil is sheared under un-drained condition. The result is that the Mohr's circle of total stress expands and the un-drained shear strength increases (Figure 4.20 b). Thus, s_u is not a fundamental soil property. The value of s_u depends on the magnitude of the initial confining pressure or the initial void ratio. Analyses of soil strength and soil stability problems using s_u are called total stress analyses (TSA).

4.10 PRACTICAL IMPLICATIONS OF THE FAILURE CRITERIA

When we interpret soil failure using Coulomb, Mohr–Coulomb, Tresca, or Taylor failure criteria, we are using a particular mechanical model. For example, Coulomb's failure criterion is based on a sliding block model. For this and the Mohr–Coulomb failure criterion, we assume that:

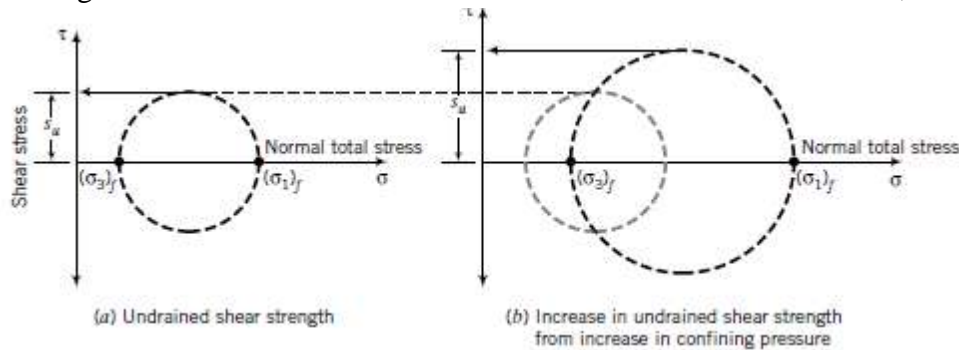


Fig.4.20 Tresca Failure Criteria

1. There is a slip plane upon which one part of the soil mass slides relative to the other. Each part of the soil above and below the slip plane is a rigid mass. However, soils generally do not fail on a slip plane. Rather, in dense soils, there are pockets or bands of soil that have reached critical state while other pockets are still dense. As the soil approaches peak shear stress and beyond, more dense pockets become loose as the soil strain-softens. At the critical state, the whole soil mass becomes loose and behaves like a viscous fluid. Loose soils do not normally show slip planes or shear bands, and strain-harden to the critical state.
2. No deformation of the soil mass occurs prior to failure. In reality, significant soil deformation (shear strains $\sim 2\%$) is required to mobilize the peak shear stress and much more (shear strains $>10\%$) for the critical state shear stress.
3. Failure occurs according to Coulomb by impending, frictional sliding along a slip plane, and according to Mohr–Coulomb when the maximum stress obliquity on a plane is mobilized. The Coulomb and Mohr–Coulomb failure criteria are based on limiting stress. Stresses within the soil must either be on the slip plane or be below it. Taylor failure criterion considers not only the forces acting on the soil mass, but also the deformation that occurs from these forces. That is, failure is a combination of the forces and the resulting deformation. Tresca's criterion, originally

proposed as a yield criterion in solid mechanics, has been adopted in soil mechanics as a failure (limiting stress) criterion. It is not the same as the Mohr–Coulomb failure criterion.

With the exception of Taylor’s criterion, none of the failure criteria provide information on the shear strains required to initiate failure. Strains (shear and volumetric) are important in the evaluation of shear strength and deformation of soils for design of safe foundations, slopes, and other geotechnical systems. Also, these criteria do not consider the initial state (e.g., the initial stresses, over consolidation ratio, and initial void ratio) of the soil. In reality, failure is influenced by the initial state of the soil.

A summary of the key differences among the four soil failure criteria is given in Table 1.

Name	Failure criteria	Soil treated as	Best used for	Test data interpretation*
Coulomb	Failure occurs by impending, frictional sliding on a slip plane.	Rigid, frictional material	Layered or fissured overconsolidated soils or a soil where a prefailure plane exists	Direct shear
Mohr–Coulomb	Failure occurs by impending, frictional sliding on the plane of maximum principal effective stress obliquity.	Rigid, frictional material	Long-term (drained condition) strength of overconsolidated fine-grained and dense coarse-grained soils	Triaxial
Tresca	Failure occurs when one-half the maximum principal stress difference is achieved.	Homogeneous solid	Short-term (undrained condition) strength of fine-grained soils	Triaxial
Taylor	Failure occurs from sliding (frictional strength) and interlocking of soil particles.	Deformable, frictional solid	Short-term and long-term strength of homogeneous soils	Direct simple shear

Example:

A cylindrical soil sample was subjected to axial principal effective stresses (σ'_1) and radial principal effective stresses (σ'_3). The soil could not support additional stresses when $\sigma'_1 = 300$ kPa and $\sigma'_3 = 100$ kPa. (1) Determine the friction angle and the inclination of the slip plane to the horizontal. (2) Determine the stresses on the failure plane. (3) Determine the maximum shear stress. (4) Is the maximum shear stress equal to the failure shear stress? Assume no significant dilational effects.

Solution:

Step 1: Find ϕ'_c

$$\sin \phi'_c = \frac{(\sigma'_1)_{cr} - (\sigma'_3)_{cr}}{(\sigma'_1)_{cr} + (\sigma'_3)_{cr}} = \frac{300 - 100}{300 + 100} = \frac{2}{4} = \frac{1}{2}$$

$$\therefore \phi'_c = 30^\circ$$

Step 2: Find θ .

$$\theta_{cr} = 45^\circ + \frac{\phi'_c}{2} = 45^\circ + \frac{30^\circ}{2} = 60^\circ$$

Step 3: Calculate the stresses on the failure plane.

$$(\sigma'_n)_{cr} = \left(\frac{\sigma'_1 + \sigma'_3}{2} - \frac{\sigma'_1 - \sigma'_3}{2} \sin \phi'_c \right)_{cr} = \left(\frac{300 + 100}{2} - \frac{300 - 100}{2} \sin 30^\circ \right)_{cr} = 150 \text{ kPa}$$

$$\tau_{cr} = \left(\frac{\sigma'_1 - \sigma'_3}{2} \right)_{cr} \cos \phi'_c = \left(\frac{300 - 100}{2} \right)_{cr} \cos 30^\circ = 86.6 \text{ kPa}$$

Step 4: Calculate the maximum shear stress.

$$\tau_{max} = \left(\frac{\sigma_1' - \sigma_3'}{2} \right) = \left(\frac{300 - 100}{2} \right) = 100 \text{ kPa}$$

Step 5: Check if the maximum shear stress is equal to the failure shear stress.

$$\tau_{max} = 100 \text{ kPa} > \tau_{cr} = 86.6 \text{ kPa}$$

The maximum shear stress is greater than the failure shear stress.

5.0 THE CONCEPT OF CRITICAL STATES

The critical state model (CSM) is a simplification and an idealization of soil behavior. However, the CSM captures the behavior of soils that are of greatest importance to geotechnical engineers. The central idea in the CSM is that all soils will fail on a unique failure surface in (p', q, e) space. Thus, the CSM incorporates volume changes in its failure criterion, unlike the Mohr–Coulomb failure criterion, which defines failure only as the attainment of the maximum stress obliquity. According to the CSM, the failure stress state is insufficient to guarantee failure; the soil structure must also be loose enough.

The CSM is a tool to make estimates of soil responses when you cannot conduct sufficient soil tests to completely characterize a soil at a site or when you have to predict the soil's response from changes in loading during and after construction. Although there is a debate about the application of the CSM to real soils, the ideas behind the CSM are simple. It is a very powerful tool to get insights into soil behavior, especially in the case of the “what-if” situation. There is also an overabundance of soil models in the literature that have critical state as their core.

5.1 DEFINITIONS OF KEY TERMS

- i) **Pre-consolidation ratio (Ro)** is the ratio by which the current mean effective stress in the soil was exceeded in the past ($R_0 = \frac{p'_c}{p'_0}$, where p'_c is the pre-consolidation mean effective stress, or, simply, pre-consolidation stress, and p'_0 is the current mean effective stress).
- ii) **Compression index (λ)** is the slope of the normal consolidation line in a plot of void ratio versus the natural logarithm of mean effective stress.
- iii) **Unloading/reloading index, or recompression index (k)**, is the average slope of the unloading/reloading curves in a plot of void ratio versus the natural logarithm of mean effective stress.
- iv) **Critical state line (CSL)** is a line that represents the failure state of soils. In (p', q) space, the critical state line has a slope M , which is related to the friction angle of the soil at the critical state. In $(e, \ln p')$ space, the critical state line has a slope 1, which is parallel to the normal consolidation line. In three dimensional (p', q, e) space, the critical state line becomes a critical state surface.

5.2 RELATION BETWEEN PARAMETERS

In order to develop the basic concepts on critical state, we are going to establish relation between certain plots using stress and strain invariants and concentrate on a saturated soil under axisymmetric loading. However, the concepts and method hold for any loading condition. Rather than plotting σ'_n versus τ , we will plot the data as p' versus q (Figure 5.1 a). This means that we must know the principal stresses acting on the element. For axisymmetric (triaxial) condition, only we need to know two principal stresses.

The Coulomb failure line in $(\sigma'_n$ versus τ) space of slope is now mapped in (p', q) space as a line of slope $M = \frac{q_f}{p'_f}$, where the subscript f denotes failure. Instead of a plot of σ'_z versus e we will plot the data as p' versus e (Figure 1b), and instead of σ'_n (log scale) versus e , we will plot p' (ln scale) versus e (Figure 1.c). The p' (ln scale) versus e plot will be referred to as the $(\ln p', e)$ plot. We will denote the slope of the normal consolidation line (NCL) in the plot of p' (ln scale) versus e as λ and the unloading/reloading (URL) line as k . The NCL is a generic normal consolidation line. In the initial development, the NCL is the same as the isotropic consolidation line (ICL). Later, we will differentiate ICL from the one-dimensional consolidation line (K₀CL). All these consolidation lines have the same slope. There are now relationships between ϕ'_{cs} and M , C_c and λ , C_r and k . The relationships for the slopes of the normal consolidation line, λ , and the unloading/ reloading line, k , are

$$\lambda = \frac{c_c}{\ln(10)} = \frac{c_c}{2.303} = 0.434c_c \text{-----} \quad \text{Eq.5.1}$$

$$k = \frac{c_r}{\ln(10)} = \frac{c_r}{2.303} = 0.434c_r \text{-----} \quad \text{Eq.5.2}$$

Both λ and k are positive for compression. For many soils, k/λ has values within the range 10 to 15. We will formulate the relationship between ϕ'_{cs} and M later. The over-consolidation ratio using stress invariants, called pre-consolidation ratio, is

$$R_0 = \frac{p'_c}{p'_0} \text{-----} \quad \text{Eq.5.3}$$

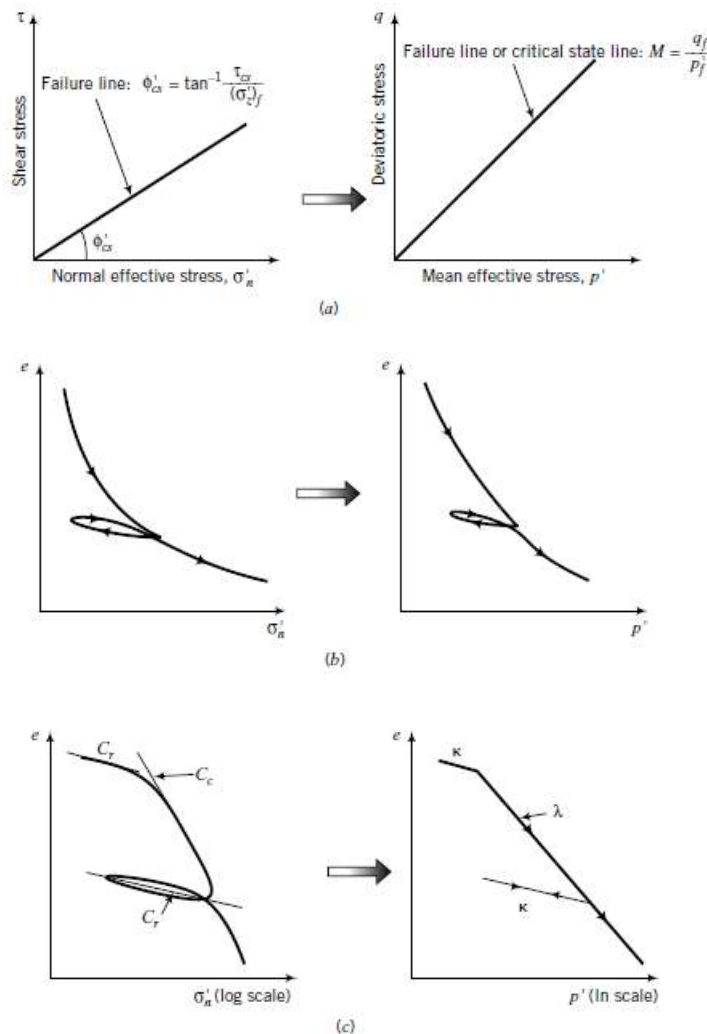


Fig.5.1: Plot between effective stress and void ratio

The concept of critical states can be defined in the following way:

The concept that soil and other granular materials, if continuously distorted until they flow as a frictional fluid, will come in to a well-defined critical state determined by two equations

$$q = Mp \text{ -----} \quad \text{Eq.5.4}$$

$$\tau = v + \lambda \ln p \text{ -----} \quad \text{Eq.5.5}$$

As a result the critical states depend on the mean effective stress p , shear stress q and soil specific volume v and are shown graphically in Figure 5.2 as two straight lines (now known as the critical state lines CSL), where e denotes the void ratio.

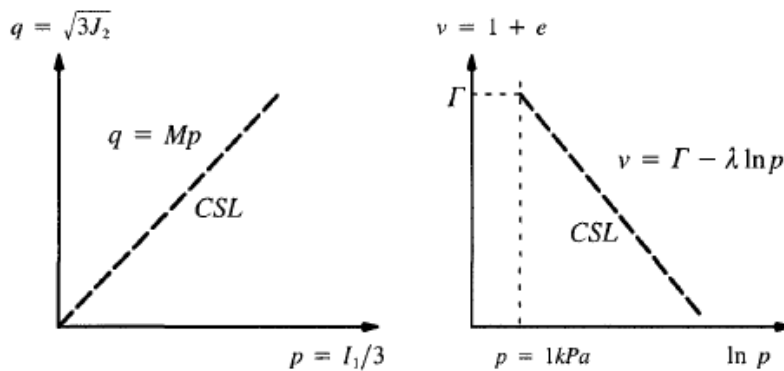


Fig.5.2: Graphical representation of specific volume with p and q

It was further explained that at the critical state, soils behave as a *frictional fluid* so that yielding occurs at constant volume and constant stresses. In other words, the plastic volumetric strain increment is zero at the critical state, since elastic strain increments will be zero due to the constant stress condition at the critical state. Also it was assumed that the critical state lines are unique for a given soil regardless of stress paths used to bring them about from any initial conditions.

In many ways, the critical states defined or assumed above may be regarded as the ultimate states anticipated by Drucker *et al.* (1957). It is also noted that the concept of steady states proposed later by Poulos (1981) is also similar to the concept of critical states. In addition, Desai and Toth (1996) and Desai (2001) proposed a concept of disturbed states for use in constitutive modeling. In effect, the critical states correspond to Desai's fully disturbed states. Given the uniqueness of the critical state lines, they are used as a convenient base of reference in formulating a strain hardening/softening plasticity model to describe the measured behaviour of soil and other granular materials (Yu, 1998).

The concept of critical states was initially developed based on limited triaxial test data obtained on reconstituted clay (Roscoe *et al.*, 1958; Parry, 1958; Schofield and Wroth, 1968; Roscoe and Burland, 1968). However over the last forty years, a lot of additional experimental data for many

other types of soil and granular material (e.g. sand, rock, natural clay, unsaturated soil and sugar) have been obtained which seems to support, at least to a very large extent, the general concept of critical states (e.g. Atkinson and Bransby, 1978; Brown and Yu, 1988; Been *et al.*, 1991; Muir Wood, 1990; Atkinson and Allman, 1992; Novello and Johnston, 1995).

5.3 CRITICAL STATE PARAMETERS

Failure Line in (p' , q) Space: The failure line in (p' , q) space is

$$q_f = Mp'_f \text{-----} \quad \text{Eq.5.6}$$

Where, q_f is the deviatoric stress at failure, M is a frictional constant, and p'_f is the mean effective stress at failure. By default, the subscript f denotes failure and is synonymous with critical state. For compression, $M=M_c$, and for extension, $M = M_e$. The critical state line intersects the yield surface at $\frac{p'_c}{2}$. We can build a convenient relationship between M and ϕ'_{cs} for axisymmetric compression and extension and plane strain conditions as follows.

5.3.1 Axisymmetric Compression

$$M_c = \frac{q_f}{p_f} = \frac{(\sigma'_1 - \sigma'_3)_f}{\left(\frac{\sigma'_1 + 2\sigma'_3}{3}\right)_f} \text{-----} \quad \text{Eq.5.7}$$

$$\text{But we know that } \left(\frac{\sigma'_1}{\sigma'_3}\right)_f = \frac{1 + \sin\phi'_{cs}}{1 - \sin\phi'_{cs}} \text{-----} \quad \text{Eq.5.8}$$

Hence

$$M_c = \frac{6\sin\phi'_{cs}}{3 - \sin\phi'_{cs}} \text{-----} \quad \text{Eq.5.9}$$

$$\text{Or } \sin\phi'_{cs} = \frac{3M_c}{6 + M_c} \text{-----} \quad \text{Eq.5.10}$$

5.3.2 Axisymmetric Extension

In an axisymmetric (triaxial) extension, the radial stress is the major principal stress. Since in axial symmetry the radial stress is equal to the circumferential stress, we get

$$p'_f = \left(\frac{2\sigma'_1 + \sigma'_3}{3}\right)_f \text{-----} \quad \text{Eq.5.11}$$

$$q_f = (\sigma'_1 - \sigma'_3)_f \text{-----} \quad \text{Eq.5.12}$$

$$M_e = \frac{q_f}{p'_f} = \frac{\left(\frac{2\sigma'_1}{\sigma'_3} + 1\right)_f}{\left(\frac{\sigma'_1}{\sigma'_3} - 1\right)_f} \text{-----} \quad \text{Eq.5.13}$$

$$M_e = \frac{6\sin\phi'_{cs}}{3 + \sin\phi'_{cs}} \text{-----} \quad \text{Eq.5.14}$$

$$\text{Hence } \sin\phi'_{cs} = \frac{3M_e}{6 - M_e} \text{-----} \quad \text{Eq.5.15}$$

An important point to note is that while the friction angle, ϕ'_{cs} , is the same for compression and extension, the slope of the critical state line in (p' , q) space is not the same (Figure 5.3). Therefore, the failure deviatoric stresses in compression and extension are different. Since $M_e <$

M_c the failure deviatoric stress of a soil in extension is lower than that for the same soil in compression.

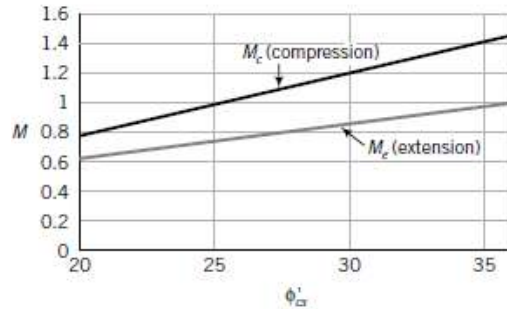


Fig.5.3: Variation of the frictional constant M with critical state friction angle

5.3.3 Plane Strain

In plane strain, one of the strains is zero, we selected, $\epsilon_2 = 0$; thus, $\sigma'_2 \neq 0$. In general, we do not know the value of σ'_2 unless we have special research equipment to measure it. If

$$\sigma'_2 = C(\sigma'_1 + \sigma'_3) \text{-----} \text{Eq.5.16}$$

where $C = 0.5$, then

$$M = M_{ps} = \sqrt{3} \sin \phi'_{cs} \text{-----} \text{Eq.5.17}$$

Taking $C = 0.5$ presumes zero elastic compressibility. The subscript p_{cs} denotes plane strain. The constant, C , using a specially designed simple shear device (Budhu, 1984) on a sand, was shown to be approximately $\frac{1}{2} \tan \phi'_{cs}$.

5.4 FAILURE LINE IN (P' , e) SPACE

Let us now find the equation for the critical state line in (p' , e) space. We will use the ($\ln p'$, e) plot, as shown in Figure 5.4 c. The CSL is parallel to the normal consolidation line and is represented by

$$e_f = e_\tau - \lambda \ln p'_f \text{-----} \text{Eq.5.18}$$

where e_τ is the void ratio on the critical state line when $p' = 1$. This value of void ratio serves as an anchor for the CSL in (p' , e) space and ($\ln p'$, e) space. The value of e_τ depends on the units chosen for the p' scale. In this chapter, we will use kPa for the units of p' .

We will now determine e_τ from the initial state of the soil. Let us isotropically consolidate a soil to a mean effective stress, p'_c , and then isotropically unload it to a mean effective stress p'_0 (Figure 5.4 a, b).

Let X be the intersection of the unloading/reloading line with the critical state line. The mean effective stress at X is $\frac{p'_c}{2}$, and from the unloading/reloading line,

$$e_x = e_0 + k \ln \left(\frac{p'_0}{\frac{p'_c}{2}} \right) \text{-----} \text{Eq.5.19}$$

where e_0 is the initial void ratio. From the critical state line,

$$e_f = e_\tau - \lambda \ln \frac{p'_c}{2} \text{-----} \quad \text{Eq.5.20}$$

Therefore, combining Equations (5.19) and (5.20), we get

$$e_\tau = e_0 + (\lambda - k) \ln \frac{p'_c}{2} + k \ln p'_0 \text{-----} \quad \text{Eq.5.21}$$

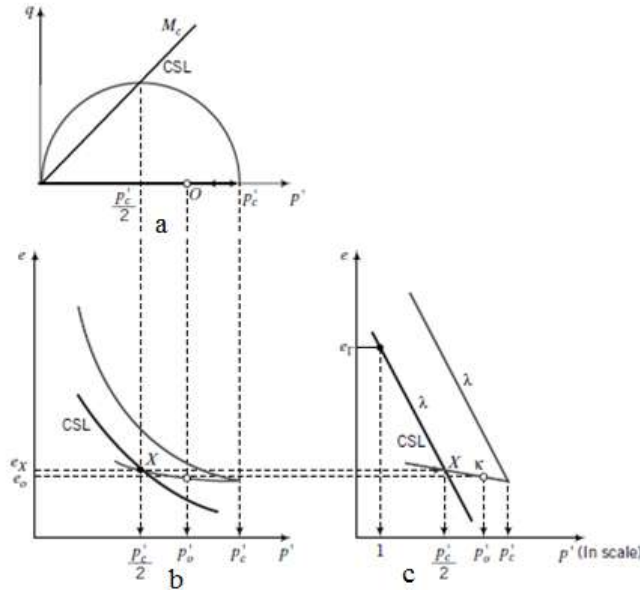


Fig. 5.4: Void ratio e_τ to anchor critical state line

EXAMPLE 1 Calculation of M and Failure Stresses in Extension

A standard triaxial CD test at a constant cell pressure, $\sigma_3 = \sigma'_3 = 120$ kPa, was conducted on a sample of normally consolidated clay. At failure, $q = \sigma_1 - \sigma_3 = 140$ kPa.

- (a) Calculate M_c .
- (b) Calculate p'_f .
- (c) Determine the deviatoric stresses at failure if an extension test were to be carried out so that failure occurs at the same mean effective stress.

Solution:

Step 1: Find the major principal stress at failure.

$$(\sigma_1)_f = (\sigma_1 - \sigma_3) + \sigma_3 = 140 + 120 = 260 \text{ kPa}$$

Step 2: Find p'_f .

$$p'_f = \left(\frac{\sigma_1 + 2\sigma_3}{3} \right)_f = \frac{260 + 2 \times 120}{3} = 166.7 \text{ kPa}$$

Step 3: Find ϕ'_{cs} .

$$\sin \phi'_{cs} = \frac{\sigma_1 - \sigma_3}{\sigma_1 + \sigma_3} = \frac{140}{260 + 120} = 0.37$$

$$\phi'_{cs} = 21.6^\circ$$

Step 4: Find M_c and M_e .

$$M_c = \frac{6 \sin \phi'_{cs}}{3 - \sin \phi'_{cs}} = \frac{6 \times 0.37}{3 - 0.37} = 0.84$$

$$M_e = \frac{6 \sin \phi'_{cs}}{3 + \sin \phi'_{cs}} = \frac{6 \times 0.37}{3 + 0.37} = 0.66$$

Step 5: Find q_f for extension.

$$q_f = \frac{0.66}{0.84} \times 140 = 110 \text{ kPa}; \quad p_f^j = \frac{q_f}{M_e} = \frac{110}{0.66} = 166.7 \text{ kPa}$$

EXAMPLE 2 Determination of λ , κ , and e_Γ

A saturated soil sample is isotropically consolidated in a triaxial apparatus, and a selected set of data is shown in the table. Determine λ , κ , and e_Γ .

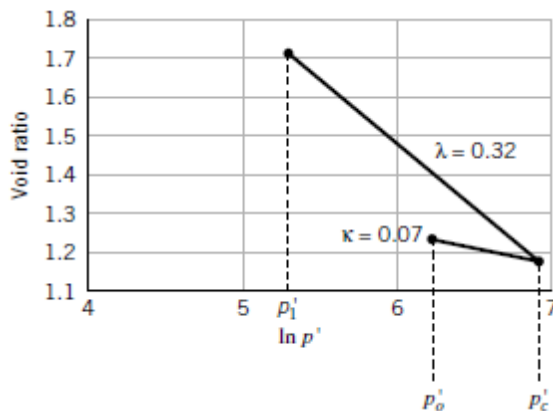
Condition	Cell pressure (kPa)	Final void ratio
Loading	200	1.72
	1000	1.20
Unloading	500	1.25

Solution:

Step 1: Make a plot of $\ln p'$ versus e .

Consider graph as shown below

Step 2: Calculate λ .
$$\lambda = -\frac{\Delta e}{\ln(p'_c) - \ln(p'_i)} = -\frac{1.20 - 1.72}{6.91 - 5.3} = 0.32$$



Step 3: Calculate κ .

From Figure

$$\kappa = -\frac{\Delta e}{\ln(p'_c) - \ln(p'_o)} = -\frac{1.20 - 1.25}{6.91 - 6.21} = 0.07$$

Step 4: Calculate e_Γ .

$$\begin{aligned} e_\Gamma &= e_o + (\lambda - \kappa) \ln \frac{p'_c}{2} + \kappa \ln p'_o \\ &= 1.25 + (0.32 - 0.07) \ln \frac{1000}{2} + 0.07 \ln 500 = 3.24 \end{aligned}$$

5.5 SOIL YIELDING

We that there is a yield surface in stress space that separates stress states that produce elastic responses from stress states that produce plastic responses. We are going to use the yield surface in (p', q) space rather than (σ'_1, σ'_3) space so that our interpretation of soil responses is independent of the axis system.

The yield surface is assumed to be an ellipse, and its initial size or major axis is determined by the pre-consolidation stress p'_c . Experimental evidence (Wong and Mitchell, 1975) indicates that an elliptical yield surface is a reasonable approximation for soils. Higher is the pre-consolidation stress, the larger the initial ellipse. We will consider the yield surface for compression, but the ideas are the same for extension except that the minor axis of the elliptical yield surface in extension is smaller than in compression. All combinations of q and p' that are within the yield surface, for example, point A in Figure 5.5, will cause the soil to respond elastically. If a combination of q and p' lies on the initial yield surface (point B , Figure 5.5), the soil yields in a similar fashion to the yielding of a steel bar. Any tendency of a stress combination to move outside the current yield surface is accompanied by an expansion of the current yield surface, such that during plastic loading the stress point (p', q) lies on the expanded yield surface and not outside, as depicted by C . Effective stress paths such as BC (Figure 5.5) cause the soil to behave elasto-plastically.

If the soil is unloaded from any stress state below failure, the soil will respond like an elastic material. As the initial yield surface expands, the elastic region gets larger. Expansion of the initial yield surface simulates strain-hardening materials such as loose sands and normally and lightly over consolidated clays. The initial yield surface can also contract, simulating strain-softening materials such as dense sands and heavily over consolidated clays. You can think of the yield surface as a balloon. Blowing up the balloon (applying pressure; loading) is analogous to the expansion of the yield surface. Releasing the air (gas) from the balloon (reducing pressure; unloading) is analogous to the contraction of the yield surface. The critical state line intersects every yield surface at its crest. Thus, the intersection of the initial yield surface and the critical state line is at a mean effective stress $\frac{p'_c}{2}$, and for the expanded yield surface it is at $\frac{p'_G}{2}$.

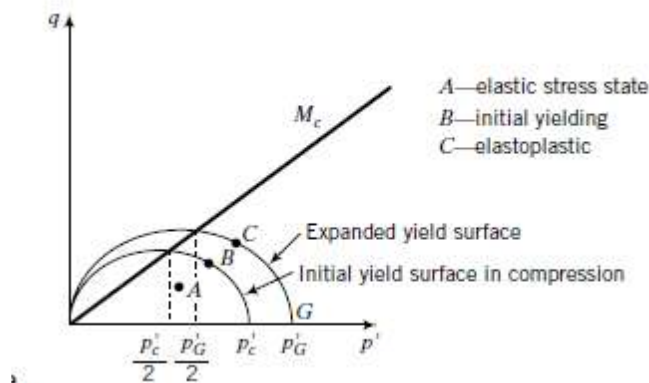


Fig.5.5: Expansion of the yield surface

5.6 PREDICTION OF THE BEHAVIOR OF NORMALLY CONSOLIDATED AND LIGHTLY OVER CONSOLIDATED SOILS (Under Drained Condition)

Let us consider a hypothetical situation to illustrate the ideas presented so far. We are going to try to predict how a sample of soil of initial void ratio e_0 will respond when tested under drained condition in a triaxial apparatus, that is, a standard CD test. You should recall that the soil sample in a CD test is isotropically consolidated and then axial loads or displacements are applied, keeping the cell pressure constant. We are going to consolidate our soil sample up to a maximum mean effective stress p'_c , and then unload it to a mean effective stress p'_0 , such that $R_0 = \frac{p'_c}{p'_0} < 2$. The limits imposed on R_0 are only for presenting the basic ideas on CSM. More details on delineating lightly over consolidated from heavily over consolidated soils will be discussed in latter on.

On a plot of p' versus e (Figure 5.6.b), the isotropic consolidation path is represented by AC. You should recall that the line AC maps as the normal consolidation line (NCL) of slope 1. Because we are applying isotropic loading, the line AC is called the isotropic consolidation line (ICL).

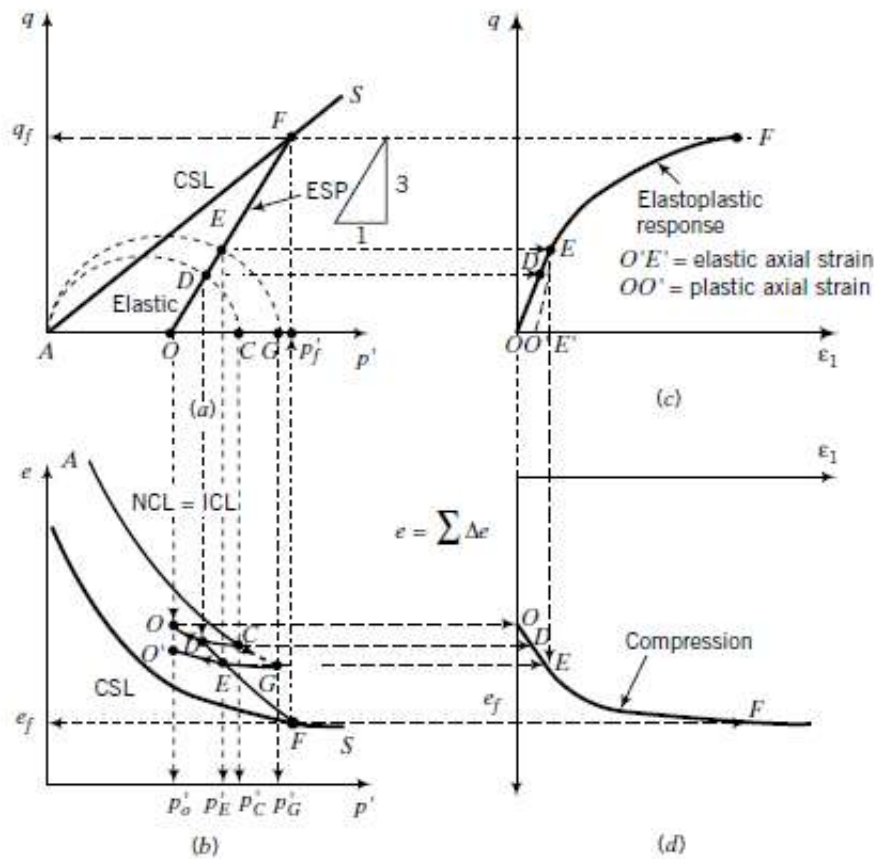


Fig.5.6: Illustrative predicted results from a triaxial CD test on a lightly over-consolidated soil

As we consolidate the soil gradually from A to C and unload it gradually to O , the stress paths followed in the (p', q) space are $A \rightarrow C$ and $C \rightarrow O$, respectively (Figure 5.5.a). We can also sketch a curve (CO , Figure 5.5.b) to represent the unloading of the soil in (p', e) space. The line CO is then the unloading/ reloading line of slope, k , in $(\ln p', e)$ space. The pre-consolidation mean effective stress, p'_c , determines the size of the initial yield surface. Since the maximum mean effective stress applied is the mean effective stress at C , then AC is the major principal axis of the ellipse representing the initial yield surface. A semi-ellipse is sketched in Figure 5.5.a to illustrate the initial yield surface for compression. We can draw a line, AS , of slope, M_c , from the origin to represent the critical-state line (CSL) in (p', q) space, as shown in Figure 5.5.a. In (p', e) space, the critical state line is parallel to the normal consolidation line (NCL), as shown in Figure 5.5 b. Of course, we do not know, as yet, the slope $M = M_c$, or the equations to draw the initial yield surface and the CSL in (p', e) space. We have simply selected arbitrary values. Later, we are going to develop equations to define the slope M , the shape of the yield surface, and the critical state line in (p', e) space or $(\ln p', e)$ space. The CSL intersects the initial yield surface and all subsequent yield surfaces at $\frac{p'_c}{2}$, where p'_c is the (generic) current pre-consolidation mean effective stress. For example, when the yield surface expands with a major axis, say AG , the CSL will intersect it at $\frac{p'_G}{2}$.

Let us now shear the soil sample at its current mean effective stress, p'_0 , by increasing the axial stress, keeping the cell pressure, σ_3 , constant, and allowing the sample to drain. Because the soil is allowed to drain, the total stress is equal to the effective stress. That is, $\Delta\sigma_1 = \Delta\sigma'_1 > 0$. But we know that the effective stress path for a standard triaxial CD test has a slope $\frac{q}{p'} = 3$. The effective stress path (ESP) is shown by OF in Figure 5.6.a. The ESP is equal to the total stress path (TSP) because this is a drained test. The effective stress path intersects the initial yield surface at D . All stress states from O to D lie within the initial yield surface and, therefore, from O to D on the ESP the soil behaves elastically.

Assuming linear elastic response of the soil, we can draw a line OD in (ε_1, q) space (Figure 5.6.c) to represent the elastic stress–strain response. At this stage we do not know the slope of OD , but later you will learn how to get this slope. Since the line CO in (p', e) space represents the unloading/reloading line (URL), the elastic response must lie along this line. The change in void ratio is $\Delta e = e_D - e_0$ (Figure 5.6.b) and we can plot the axial strain (ε_1) versus e response, as shown by OD in Figure 5.6.d. Further loading from D along the stress path OF causes the soil to yield. The initial yield surface expands (Figure 5.6.a) and the stress–strain is no longer elastic but elasto-plastic. At some arbitrarily chosen small increment of loading beyond initial yield, point E along the ESP, the size (major axis) of the yield surface is p'_G (G in Figure 5.6.a). There must be a corresponding point G on the NCL in (p', e) space, as shown in Figure 5.6.b. The increment of loading shown in Figure 5.6 is exaggerated.

Normally, the stress increment should be very small because the soil behavior is no longer elastic. The stress is now not directly related to strain but is related to the plastic strain increment. The total change in void ratio as you load the sample from D to E is DE (Figure

5.6.b). Since E lies on the expanded yield surface with a past mean effective stress, p'_G , then E must be on the unloading line, GO' , as illustrated in Figure 5.6.b. If you unload the soil sample from E back to O (Figure 5.6.a), the soil will follow an unloading path, EO' , parallel to OC , as shown in Figure 1.b. In the stress–strain plot, the unloading path will be EO' , (Figure 5.6.c). The length OO' , on the axial strain axis is the plastic (permanent) axial strain, while the length EO' is the elastic axial strain. We can continue to add increments of loading along the ESP until the CSL is intersected. At this stage, the soil fails and cannot provide additional shearing resistance to further loading. The deviatoric stress, q , and the void ratio, e , remain constant. The failure stresses are p'_f and q_f (Figure 5.6.a) and the failure void ratio is e_f (Figure 5.6.b). In general, it is the ratio $\frac{q_f}{p'_f} = M$ and ef that are constants. For each increment of loading, we can determine Δe and plot ε_1 versus $\sum \Delta e$, as shown in Figure 5.6.d. We can then sketch the stress–strain curve and the path followed in (p', e) space. Let us summarize the key elements so far about our model.

1. During isotropic consolidation, the stress state must lie on the mean effective stress axis in (p', q) space and also on the NCL in (p', e) space.
2. All stress states on an ESP within and on the yield surface must lie on the unloading/reloading line through the current pre consolidation mean effective stress. For example, any point on the semi ellipse, AEG , in Figure 5.6.a has a corresponding point on the unloading/reloading line, $O'G$. Similarly, any point on the ESP from, say, E will also lie on the unloading/reloading line $O'G$. In reality, we are projecting the mean effective stress component of the stress state onto the unloading/reloading line.
3. All stress states on the unloading/reloading line result in elastic response.
4. Consolidation (e.g., stress paths along the p' axis) cannot lead to soil failure. Soils fail by the application of shearing stresses following ESP with slopes greater than the slope of the CSL for compression.
5. Any stress state on an ESP directed outward from the current yield surface causes further yielding. The yield surface expands.
6. Unloading from any expanded yield surface produces elastic response.
7. Once yielding is initiated, the stress–strain curve becomes nonlinear, with an elastic strain component and a plastic strain component.
8. The critical state line intersects each yield surface at its crest. The corresponding mean effective stress is one-half the mean effective stress of the major axis of the ellipse representing the yield surface.
9. Failure occurs when the ESP intersects the CSL and the change in volume is zero.
10. The soil must yield before it fails.
11. Each point on one of the plots in Figure 5.5 has a corresponding point on another plot. Thus, each point on any plot can be obtained by projection, as illustrated in Figure 5.5 of course; the scale of the axis on one plot must match the scale of the corresponding axis on the other plot. For example, point F on the failure line, AS , in (p', q) space must have a corresponding point F on the failure line in (p', e) space.

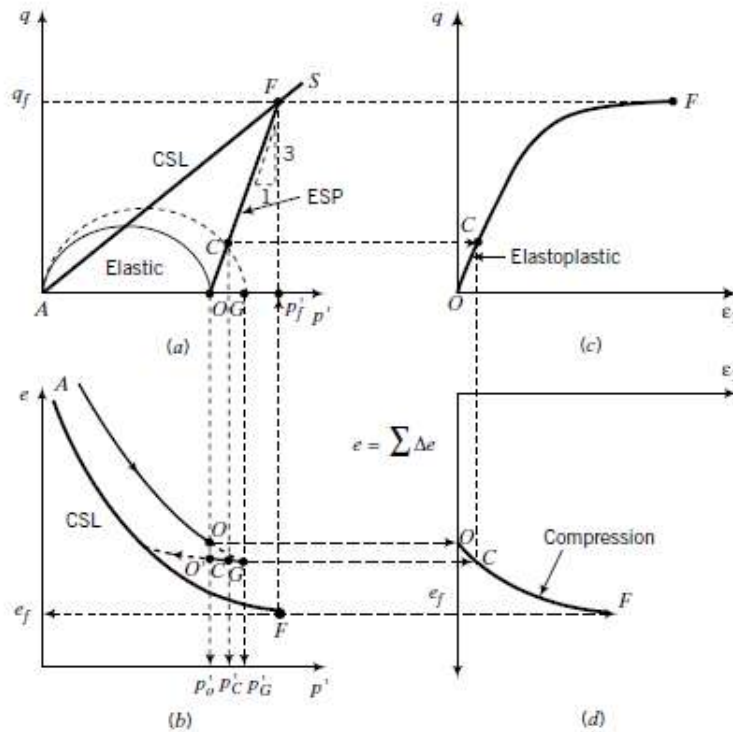


Fig.5.7: Illustrative predicted results from a CD triaxial test on a normally consolidated soil

In the case of a normally consolidated soil, the past mean effective stress is equal to the current mean effective stress (O in Figure 5.7 a, b). The point O is on the initial yield surface. So, upon loading, the soil will yield immediately. There is no initial elastic region. An increment of effective stress corresponding to C in Figure 5.7 will cause the initial yield surface to expand. The pre consolidation mean effective stress is now P'_G and must lie at the juncture of the normal consolidation line and the unloading/ reloading line. Since C is on the expanded yield surface, it must have a corresponding point on the unloading/reloading line through G . If you unload the soil from C , you will now get an elastic response ($C \rightarrow O'$, Figure 5.6.b). The soil sample has become over consolidated. Continued incremental loading along the ESP will induce further incremental yielding until failure is attained.

5.7 PREDICTION OF THE BEHAVIOR OF NORMALLY CONSOLIDATED AND LIGHTLY OVER-CONSOLIDATED SOILS (Under Un-drained Condition)

Instead of a standard triaxial CD test, we could have conducted a standard triaxial CU test after consolidating the sample. The slope of the TSP is 3. We do not know the ESP as yet. Let us examine what would occur to a lightly over consolidated soil under un-drained condition according to our CSM. We will use the abscissa as a dual axis for both p' and p (Figure 5.8). We know that for un-drained condition the soil volume remains constant, that is, $\Delta e = 0$. Constant volume does not mean that there is no induced volumetric strain in the soil sample as it is sheared. Rather, it means that the elastic volumetric strain is balanced by an equal and opposite amount of plastic volumetric strains. We also know that the ESP for a linear elastic soil is

vertical, that is, the change in mean effective stress, $\Delta p'$ is zero. Because the change in volume is zero, the mean effective stress at failure can be represented by drawing a horizontal line from the initial void ratio to intersect the critical state line in (p', e) space, as illustrated by OF in Figure 3b. Projecting a vertical line from the mean effective stress at failure in (p', e) space to intersect the critical state line in (p', q) space gives the deviatoric stress at failure (Figure 5.8a). The initial yield stresses (p'_y, q_y) , point D in Figure 5.8a, are obtained from the intersection of the ESP and the initial yield surface. Points O and D are coincident in the (p', e) plot, as illustrated in Figure 3b, because $\Delta p' = 0$. The ESP (OD in Figure 5.8 a) produces elastic response. Continued loading beyond initial yield will cause the initial yield surface to expand. For example, any point E between D and F on the constant void ratio line will be on an expanded yield surface (AEG) in (p', q) space. Also, point E must be on a URL line through G (Figure 5.8 b). The ESP from D curves left toward F on the critical state line as excess pore water pressure increases significantly after initial yield. The TSP has a slope of 3, as illustrated by OX in Figure 5.8 a. The difference in mean stress between the total stress path and the effective path gives the change in excess pore water pressure. The excess pore water pressures at initial yield and at failure are represented by the horizontal lines DW and FT , respectively.

The un-drained shear response of a soil is independent of the TSP. The shearing response would be the same if we imposed a TSP OM (Figure 5.8 a), of slope, say, 2 (V): 1 (H) rather than 3 (V): 1 (H), where V and H are vertical and horizontal values. The TSP is only important in finding the total excess pore water pressure under un-drained loading. The intersection of the TSP with the critical state line is not the failure point, because failure and deformation of a soil mass depend on effective stress, not total stress. By projection, we can sketch the stress–strain response and the excess pore water pressure versus axial strain, as illustrated in Figure 5.8 c, d.

For normally consolidated soils, yielding begins as soon as the soil is loaded (Figure 5.9). The ESP curves toward F on the failure line. A point C on the constant volume line, OF , in Figure 5.9b will be on an expanded yield surface and also on the corresponding URL (Figure 5.9 a, b). The excess pore water pressures at C and F are represented by the horizontal lines CT and FW , respectively.

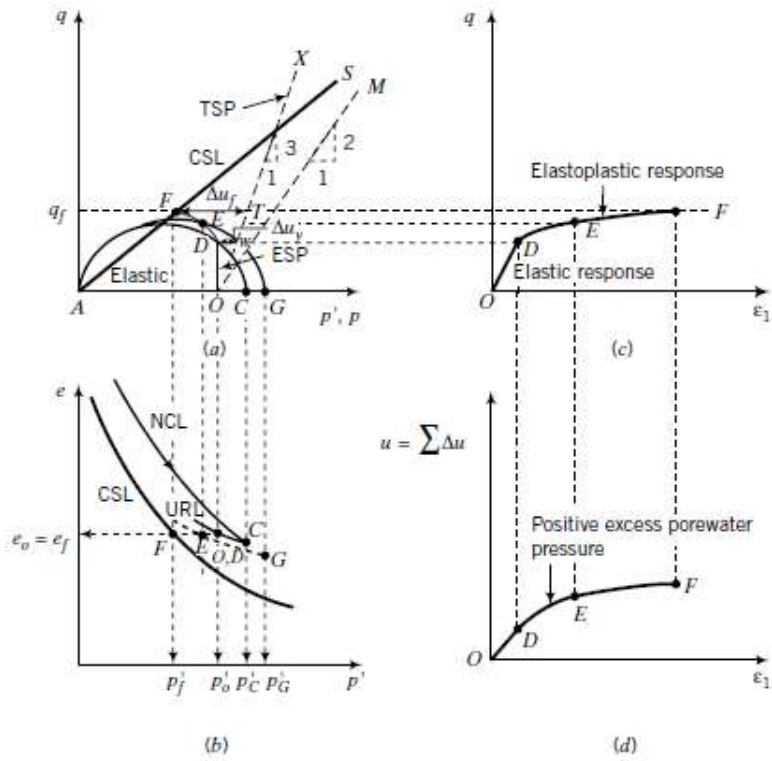


Fig.5.8: Illustrative predicted results from a triaxial CU test on a lightly over consolidated soil using the CSM

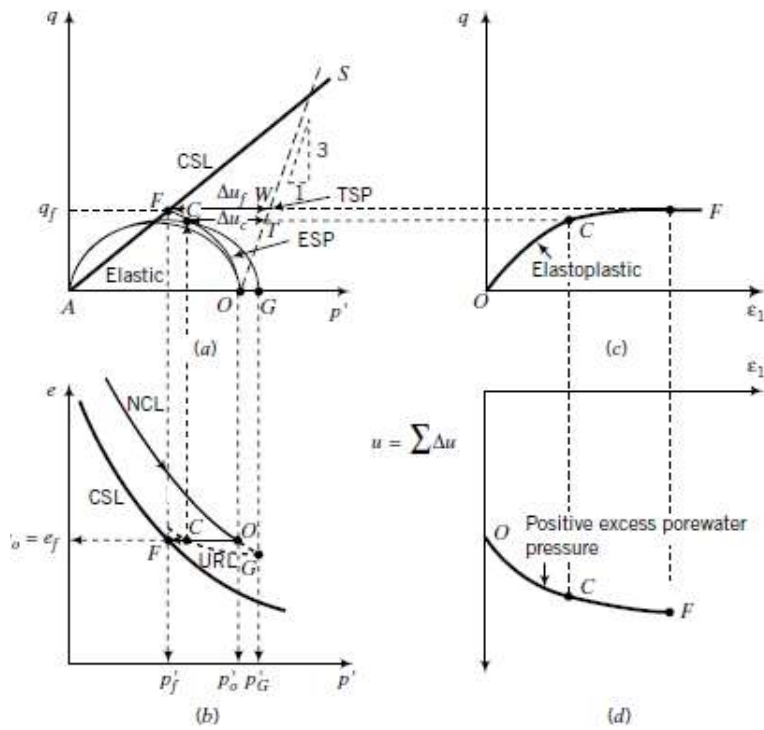


Fig.5.9: Illustrative predicted results from a triaxial CU test on a normally consolidated soil using the CSM

Let us summarize the key elements for un-drained loading of lightly over consolidated and normally consolidated soils from our model.

1. Under un-drained loading, also called constant-volume loading, the total volume remains constant. This is represented in (p', e) space by a horizontal line from the initial mean effective stress to the failure line.
2. The portion of the ESP in (p', q) space that lies within the initial yield surface is represented by a vertical line from the initial mean effective stress to the initial yield surface. The soil behaves elastically, and the change in mean effective stress is zero.
3. Normally consolidated soils do not show an initial elastic response. They yield as soon as the loading is applied.
4. Loading beyond initial yield causes the soil to behave as a strain-hardening elasto-plastic material. The initial yield surface expands.
5. The difference in mean total and mean effective stress at any stage of loading gives the excess pore water pressure at that stage of loading.
6. The response of soils under un-drained condition is independent of the total stress path.

5.8 PREDICTION OF THE BEHAVIOR OF HEAVILY OVER-CONSOLIDATED SOILS

(Under Drained and Un-drained Condition)

So far we have considered normally and lightly over consolidated soils ($R_0 \leq 2$). What is the situation regarding heavily over-consolidated soils, that is, $R_0 > 2$? Whether a soil behaves in a normally consolidated or a lightly over-consolidated or a heavily over-consolidated manner depends not only on R_0 but also on the effective stress path. We can model a heavily over-consolidated soil by unloading it from its pre-consolidation stress so that, $\frac{p'_c}{p'_0} > 2$, as shown by point O in Figure 5.10.a, b.

Heavily over-consolidated soils have initial stress states that lie to the left of the critical state line in $(p' e)$ space. The ESP for a standard triaxial CD test has a slope of 3 and intersects the initial yield surface at D . Therefore, from O to D the soil behaves elastically, as shown by OD in Figure 1.b, c. The intersection of the ESP with the critical state line is at F (Figure 5.10.a), so that the yield surface must contract as the soil is loaded to failure beyond initial yield. The initial yield shear stress is analogous to the peak shear stress for dilating soils. From D , the soil volume expands (Figure 5.10.b, d), and the soil strain softens (Figure 5.10.c) to failure at F . Remember that soil yielding must occur before failure. So, the soil must follow the path $O \rightarrow S \rightarrow D \rightarrow S \rightarrow F$ and not $O \rightarrow S \rightarrow F \rightarrow S \rightarrow D$.

The simulated volumetric response is shown in Figure 5.10.d. From O to D (the elastic phase), the soil contracts. After initial yielding, the soil expands (dilates) up to failure and remains at constant volume (constant void ratio) thereafter.

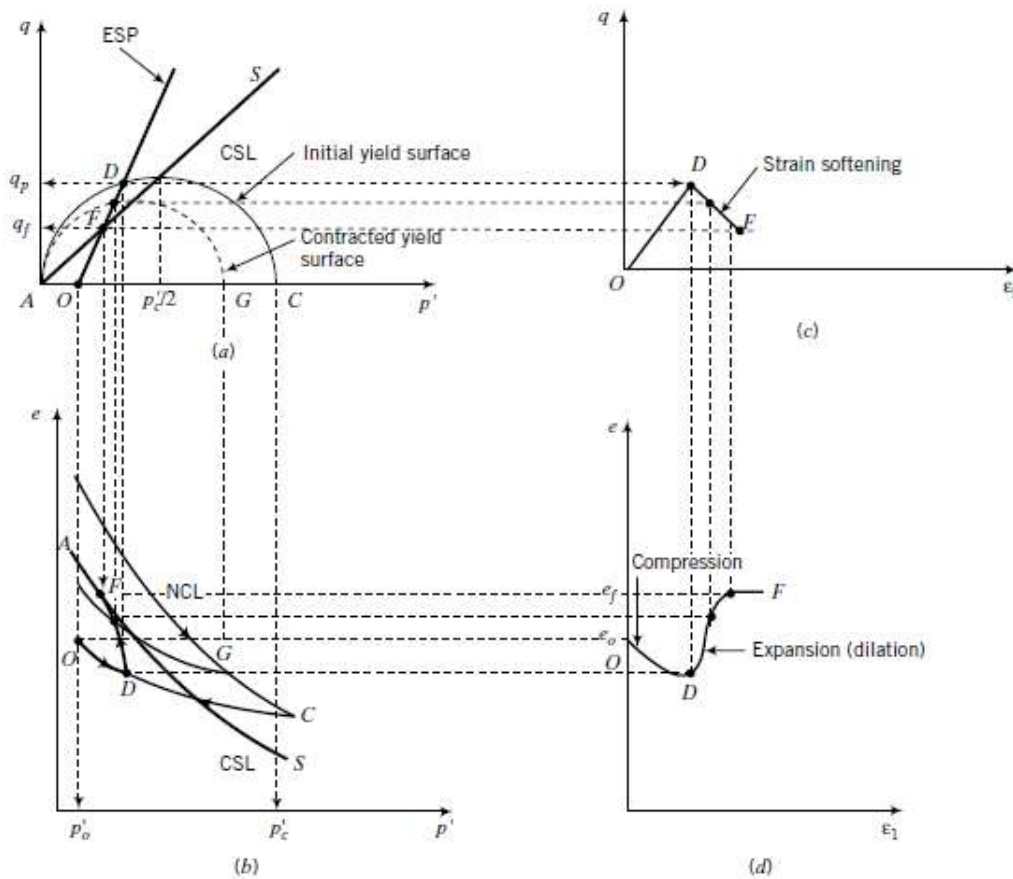


Fig.5.10: Illustrative predicted results from a triaxial CD test on a heavily over consolidated soil ($R_o > 2$) using the CSM.

The CSM simulates the mechanical behavior of heavily over-consolidated soils as elastic materials up to the peak shear stress and thereafter elasto-plastically as the imposed loading causes the soil to strain-soften toward the critical state line. In reality, heavily over-consolidated soils may behave elasto-plastically before the peak shear stress is achieved, but this behavior is not captured by the simple CSM described here.

In the case of a standard triaxial CU test on heavily over consolidated soils, the path to failure in (p', e) Space is OF , as shown in Figure 5.11.b, because no change in volume occurs. In the (p', q) space (Figure 5.11.a), the soil will yield at D and then fail at F . So the path to failure is $O \rightarrow S \rightarrow D \rightarrow S \rightarrow F$. All stress states from O to D are within the initial yield surface, so the soil behaves like an elastic material. The ESP is then represented by a vertical line. Any stress state between D and F must have a corresponding point at the intersection of a URL line and the constant volume line, OF (Figure 5.11. b). The yield surface from D to F contracts.

The tendency for the soil to contract from O to D induces positive excess pore water pressures, while the tendency to expand (D to F) induces negative excess pore water pressures (Figure 5.11. d). The excess pore water pressures at initial yield, Δu_y and at failure, Δu_f are shown in the inset of Figure 5.11. a. The excess pore water pressure at failure is negative ($p'_f > p_f$).

Let us summarize the key elements for un-drained loading of heavily over-consolidated soils from the model.

1. Under un-drained loading, the total volume remains constant. This is represented in (p', e) space by a horizontal line from the initial mean effective stress to the failure line.
2. The portion of the ESP in (p', q) space that lies within the initial yield surface is represented by a vertical line from the initial mean effective stress to the initial yield surface. The soil behaves elastically, and the change in mean effective stress is zero.
3. After initial yield, the soil may strain-soften (the initial yield surface contracts) or may strain-harden (the initial yield surface expands) to the critical state.
4. During elastic deformation under drained condition, the soil volume decreases (contracts), and after initial yield the soil volume increases (expands) to the critical state and does not change volume thereafter.
5. During elastic deformation under un-drained condition, the soil develops positive excess pore water pressures, and after initial yield the soil develops negative excess pore water pressures up to the critical state. Thereafter, the excess pore water pressure remains constant.
6. The response of the soil under un-drained condition is independent of the total stress path.

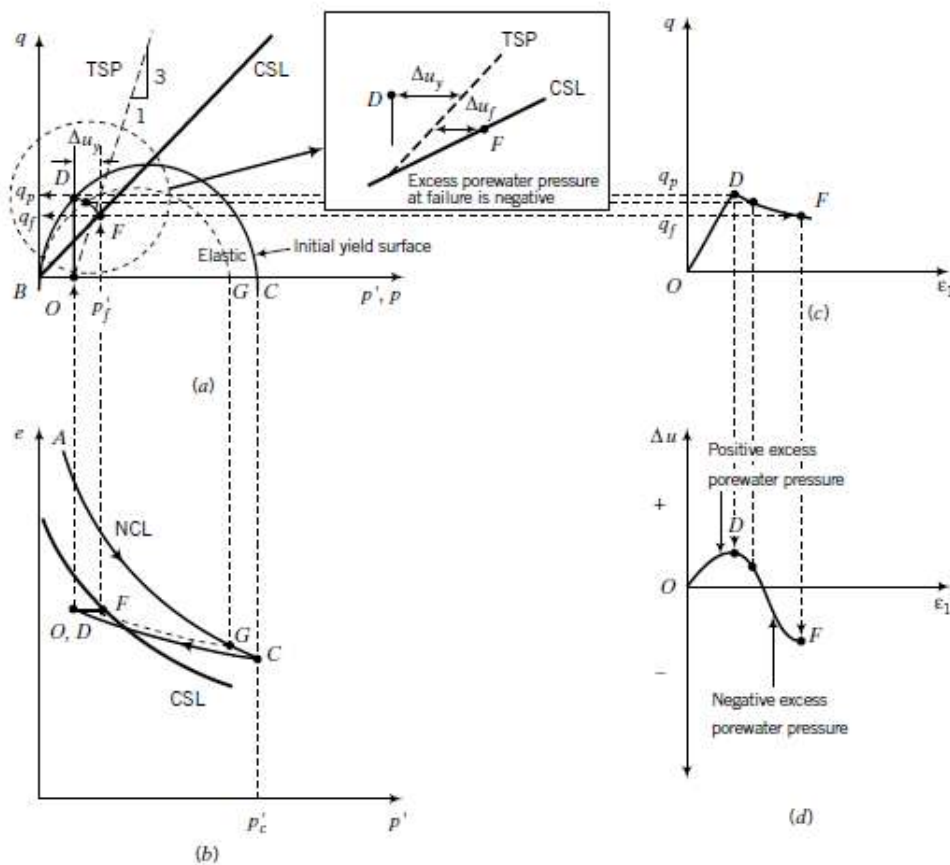


Fig.5.11: Illustrative predicted results from a triaxial CU test on a heavily over consolidated soil ($R_o > 2$) using the CSM.

5.9 ROSCOE AND HVORSLEV SURFACES FOR UNSATURATED SILTY SOIL

In the 1950s and 1960s, a new approach to soil mechanics was formulated on the basis of critical state concepts at Cambridge University. It provides a framework where the shear distortion of a saturated soil during yielding can be related to its stress and volume state (Roscoe et al. 1958; Schofield and Worth 1968). In particular, the framework can explain the differences in shear behavior between an over consolidated and a normally consolidated soil in the space of $\frac{q}{p'_e}$: $\frac{p'}{p'_e}$ to reach the critical state (Figure 5.12), where p' , q , and p'_e are the mean effective stress, deviator stress, and equivalent pressure, respectively.

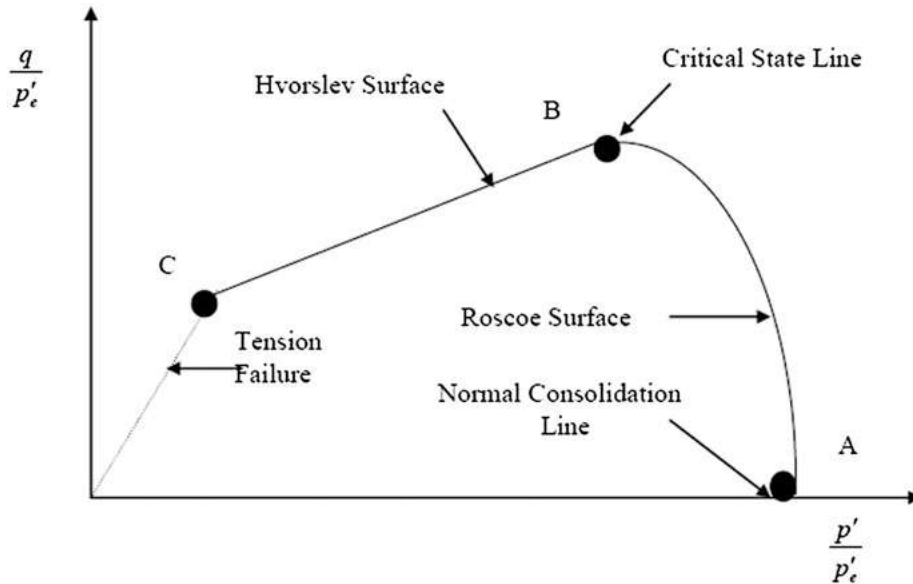


Fig.5.12: State boundary surface for saturated soil

A soil that is wetter (sometimes referred to as looser) than the critical state will contract in volume under shear to achieve the critical state, or if volume change is prevented (undrained condition) then increases in pore-water response will result so that the effective stress state moves toward the critical state. A soil that is drier (or denser) than the critical state will dilate, or if volume change is prevented then the result will decrease the pore-water pressure. The behavior of saturated soils is controlled by effective stress. The critical state theory is a three-dimensional (3D) approach for saturated soils and is defined in terms of three state variables: p' , q , and specific volume, v . For axi-symmetric conditions, these variables are defined as

$$p' = \frac{\sigma_1 + 2\sigma_3}{3} - u_w = p - u_w \text{-----} \quad \text{Eq.5.22}$$

$$q = \sigma_1 - \sigma_3 \text{-----} \quad \text{Eq.5.23}$$

$$v = 1 + e \text{-----} \quad \text{Eq.5.24}$$

Where σ_1 and σ_3 major and minor principal stresses; and e void ratio.

When the soil is under shearing, it will eventually reach a critical state condition, and these critical states are located on a unique line in the q : p' , v space. For normally consolidated soil,

all drained and un-drained stress paths appear to lie on a 3D surface bounded by the critical state line (CSL) at the top and the normal consolidation line (NCL) at the bottom. Both sets of stress paths lie on this surface. This surface is called the Roscoe surface or state boundary surface. The Hvorslev surface is another state boundary surface and links up with the Roscoe surface at the CSL (Fig. 1). This surface is a straight line in the normalized space of $\frac{q}{p'_e} : \frac{p'}{p'_e}$, where p'_e is the equivalent pressure and is defined as

$$p'_e = \exp \left[\frac{N(0) - v}{\lambda(0)} \right] \dots \dots \dots \text{Eq.5.25}$$

Where $N(0)$ and $\lambda(0)$ are the intercept (at $p' = 1$ kPa) and slope of the saturated virgin line, respectively; and v is specific volume.

The Hvorslev surface cannot extent to the $q=p'_e$ axis because of the no tension line. The significant feature of this surface is that the shear strength of a sample is a function of the mean net stress (p') and specific volume. Therefore, the complete state boundary surface consists of the Roscoe and Hvorslev surfaces, which meet at the CSL. It limits the behavior of drained and undrained tests on normally consolidated and over consolidated samples and unifies a wide range of the behavior of soil samples. Researchers, such as Marto (1996) and Moradi (1998), showed the Roscoe and Hvorslev surfaces by conducting compression and extension triaxial tests on soil samples. Houlsby et al. (1982) presented the Roscoe-Hvorslev model based on elastic-perfectly plastic behavior. Tanaka et al. (1986) also adapted the Hvorslev surface for a supercritical state, which is defined as the portion of the $p'-q$ plane on the right of the intersection between the CSL and the Cam-clay ellipse. The portion on its left is the subcritical region (de Souza Neto et al. 2009). Mita et al. (2004) conducted compression and extension tests on over consolidated clay and found a 3D Hvorslev modified **Cam-clay** model for over consolidation clay.

Cam Clay was originated by the Cambridge soil mechanics group in the 1960s. The problem to be considered is *simple shearing*, illustrated in Figure 5.13. A sample of soil is subjected to applied normal and shearing tractions, σ and τ , on its upper surface. If the sample happens to be saturated, we consider σ to be the effective stress.

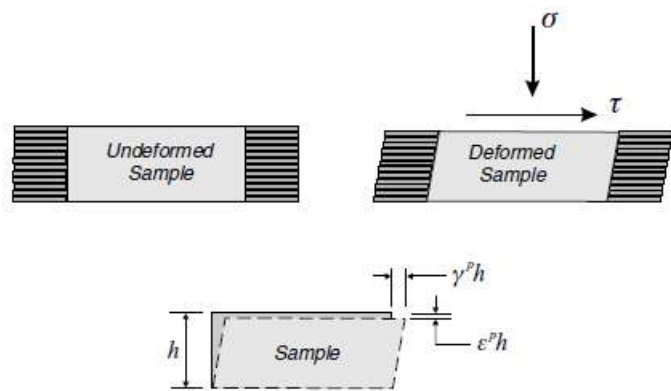


Fig.5.13: Schematic diagram showing a simple shear test.

The soil is laterally constrained so that no extensional deformation occurs in the horizontal direction. This can be accomplished using a sort of 'pancake' container consisting of layers of rigid material that may slide over each other, permitting shearing strain but no extensional strain. It is not a simple device, but that is not our concern. The essential thing is that the only extensional strain is the vertical strain, denoted by ϵ^p . The only other non-zero strain is the shear strain, denoted by γ^p . We denote both strains as plastic. The theory to be derived will overlook elastic strains for the moment, but they will be considered later.

The originators of the Cam Clay model used the triaxial test as their example problem, and it also has only two stress and two strain components, but those components are derived from invariants and are slightly more complex than the simple stresses and strains considered here.

First, we want to establish a yield surface. In the context of our example problem, this will be a function of the form $f(\sigma, \tau)$. To begin, assume the soil sample is in a yield state and write down the rate of plastic work:

$$\dot{W}_p = \sigma \dot{\epsilon}^p + \tau \dot{\gamma}^p \text{-----} \tag{Eq.5.26}$$

\dot{W}_p represents plastic, irrecoverable work done by the applied tractions. It postulates that \dot{W}_p must equal a specified function called the *dissipation function*, \dot{D} . It can be shown that the dissipation function should be a homogeneous function of the plastic strain rates multiplied by coefficients that depend upon the stresses. If we consider the case where σ is constant then it is reasonable to assume that the plastic extensional strain ϵ^p is at most a function of the plastic shear strain γ^p . Then the dissipation function \dot{D} can be written as a function of $\dot{\gamma}^p$ only. Also, for a frictional material, the rate of dissipation should depend on the normal stress σ . The Cambridge workers postulated a dissipation function with the form

$$\dot{D} = k\sigma \dot{\gamma}^p \text{-----} \tag{Eq.5.27}$$

where k is a material parameter that is constant for any particular soil. Setting the right-hand sides of (4) and (5) equal and rearranging gives

$$\frac{\dot{\epsilon}^p}{\dot{\gamma}^p} = k - \frac{\tau}{\sigma} \text{-----} \tag{Eq.5.28}$$

where we assume the shear strain rate $\dot{\gamma}^p$ to be strictly positive.

Suppose we alter both stresses by small amounts $\delta\sigma$ and $\delta\tau$. Then the rate of plastic work would also be altered by some amount $\delta\dot{W}_p$. Drucker's postulate states that, so long as the body remains in equilibrium, $\delta\dot{W}_p$ should always be equal to or greater than zero. Therefore

$$\delta\dot{W}_p = \delta\sigma \dot{\epsilon}^p + \delta\tau \dot{\gamma}^p \text{-----} \tag{Eq.5.29}$$

In the limiting case where the equality holds this expression embodies the normality condition. If we take the equality, we may write

$$\frac{\delta\tau}{\delta\sigma} + \frac{\dot{\epsilon}^p}{\dot{\gamma}^p} = \frac{d\tau}{d\sigma} + k - \frac{\tau}{\sigma} = 0 \text{-----} \tag{Eq.5.30}$$

where (7) has been used and δs have been replaced by ds . We can integrate (9) to give

$$\tau = \sigma(C_1 - k \ln \sigma) \text{-----} \tag{Eq.5.31}$$

Where C_1 is a constant of integration. This expression represents Cam Clay yield surface; however, an initial condition is still needed to find the constant C_1 .

To establish C_1 , note that equation (5.28) says that when $\sigma = \frac{\tau}{k}$, we are at the critical state.

Suppose we define a *critical state stress*, σ_c , which is equal to $\frac{\tau}{\sigma}$. In general, σ will be different from σ_c , but if they do coincide the particle packing will be at its critical state and there will be no further volume change. In that state, (5.31) would read as

$$k\sigma_c = \sigma_c(C_1 - k \ln \sigma_c) \text{-----} \text{Eq.5.32}$$

We can solve this equation for C_1 and along with the Eq. (10) to find the following expression:

$$\tau + k\sigma \left[\ln \left(\frac{\sigma}{\sigma_c} \right) - 1 \right] = 0 \text{-----} \text{Eq.5.33}$$

This equation relates the stresses σ and τ during yielding and hence represents our Cam Clay yield surface. A graph of (Eq.5.33) is shown in Figure 5.14.

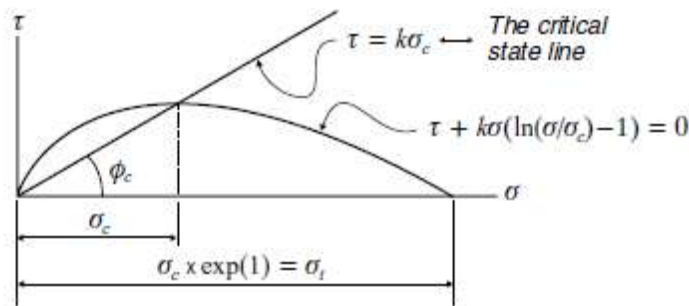


Fig. 5.14: Cam Clay yield surface in a simple shear test.

The yield criterion can be written in terms of the invariants q and p as follows:

$$q + Mp \left(\ln \frac{p}{p_c} - 1 \right) = 0 \text{-----} \text{Eq.5.34}$$

Here both M and p_c are material parameters, while q and p are the deviatoric and the mean stress, respectively. In the π -plane the Cam Clay surface will be circular just as the Drucker–Prager surface was. If we plot (Eq.13) we find the situation depicted in Figure 5.15.

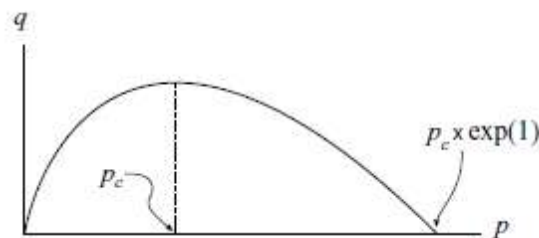


Fig.5.15: Cam Clay yield surface in (q, p) -space.

The pointed vertex at the tip of the Cam Clay surface was viewed by some researchers as being a weakness of the original Cam Clay model. The Modified Cam Clay

eliminated the point and introduced an elliptical surface with the form

$$q^2 = M^2 p(2p_c - p) \text{----- Eq.5.35}$$

The shape of the yield surface is now as shown in Figure 5.16.

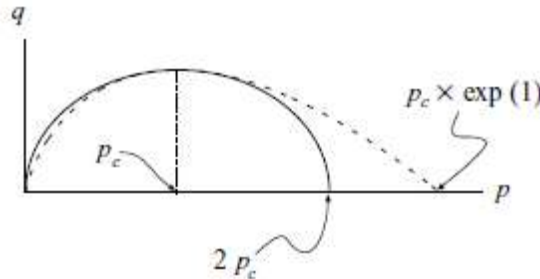


Fig.5.16: Modified Cam Clay yield surface.

The original Cam Clay surface is also shown as a dashed line. The two surfaces agree exactly when $p = p_c$, but the modified surface closes on the mean stress axis at a value of $2p_c$ rather than at $2.718p_c$ for the original model.

Example 1

The values of the critical state parameters for a particular type of clay are:

$$N = 2.1, \lambda = 0.087, \Gamma = 2.05, M = 0.95.$$

Two samples of this soil are consolidated under a confining pressure of 300 kPa. One sample has been subjected to a drained triaxial test whilst the second sample has been sheared in an undrained condition. Determine:

- the deviator stress at the critical state for both the drained and undrained tests,
- the pore pressure in the undrained test at the critical state,
- the volumetric strain in the drained test when the sample approaches the critical state.

Solution:

(a) Projection of the critical state line (CSL) onto the p' - q' plane defines the state of stress at the critical state and is a line that passes through the origin with gradient M .

$$q' = Mp'$$

where $q' = \sigma'_1 - \sigma'_3$ and $p' = \frac{\sigma'_1 + 2\sigma'_3}{3}$.

The initial state of the sample is point C in Figure . It can be shown that the stress path of the drained test on the p' - q' plane has a slope of 3 vertical to 1 horizontal (line CD). The stress path for the undrained test is represented by CU . Points D and U that are located on the critical state line represent the states of the two samples at critical state.

For the drained test the equation of the drained path (line CD in Figure is:

$$q' = 3(p' - 300.0).$$

This ensures the slope of 3 vertical, 1 horizontal on the p' - q' plane. Substituting q' in the equation of CSL :

$q' = 0.95 p' = 3(p' - 300.0)$, thus
 p' (at critical state) = 439.0 kPa.
 Substituting the above value of p'

$$q' = \sigma'_1 - \sigma'_3 = 0.95 \times 439.0 = 417.0 \text{ kPa.}$$

The state of the sample subjected to an isotropic compression or confining pressure σ_3 is defined by a relationship between v and p' called the normal compression line (*NCL*), as shown in Figures 1.a,b . Specific volume v is a dimensionless parameter and represents a volume in which the solids occupy a unit volume. From a phase diagram it can be shown that $v = 1 + e$ where e is the void ratio. The normal compression line is established by means of a triaxial compression test. The equation of the normal compression line (*NCL*) in $v, \ln p'$ coordinate system is:

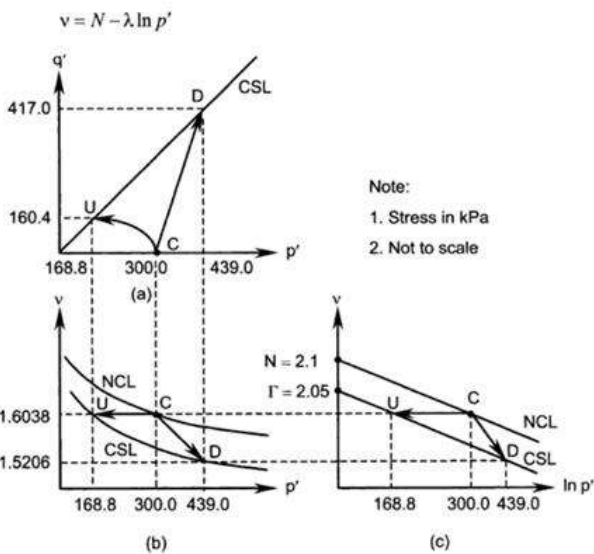


Fig: 1

For the undrained test we first substitute numerical values in the *NCL* equation and calculate the corresponding specific volume during the test and at failure:

$$v = 2.1 - 0.087 \times \ln 300.0 = 1.6038.$$

The magnitude of p' at critical state is calculated by substituting the specific volume in the *CSL* equation:

The projection of the *CSL* on to the $v, \ln p'$ coordinate system is approximated by a line parallel to the *NCL* (Figure 1 (c)):

$$v = \Gamma - \lambda \ln p'$$

$$1.6038 = 2.05 - 0.087 \times \ln p' \rightarrow p' = 168.8 \text{ kPa.}$$

The deviator stress at the critical state is:

$$q' = \sigma'_1 - \sigma'_3 = Mp' = 0.95 \times 168.8 = 160.4 \text{ kPa.}$$

(b) From the definition of p' we have:

$$p' = (\sigma'_1 + 2\sigma'_3)/3 = (\sigma'_1 - \sigma'_3 + \sigma'_3 + 2\sigma'_3)/3 = (q' + 3\sigma'_3)/3,$$

$$p' = (160.4 + 3\sigma'_3)/3 = 168.8,$$

$$\sigma'_3 = 115.3 \text{ kPa.}$$

$$u = 300.0 - 115.3 = 184.7 \text{ kPa.}$$

where ΔV is the volume change, V is the initial volume; ε_1 , ε_2 , and ε_3 are the axial strains in the direction of major principal stresses. The above equation can be expressed in terms of specific volume:

$$\varepsilon_V = \frac{\Delta v}{v}$$

$$\text{Thus } \varepsilon_V = (1.6038 - 1.5206)/1.6038 = 0.0519 = 5.19\%.$$

The results are illustrated in Figure 1.

(c) Calculate the specific volume at critical state (drained test):

$$v = \Gamma - \lambda \ln p' = 2.05 - 0.087 \ln 168.8 = 1.5206.$$

The general definition of volumetric strain is expressed by:

$$\varepsilon_V = \frac{\Delta V}{V} \approx \varepsilon_1 + \varepsilon_2 + \varepsilon_3$$

Example 2:

In a drained triaxial test carried out on a sample of the clay of Example 1. the sample was first consolidated under a confining pressure of 400 kPa. It was then unloaded to 300 kPa and, after equilibrium was reached, it was sheared in drained conditions. If the κ value is 0.037, calculate the volumetric strain at failure.

Solution:

The equation of expansion line (unloading) in v , $\ln p'$ coordinate system (Figure 2.(c)) is in the form:

$$v = v_\kappa - \kappa \ln p'$$

$$\kappa = -\frac{v_C - v_{C_1}}{\ln p'_C - \ln p'_{C_1}}$$

is the slope of the expansion line and v_κ is the magnitude of v at $p' = 1$ kPa. The parameter v_κ is not a constant for the soil and its magnitude depends on the magnitude of p'_{C_1} .

Note in this example $p'_{C_1} = 400$ kPa, and $p'_C = 300$ kPa. Alternatively:

$$(v - v_C)/(\ln p' - \ln p'_C) = -\kappa, \text{ or: } (v - v_{C_1})/(\ln p' - \ln p'_{C_1}) = -\kappa$$

Calculate the specific volume for $p' = 400.0$ kPa on the *NCL*:

$$v_{400} = 2.1 - 0.087 \times \ln 400.0 = 1.5787.$$

Calculate the specific volume after unloading to $p' = 300.0$ kPa:

$$\kappa = \frac{-(v_{300} - v_{400})}{(\ln 300.0 - \ln 400.0)} = 0.037, \quad \frac{-(v_{300} - 1.5787)}{(\ln 300.0 - \ln 400.0)} = 0.037 \rightarrow v_{300} = 1.5893.$$

From part (c) of Example 1 the specific volume at critical state is 1.5206.

Volumetric strain from equilibrium conditions at $p' = 300.0$ kPa and $v = 1.5893$ to critical state at $p' = 439.0$ kPa and $v = 1.5206$ is:

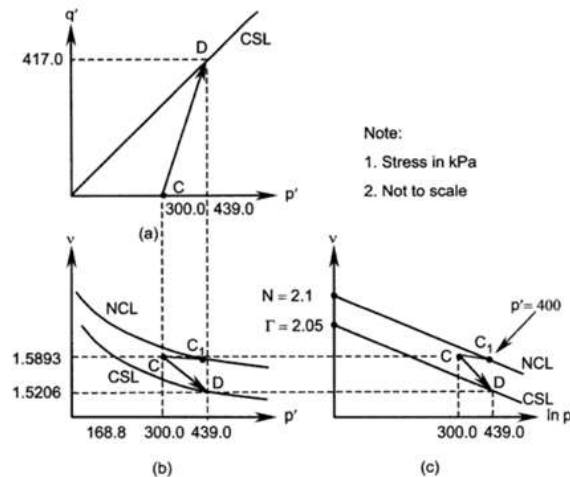
$$\varepsilon_V = (1.5893 - 1.5206) / 1.5893,$$

$$\varepsilon_V = 0.0432 = 4.32\% \text{ (compression).}$$

This is less than 5.19% obtained in Example 1. due to its lightly overconsolidated state. However the deviator stress at critical state is the same as the drained sample of Problem 4.10. Volumetric strain during unloading from $p' = 400.0$ kPa to $p' = 300.0$ kPa is:

$$\varepsilon_V = \frac{1.5787 - 1.5893}{1.5787},$$

$$\varepsilon_V = -0.0067 = -0.67\% \text{ (expansion).}$$



Example 3

The critical state parameters of a soil are:

$$M = 0.857, \lambda = 0.095, N = 2.1, \Gamma = 2.05, \kappa = 0.045.$$

Specimens of this soil have been consolidated and unloaded to obtain an initial void ratio of 0.62.

(a) If the specimens are subjected to an undrained triaxial test, find the minimum overconsolidation ratio ($OCR = m$) above which the pore pressure at the critical state becomes negative,

(b) calculate the volumetric strains for three specimens of $OCR = 1$, $OCR = m$ (as defined above) and $OCR = 8$ that are subjected to drained triaxial tests.

Sol:

(a) We consider the case where the pore pressure at failure becomes zero. At this state the effective stress path and the total stress path intersect each other on the *CSL* ($p'-q'$ plane) so that the q' is the same for both stress paths at this point (critical state).

At the critical state the specific volume is: $v = 1 + e = 1 + 0.62 = 1.62$.

Using Equation 4.14 the value of p' at $v = 1.62$ becomes:

$$v = \Gamma - \lambda \ln p' = 1.62 = 2.05 - 0.095 \ln p',$$

$$p' = 92.4 \text{ kPa.}$$

The deviator stress at the critical state is calculated as

$$q' = Mp' = 0.857 \times 92.4 = 79.2 \text{ kPa.}$$

The progress of the undrained triaxial test in terms of the total stresses, on the $p'-q'$ plane, is a line with the slope of 3 vertical to 1 horizontal.

Referring to Figure 4.9(a) the equation of the total stress path may be written as follows:

$$\frac{q - 79.2}{p - 92.4} = 3, \text{ which has a slope of 3 vertical, 1 horizontal.}$$

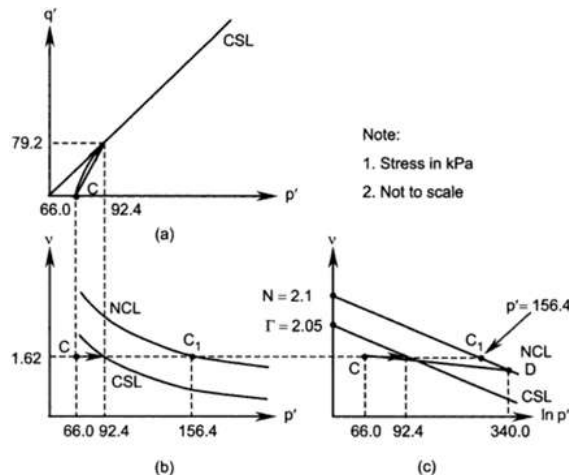
$$\kappa = -\frac{v_C - v_D}{\ln p'_C - \ln p'_D} \rightarrow 0.045 = -\frac{1.62 - v_D}{\ln 66.0 - \ln p'_D}.$$

Point D is located on the normal compression line; thus

$$v_D = N - \lambda \ln p'_D = 2.1 - 0.095 \ln p'_D.$$

For $q = 0, p = p'_C = 66.0 \text{ kPa}$.

This means an unloading (after consolidation) has yielded $p'_C = 66.0 \text{ kPa}$ as the initial state for triaxial test. In order to find the corresponding preconsolidation pressure (the isotropic compression where the sample was unloaded; point D in Figure 3 (c)) on the normal compression line we intersect this line with the expansion (or unloading) line. For this purpose first we define the slope of the expansion line



$$OCR = \exp\left(\frac{1.62 - 1.5462}{0.045}\right) = 5.15.$$

For the OCR values lower than 5.15 ($p'_D < 340.0$ kPa) the pore pressure at the critical state is positive; for the OCR values higher than 5.15 ($p'_D > 340.0$ kPa) the pore pressure is negative. The pore pressure can be calculated in a way similar to part (b) of Example 1.0. As an example if $p'_D = 400.0$ kPa:

$$v_D = N - \lambda \ln p' = 2.1 - 0.095 \ln 400.0 = 1.5308.$$

Using the definition of the slope of the expansion line:

$$\kappa = -\frac{v_C - v_D}{\ln p'_C - \ln p'_D} \rightarrow 0.045 = -\frac{1.62 - 1.5308}{\ln p'_C - \ln 400}$$

$$p'_C = 55.1 \text{ kN} < 66.0 \text{ kPa}.$$

Substituting v_D in the equation of the expansion line:

$$0.045 = -\frac{1.62 - (2.1 - 0.095 \ln p'_D)}{\ln 66.0 - \ln p'_D}.$$

Solving for p'_D :

$$p'_D = 340.0 \text{ kPa}.$$

From the definition of p' we have (part (b) of Example No. 1

$$p' = (\sigma'_1 + 2\sigma'_3)/3 = (\sigma'_1 - \sigma'_3 + \sigma'_3 + 2\sigma'_3)/3 = (q' + 3\sigma'_3)/3 = 92.4 \text{ kPa}.$$

$$p' = (\sigma'_1 + 2\sigma'_3)/3 = (79.2 + 3\sigma'_3)/3 = 92.4 \rightarrow \sigma'_3 = 66.0 \text{ kPa}.$$

$$u = 55.1 - 66.0 = -10.9 \text{ kPa}.$$

The results of part (a) are shown in Figure 3.

(b) For $OCR = 1$:

$$v_D = 1.62 = N - \lambda \ln p' = 2.1 - 0.095 \ln p'_D,$$

$$p'_D = 156.4 \text{ kPa}.$$

The p' value at the critical state is:

$$q' = 3(p' - 156.4) = 0.857 p' \rightarrow p' = 218.9 \text{ kPa}.$$

The corresponding specific volume at the critical state:

$$v = \Gamma - \lambda \ln p' = 2.05 - 0.095 \ln 218.9 = 1.5381.$$

$$\varepsilon_V = \frac{(1.62 - 1.5381)}{1.62} = 0.0506 = 5.06\% \approx 5.1\% \text{ (compression)}.$$

For $OCR = 5.15$, $p' = 92.4$ kPa.

$$v = \Gamma - \lambda \ln p' = 2.05 - 0.095 \ln 92.4 = 1.62.$$

$$\varepsilon_V = \frac{(1.62 - 1.62)}{1.62} = 0.0 = 0.0\%.$$

$$v_D = N - \lambda \ln p'_D = 1.5264 = 2.1 - 0.095 \ln p'_D \rightarrow p'_D = 419.0 \text{ kPa}.$$

$$p'_C = 419.0/8 = 52.4 \text{ kPa}.$$

$$q' = 3(p' - 52.4) = 0.857 p',$$

$$p' = 73.3 \text{ kPa.}$$

The corresponding specific volume at critical state:

$$v = \Gamma - \lambda \ln p' = 2.05 - 0.095 \ln 73.3 = 1.6420.$$

$$\varepsilon_V = \frac{(1.62 - 1.642)}{1.62} = -0.0136 = -1.36\% \text{ (expansion).}$$

For $OCR = 8$:

$$\kappa = -\frac{v_C - v_D}{\ln p'_C - \ln p'_D} \rightarrow 0.045 = -\frac{1.62 - v_D}{\ln(1/8)}.$$

$$v_D = 1.5264.$$

5.10 CRITICAL VOID RATIO, EFFECT OF DILATION IN SANDS

5.10.1 Interpretation of the shear strength of soils:

We will interpret the shear strength of soils based on their capacity to dilate. Dense sands and over consolidated clays ($OCR > 2$) tend to show peak shear stresses and expand (positive dilation angle), while loose sands and normally consolidated and lightly over consolidated clays do not show peak shear stresses except at very low normal effective stresses and tend to compress (negative dilation angle). In our interpretation of shear strength, we will describe soils as dilating soils when they exhibit peak shear stresses at $\alpha > 0$, and non dilating soils when they exhibit no peak shear stress and attain a maximum shear stress at $\alpha=0$. However, a non dilating soil does not mean that it does not change volume (expand or contract) during shearing. The terms *dilating* and *nondilating* refer only to particular stress states (peak and critical) during soil deformation.

The peak shear strength of a soil is provided by a combination of the shearing resistance due to sliding (Coulomb's frictional sliding), dilatancy effects, crushing, and rearrangement of particles. At low normal effective stresses, rearrangement of soil particles and dilatancy are more readily facilitated than at high normal effective stresses. At high normal effective stresses, particle crushing significantly influences the shearing resistance. However, it is difficult to determine the amount of the shear strength contributed by crushing and the arrangement of particles from soil test results.

We will refer to key soil shear strength parameters using the following notation. The peak shear strength, τ_p , is the peak shear stress attained by a dilating soil (Figure 5.17). The dilation angle at peak shear stress will be denoted as α_p . The shear stress attained by all soils at large shear strains ($\tau_{zx} > 10\%$), when the dilation angle is zero, is the critical state shear strength denoted by τ_{cs} . The void ratio corresponding to the critical state shear strength is **the critical void ratio** denoted by e_{cs} . The effective friction angle corresponding to the critical state shear strength and critical void ratio is ϕ'_{cs} .

The peak effective friction angle for a dilating soil according to Coulomb's model is

$$\phi'_p = \phi'_{cs} + \alpha_p \text{-----} \quad \text{Eq.5.35}$$

Type I soils: loose sands, normally consolidated and lightly over consolidated clays ($OCR \leq 2$) are observed to:

Show gradual increase in shear stresses as the shear strain increases (strain-hardens) until an approximately constant shear stress, which we will call the critical state shear stress, τ_{CS} , is attained (Figure 5.17.a).

Type II soils: dense sands and heavily over consolidated clays ($OCR > 2$) are observed to:

Show a rapid increase in shear stress reaching a peak value, τ_p , at low shear strains (compared to Type I soils) and then show a decrease in shear stress with increasing shear strain (strain-softens), ultimately attaining a critical state shear stress (Figure 5.17.a).

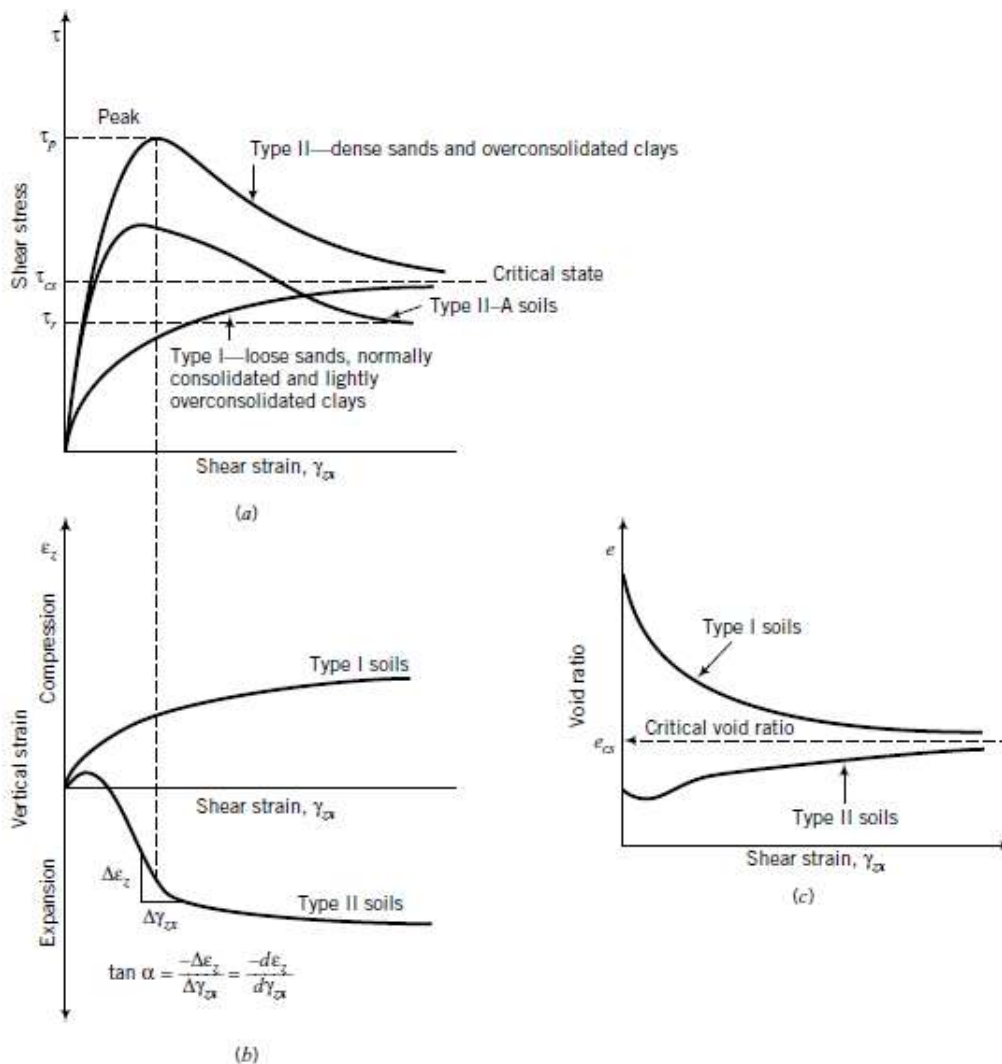


Fig.5.17: Response of soils to shearing

All soils, regardless of their initial state of stress, will reach a critical state characterized by continuous shearing at constant shear-to-normal-effective-stress ratio and constant volume. The initial void ratio of a soil and the normal effective stresses determine whether the soil will dilate or not. Dilating soils often exhibit (1) a peak shear stress and then strain-soften to a constant

shear stress, and (2) initial contraction followed by expansion toward a critical void ratio. Non dilating soils (1) show a gradual increase of shear stress, ultimately reaching a constant shear stress, and (2) contract toward a critical void ratio.

5.11 EFFECT OF DILATION ON SANDS

5.11.1 Effects of dilation on Coulomb's failure envelope

In real soils, the particles are randomly distributed and often irregular. Shearing of a given volume of soil would cause impending slip of some particles to occur up the failure plane while others occur down the plane. The general form of Equation of failure plane can be expressed as

$$\tau_f = \sigma'_{nf} \tan(\phi' \pm \alpha) \text{-----} \text{Eq.5.35}$$

Where the positive sign refers to soils in which the net movement of the particles is initiated up the plane and the negative sign refers to net particle movement down the plane.

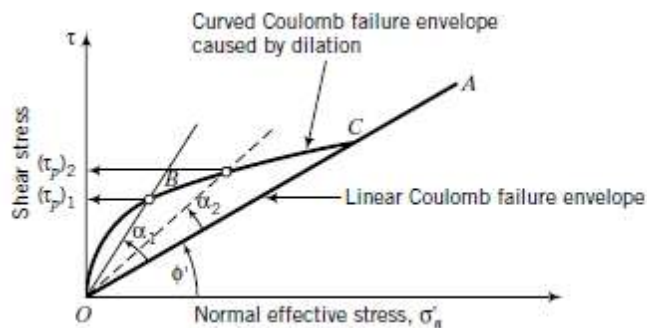


Fig.5.18: Effect of dilation on Coulomb's failure envelope

We will call the angle, α , the dilation angle. It is a measure of the change in volumetric strain with respect to the change in shear strain. Soils that have positive values of α expand during shearing, while soils with negative values of α contract during shearing. In Mohr's circle of strain (Figure 5.19), the dilation angle is

$$\alpha = \sin^{-1} \left(-\frac{\Delta\varepsilon_1 + \Delta\varepsilon_3}{\Delta\varepsilon_1 - \Delta\varepsilon_3} \right) = \sin^{-1} \left[-\frac{\Delta\varepsilon_1 + \Delta\varepsilon_3}{(\Delta\gamma_{cs})_{max}} \right] \text{-----} \text{Eq.5.36}$$

Where, Δ denotes change. The negative sign is used because we want α to be positive when the soil is expanding. You should recall that compression is taken as positive in soil mechanics.

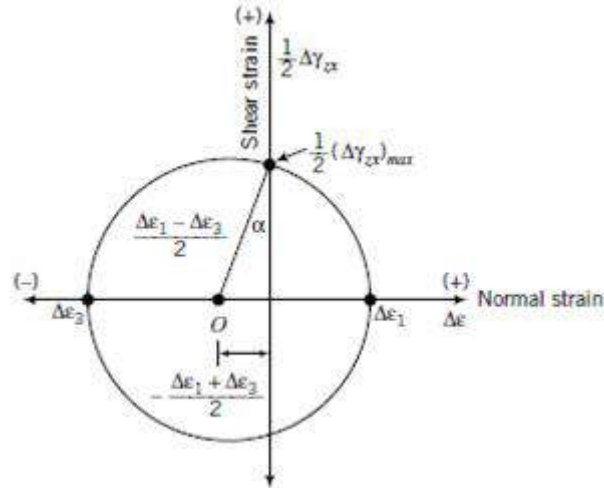


Fig.5.19: Mohr's circle of strain and angle of dilation

Dilation is not a peculiarity of soils, but occurs in many other materials, for example, rice and wheat. The ancient traders of grains were well aware of the phenomenon of volume expansion of grains. However, it was Osborne Reynolds (1885) who described the phenomenon of dilatancy and brought it to the attention of the scientific community. Dilation can be seen in action at a beach. If you place your foot on beach sand just following a receding wave, you will notice that the initially wet, saturated sand around your foot momentarily appears to be dry (whitish color). This occurs because the sand mass around your foot dilates, sucking water up into the voids. This water is released, showing up as surface water, when you lift up your foot.

5.12 IMPORTANT POINTS

1. Shear failure of soils may be modeled using Coulomb's frictional law, $\tau_f = \sigma'_{n_f} \tan(\phi' \pm \alpha)$, where τ_f is the shear stress when slip is initiated, σ'_{n_f} is the normal effective stress on the slip plane, ϕ' is the friction angle, and α is the dilation angle.
1. Shear failure of soils may be modeled using Coulomb's frictional law, $\tau_f = \sigma'_{n_f} \tan(\phi' \pm \alpha)$, where τ_f is the shear stress when slip is initiated, σ'_{n_f} is the normal effective stress on the slip plane, ϕ' is the friction angle, and α is the dilation angle.
2. The effect of dilation is to increase the shear strength of the soil and cause the Coulomb's failure envelope to be curved.
3. Large normal effective stresses tend to suppress dilation.
4. At the critical state, the dilation angle is zero.